PART I: TEMPERATURE GRADIENTS IN TURBULENT GAS STREAMS EFFECT OF VISCOUS DISSIPATION ON THE EVALUATION OF TOTAL CONDUCTIVITY

PART II: THERMAL TRANSFER FROM SMALL WIRES IN THE BOUNDARY FLOW ABOUT A CYLINDER

Thesis by

Emilio Cesare Venezian

In Partial Fulfillment of the Requirements

For the Degree of

Doctor of Philosophy

California Institute of Technology

Pasadena, California

1962

ACKNOWLEDGMENT

The author wishes to express his gratitude for the patient and helpful guidance of Dr. B. H. Sage during the entire course of his studies. The cooperation of Mr. H. H. Reamer is also acknowledged. H. E. Smith assisted in collecting the experimental data reported in the second part of this work. Virginia Berry and other members of the staff assisted in many of the computations and graphical manipulations of the data.

The Peter E. Fluor Foundation generously supported the research program. The author was recipient of the Peter E. Fluor Fellowship during the period in which the work presented was carried out. This financial assistance is gratefully acknowledged.

FOREWORD

An article entitled "Temperature Gradients in Turbulent Gas Streams. Effect of Viscous Dissipation on the Evaluation of Total Conductivity," co-authored by E. C. Venezian and B. H. Sage, and based on the material presented in Part I of this thesis, has been accepted for publication by the "A. I. Ch. E. Journal."

ABSTRACT

PART I

Values of the total conductivity for air in turbulent flow were originally reported without regard to effects of viscous dissipation. The reported values were corrected for such effects by utilizing measurements taken at the time of the original investigation. The total conductivity obtained by taking into account dissipation effects was found to be independent of the average temperature gradient with which measurements were made.

PART II

The heat transfer characteristics from a 0. 001-inch diameter platinum wire in the boundary flow about a 1-inch copper cylinder were measured at Reynolds numbers, based on the cylinder diameter, of about 1750, 3500, and 7100. The results are presented in terms of the Nusselt number for the wire as a function of position for the three Reynolds numbers investigated. Comparison of the measured Nusselt numbers with values predicted from calculated velocity distributions indicate that, in the vicinity of the cylinder wall, the Nusselt number is not a unique function of the Reynolds number based on the wire diameter.

TABLE OF CONTENTS

LIST OF FIGURES

LIST OF FIGURES (Continued)

LIST OF FIGURES (Concluded)

PART III

LIST OF TABLES

PART I

TEMPERATURE GRADIENTS IN TURBULENT GAS STREAMS

EFFECT OF VISCOUS DISSIPATION ON THE EVALUATION OF TOTAL CONDUCTIVITY

INTRODUCTION

In the period from 1947 to 1956 a series of measurements was made at the Chemical Engineering Laboratory of the California Institute of Technology (1, 2, 3, 4, 5, 6, 7, 8, 9, 10, 11, 12)* to determine the total viscosity and total conductivity of air in turbulent flow as a function of the flow conditions. An additional objective was to obtain experimental data for an evaluation of the analogy between heat and momentum transport proposed by Reynolds (13), and for various modifications of this analogy (14, 15, 16). The present work consists of a supplemental evaluation of the experimental data by taking into account the effect of viscous dissipation in the calculation of the total conductivity.

Following von Karman (14), the total viscosity may be defined as:

$$\underline{\epsilon}_m = \frac{\tau/\rho}{d\overline{u}/dy} \qquad (1)^{**}$$

The total conductivity is defined by a similar expression:

$$\underline{\epsilon}_c = \frac{-\dot{q}}{\sigma C_p \frac{\partial \overline{t}}{\partial y}} \qquad (2)$$

From these quantities, the eddy viscosity and conductivity are defined by the equations

$$\epsilon_m = \underline{\epsilon}_m - \nu \qquad (3)$$

$$\epsilon_c = \underline{\epsilon}_c - \kappa \qquad (4)$$

---

*Numbers in parentheses indicate references listed on page 30.

**Definitions of the symbols used are given on page 32.

The statement of Reynolds' analogy is usually (14, 16) expressed by the equation

$$\epsilon_m = \epsilon_c \tag{5}$$

In postulating the analogy between momentum and energy transport, Reynolds (13) used equations which are not wholly consistent with modern concepts; however, if these equations are interpreted at the microscopic level a more proper statement of the analogy would be

$$\epsilon_m = \gamma\epsilon_c \tag{6}$$

Since the modified analogies of von Karman and Martinelli are based on equation 5, it appears reasonable to refer to this as the "modified Reynolds' analogy," and to reserve the name "Reynolds' analogy" for equation 6.

EXPERIMENTAL METHODS

The experimental methods used in the determination of the total viscosity and conductivity have been discussed in considerable detail (1, 2, 3, 5, 6). To aid in the understanding of the analysis a brief summary of the equipment and methods is given.

A schematic diagram of the system is shown in fig. 1. The equipment consisted of a closed-loop wind-tunnel formed by two polished copper plates, A and B, 13.5 feet long and 13 inches wide. The distance between the plates was approximately 0.7 inches but varied slightly with the experimental conditions (1). A blower, C, with variable speed drive was used to supply air at various gross velocities to the channel. Heaters and refrigeration coils, D, were provided for conditioning the air prior to entry into the channel through the converging section, E. Each plate was supplied with an oil bath, these baths were independent, so that the temperature of the heat transfer medium could be adjusted to give the desired temperature at the upper and lower copper plates. Each bath was provided with a thyratron-controlled immersion heater for fine regulation of the temperature.

The upper plate was provided with two calorimeters, F and G, for the determination of heat flux. The construction of these calorimeters, as well as their operation, is discussed in detail by Page (5) and Cavers (6). In principle, the surface of the calorimeter was maintained at the same temperature as the copper plate immediately adjacent

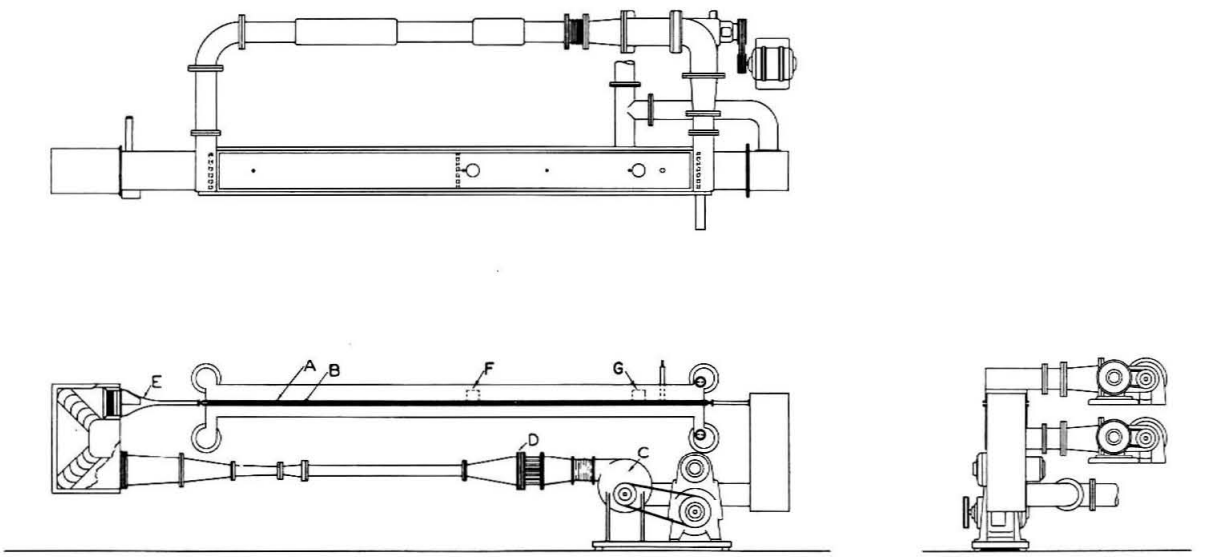

Figure 1: Schematic Diagram of Equipment

to it by proper adjustment of an electrical heater inside the calorimeter. The current and potential difference across this heater then gave a direct measure of the heat flux.

In order to obtain accurate information on the temperature distribution in the flowing stream, a platinum resistance thermometer was provided. This thermometer could also be used as a hot-wire anemometer for the determination of velocity profiles. A Pitot tube was also used to determine velocity distributions over the central portion of the channel, and served as a standard for the calibration of the hot-wire anemometer. Figure 2 shows these instruments installed in the channel.

Besides the temperature and velocity distributions the data obtained included the separation between the plates, the heat flux at the upper wall, and the pressure gradient along the channel. The conditions under which the tests were performed are listed in Table I.*

---

*Tables are presented on page 35.

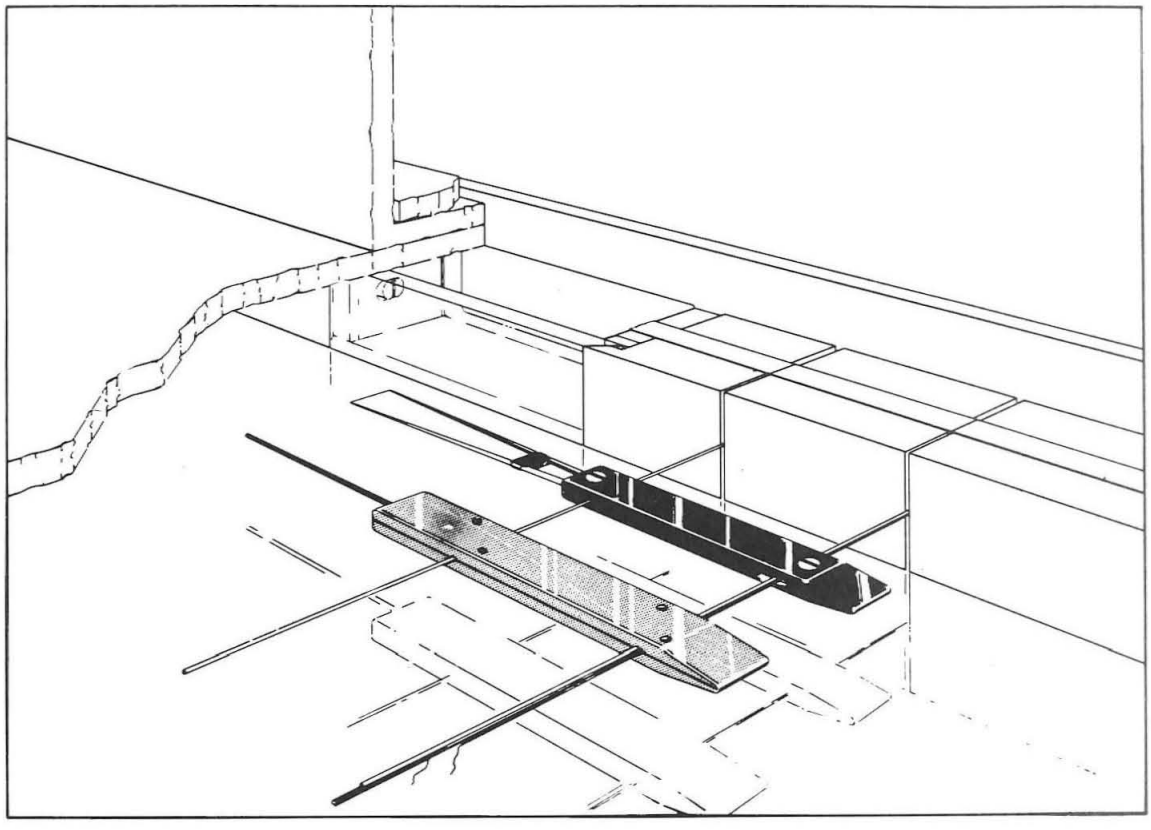

Figure 2: Hot Wire Anemometer and Pitot Tube

ANALYSIS

The total conductivity as defined by equation 2 is based on the local heat flux which, in general, is not equal to the heat flux at the boundaries. Since information on the local heat flux was not available, this flux was originally assumed to be equal to the heat flux at the upper wall (5, 6). The heat flux, however, is a function of position if the viscous dissipation in the stream is considered.

The coordinate systems used in this analysis are shown in fig. 3. For steady, two-dimensional flow which is uniform as regards momentum transport and nearly uniform as regards energy transport, the energy equation may be written as (17, 18):

$$\frac{d\dot{q}}{dy} = \phi - \sigma C_p \overline{u}_x \frac{\partial \overline{t}}{\partial x} \tag{7}$$

where

$$\phi = \eta \left(\frac{\partial \overline{u}_x}{\partial y} \right)^2 + \eta \sum_{i=1}^{3} \sum_{k=1}^{3} \overline{\frac{\partial u_i'}{\partial x_k} \left(\frac{\partial u_i'}{\partial x_k} + \frac{\partial u_k'}{\partial x_i} \right)} \tag{8}$$

Since the temperature in the tests considered* decreases with decreasing distance from the lower plate, equation 8 may be integrated directly to

$$\dot{q} = \dot{q}_a + \int_{y_o}^{y} \left(\phi - \sigma C_p \overline{u}_x \frac{\partial \overline{t}}{\partial x} \right) dy \tag{9}$$

---

*Test 61 constitutes an exception to this statement. The modifications required in the analysis, however, are minor.

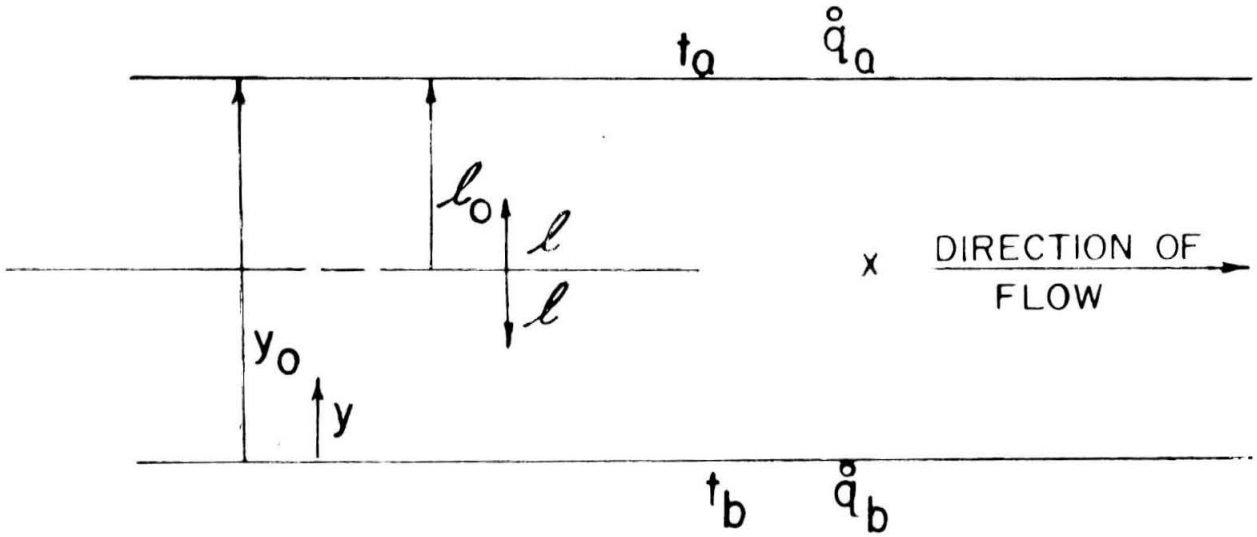

Figure 3: Coordinate Systems Used in the Analysis

For the conditions of interest, it can be shown (19, 20) that

$$-\rho\,\overline{u_x' u_y'}\,\frac{\partial \bar{u}_x}{\partial y} = \eta \sum_{i=1}^{3}\sum_{k=1}^{3} \overline{\frac{\partial u_i'}{\partial x_k}\left(\frac{\partial u_i'}{\partial x_k} + \frac{\partial u_k'}{\partial x_i}\right)} - \psi \qquad (10)$$

where

$$\psi = \frac{\partial}{\partial y}\,\overline{\eta u_x'\left(\frac{\partial u_y'}{\partial x} + \frac{\partial u_x'}{\partial y}\right)} - \frac{\partial}{\partial y}\,\overline{u_y'\left(P' + \sum_{j=1}^{3}\frac{\rho}{2}u_j'^2\right)} \qquad (11)$$

From equations 8, 9, and 10, it follows that

$$\dot{q} = \dot{q}_a + \int_{y_o}^{y}\left[\left(\eta\frac{\partial \bar{u}_x}{\partial y} - \rho\,\overline{u_x' u_y'}\right)\frac{\partial \bar{u}_x}{\partial y} + \psi - \sigma C_p \bar{u}_x \frac{\partial \bar{t}}{\partial x}\right]dy \qquad (12)$$

For the restricted case under consideration, the Navier-Stokes equations may be written in the form

$$\rho\,\frac{\partial(u_y' u_z')}{\partial y} = 0 \qquad (13)$$

$$-\frac{\partial \bar{P}}{\partial y} - \rho\,\frac{\partial \overline{(u_y')^2}}{\partial y} = 0 \qquad (14)$$

$$-\frac{\partial \bar{P}}{\partial x} + \frac{\partial}{\partial y}\left(\eta\,\frac{\partial \bar{u}_x}{\partial y}\right) - \rho\,\frac{\partial \overline{(u_x' u_y')}}{\partial y} = 0 \qquad (15)$$

The derivation of these equations is available in the literature (17, 21) for the case of constant viscosity. The extension to the case of variable viscosity is immediate. When equation 13 is integrated with respect to y, and the boundary conditions of zero velocity at the walls are used, there is obtained

$$\overline{u_y' u_z'} = 0 \qquad (16)$$

Upon differentiating equation 14 with respect to x, there results

$$- \frac{\partial}{\partial y} \left(\frac{\partial \overline{P}}{\partial x} \right) = \frac{\partial}{\partial x} \rho \frac{\partial \overline{(u_y')^2}}{\partial y} \tag{17}$$

Since the flow has been assumed to be uniform and fully-developed, it follows that

$$\frac{\partial}{\partial x} \rho \frac{\partial \overline{(u_y')^2}}{\partial y} = 0 \tag{18}$$

Combining equation 17 with equation 18 yields the result

$$- \frac{\partial}{\partial y} \left(\frac{\partial \overline{P}}{\partial x} \right) = 0 \tag{19}$$

which implies that the derivative $\frac{\partial \overline{P}}{\partial x}$ is independent of y. Making use of this result, equation 15 may be integrated to give

$$\eta \frac{\partial \overline{u}_x}{\partial y} - \rho \, u_x' u_y' = \frac{\partial \overline{P}}{\partial x} y + \tau_{ob} \tag{20}$$

where

$$\tau_{ob} = \left(\eta \frac{\partial \overline{u}_x}{\partial y} \right)_{y=0} \tag{21}$$

Combining equations 12 and 20, there results

$$\dot{q} = \dot{q}_a + \int_{y_o}^{y} \left[\left(\tau_{ob} + \frac{\partial \overline{P}}{\partial x} y \right) \frac{\partial \overline{u}_x}{\partial y} + \psi - \sigma C_p \overline{u}_x \frac{\partial \overline{t}}{\partial x} \right] dy \tag{22}$$

Data for the determination of the local heat flux by equation 22

is not available from the experiments of interest. However, there is sufficient data in the literature to estimate the relative importance of the terms of the integrand at a Reynolds number of about 50, 000. An average value of the first term in the integrand, as obtained from the data of Page (5), is 0. 15 Btu/cu. ft. /sec. This term vanishes at the center of the channel and assumes its largest value at the wall. The local value of ψ may be obtained from the data of Laufer (21, 22, 23) the maximum value of this quantity is no larger than 0. 001 Btu/cu. ft. / sec., and occurs close to the wall. The data of Mason (4) indicates that axial temperature gradients of at most 0. 05 ^{o}F/ft. may be expected, under these conditions the value of the third term in the integrand is of about 0. 007 Btu/cu. ft. /sec.

From this data it is apparent that neglecting the last two terms in the integrand in equation 23 would introduce an error no larger than 5% in the value of the integral. With these approximations, the value of the local heat flux is related to experimentally determined quantities by the expression

$$\dot{q} = \dot{q}_a + \int_{y_o}^{y} \left(\tau_{ob} + \frac{\partial \overline{P}}{\partial x} \right) \frac{\partial \overline{u}_x}{\partial y} \, dy \tag{23}$$

$$= \dot{q}_a + \dot{q}_j \tag{24}$$

where

$$\dot{q}_j = \int_{y_o}^{y} \left(\tau_{ob} + \frac{\partial \overline{P}}{\partial x} \right) \frac{\partial \overline{u}_x}{\partial y} \, dy \tag{25}$$

Equations 2 and 23 may be used for the calculation of the total conductivity from the available experimental data. In the present case, however, values of the total conductivity uncorrected for viscous dissipation

$$\underline{\epsilon}_c^* = \frac{-\dot{q}_a}{\sigma C_p (\frac{\partial \bar{t}}{\partial y})} \tag{26}$$

were available, and the calculations were facilitated by rewriting equation 2 in the form

$$\underline{\epsilon}_c = \frac{-\dot{q}_a}{\sigma C_p (\frac{\partial \bar{t}}{\partial y})} (1 + \frac{\dot{q}_a}{\dot{q}_j}) \tag{27}$$

$$= \underline{\epsilon}_c^* (1 + \frac{\dot{q}_a}{\dot{q}_j}) \tag{28}$$

The quantity $\dot{q}_j$ was calculated by equation 25 using experimental values of the velocity gradient and of the pressure gradient whenever possible. When this data was not available, the velocity distribution was assumed to be the same as that for tests at essentially the same Reynolds number. The pressure gradient, when not available from the experiments, was calculated from established correlations (10). The thermal flux at the upper wall, $\dot{q}_a$, was available for all the tests used.

The values of the corrected total conductivity in the region $0.1 \leq y/y_o \leq 0.9$ are presented in Table II, together with the values of the uncorrected total conductivity and of the factor $(1 + \frac{\dot{q}_j}{\dot{q}_a})$. Figure 4 shows the variation of the factor $(1 + \frac{\dot{q}_j}{\dot{q}_a})$ with position in the channel

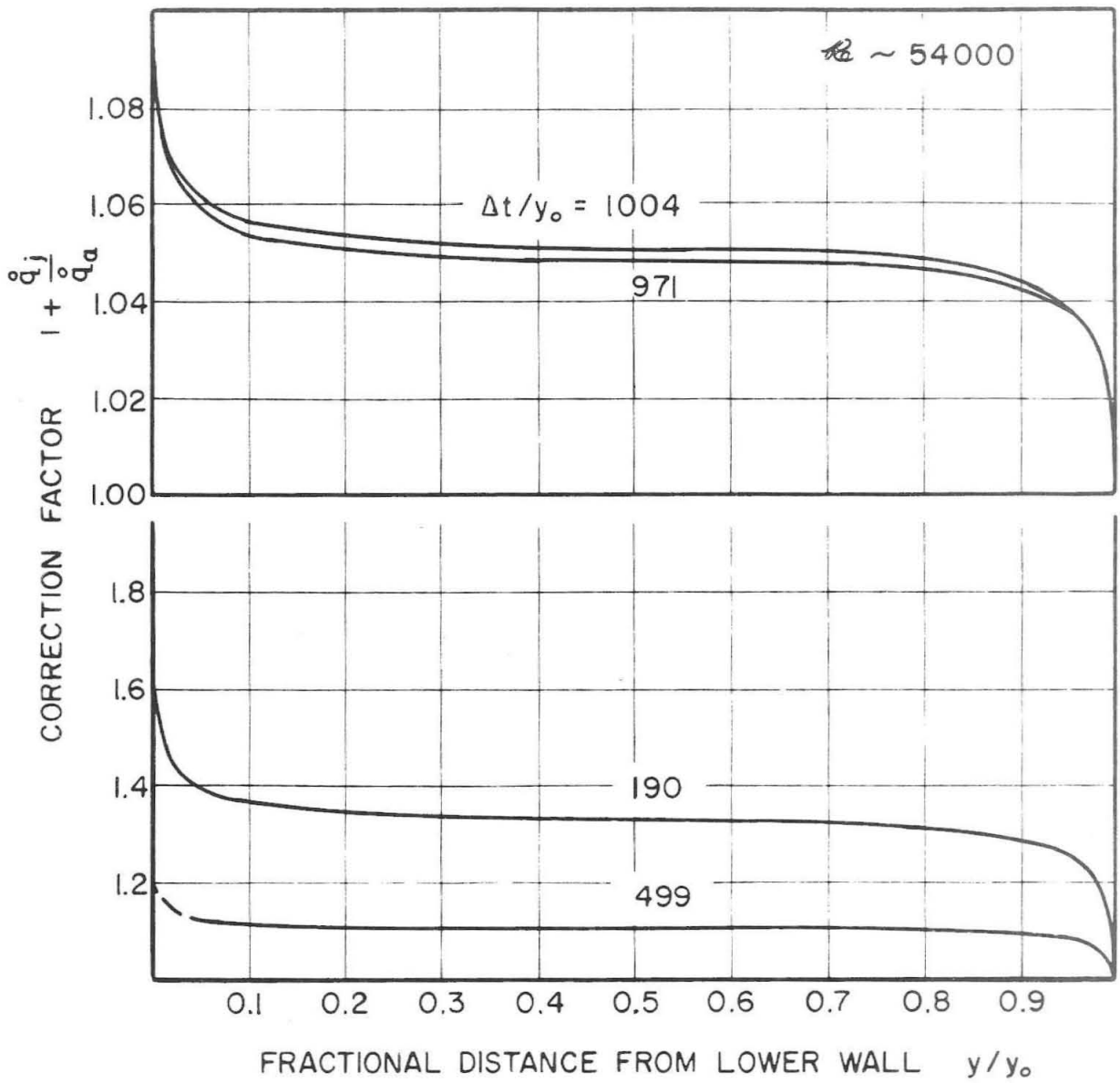

Figure 4: Effect of Position on the Correction Factor

for a Reynolds number

$$Re = \frac{\int_0^{y_o} \overline{u}_x \, dy}{\nu_{y/y_o=0.5}} \tag{29}$$

of about 54, 000, using the average temperature gradient, $\Delta t/y_o$, as a parameter. The variation of the maximum value of this factor with Reynolds number and average temperature gradient is shown in fig. 5.

The data presented in Table II was smoothed with respect to Reynolds number and position. The values so obtained, which represent the average of values obtained at different values of the average temperature gradient, are listed in Table III and depicted in fig. 6. Table IV presents the standard error of estimate of the experimental data from the smooth values. The standard error of estimate is defined as

$$\sigma_e = \left[\frac{\sum_{i=1}^{N} (f_{exp,i} - f_{sm,i})^2}{N - 1} \right]^{1/2} \tag{30}$$

Cavers (6, 11) reported values of the total conductivity in the vicinity of the walls in terms of the parameter $\frac{\epsilon_c}{\kappa} \frac{\ell_o}{\ell}$. This parameter is expressible as a unique function of

$$y^+ = \frac{(1 - \frac{\ell}{\ell_o}) u_* \ell_o}{\nu} \tag{31}$$

provided the dimensionless velocity u/u_* is also a function of y^+ alone, and provided Reynolds' analogy holds with

$$\gamma = Pr_m \tag{32}$$

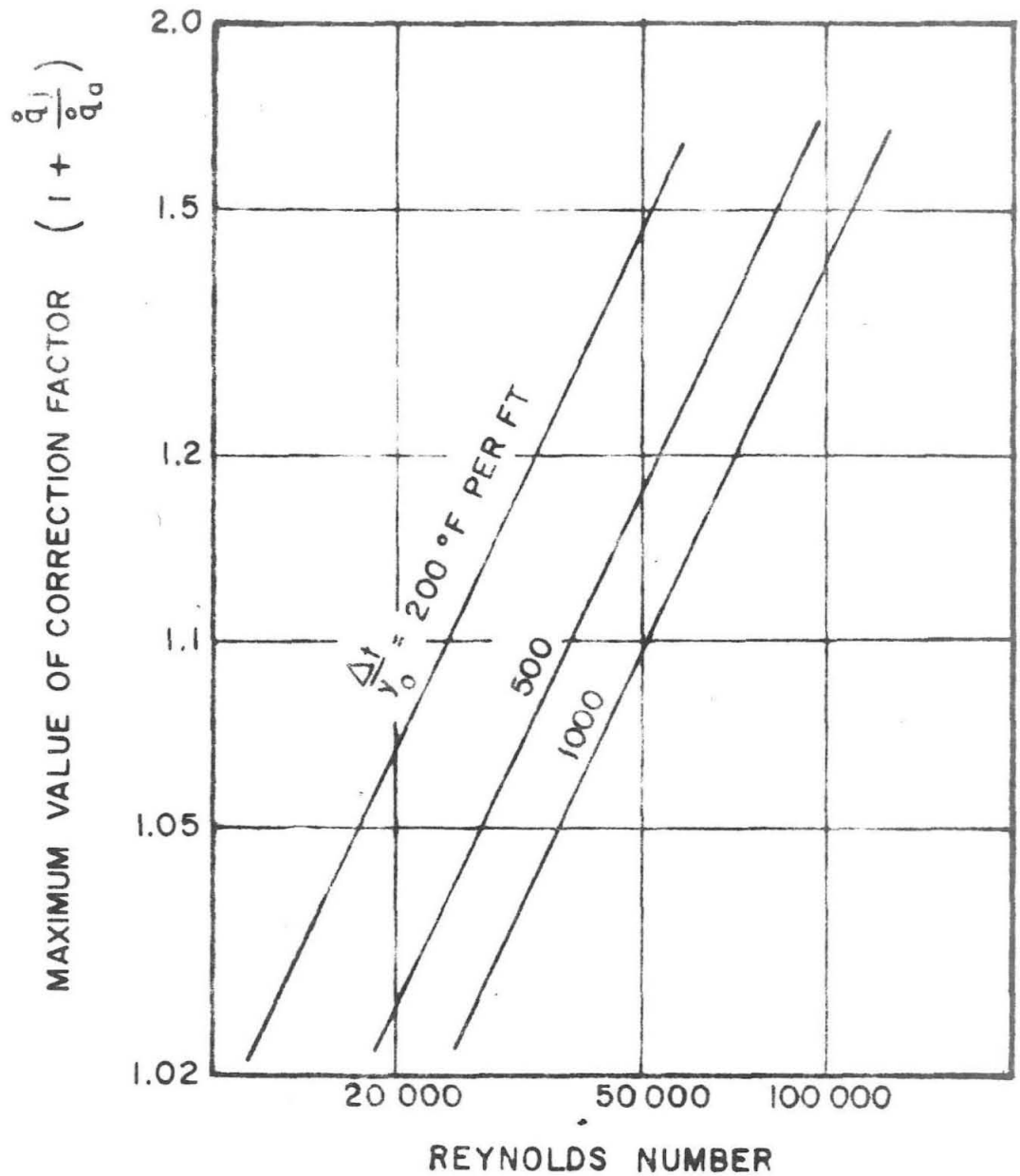

Figure 5: Effect of Reynolds Number on the Maximum Correction Factor

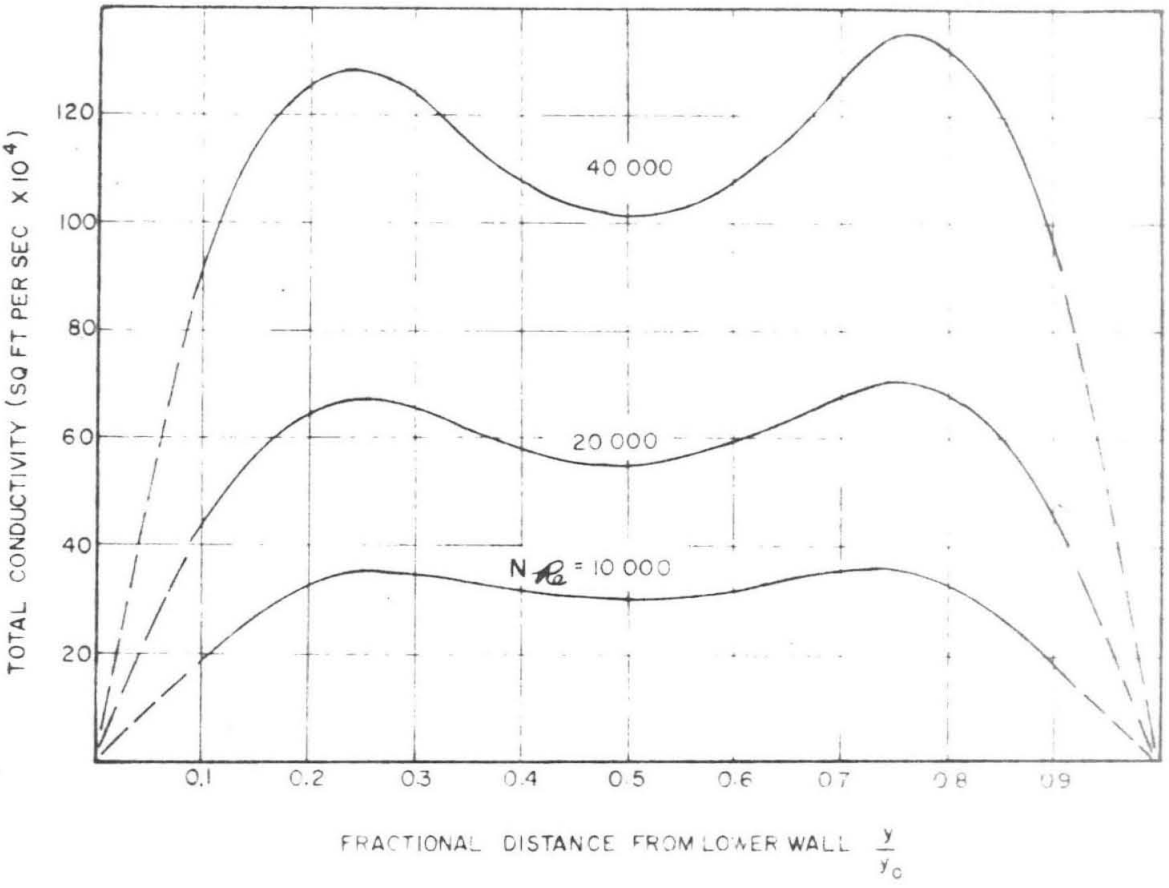

Figure 6: Smooth Values of the Corrected Total Conductivity

Values of the total conductivity parameter $\frac{\epsilon_c}{\kappa}\frac{\ell_o}{\ell}$ corrected for viscous dissipation are given in Table V. Figure 7 shows the effect of the distance parameter on the total conductivity parameter at the upper and lower wall. The full curve shows the line of best fit to the data corrected for viscous dissipation, and the dashed curves represent the line of best fit to the uncorrected data (11). Data for both upper and lower walls is shown in fig. 8. The corrected and uncorrected data are represented by the full and dashed curve, respectively. Table VI records the coordinates of the lines of best fit to the corrected data, and the standard error of estimate of the experimental points from these lines.

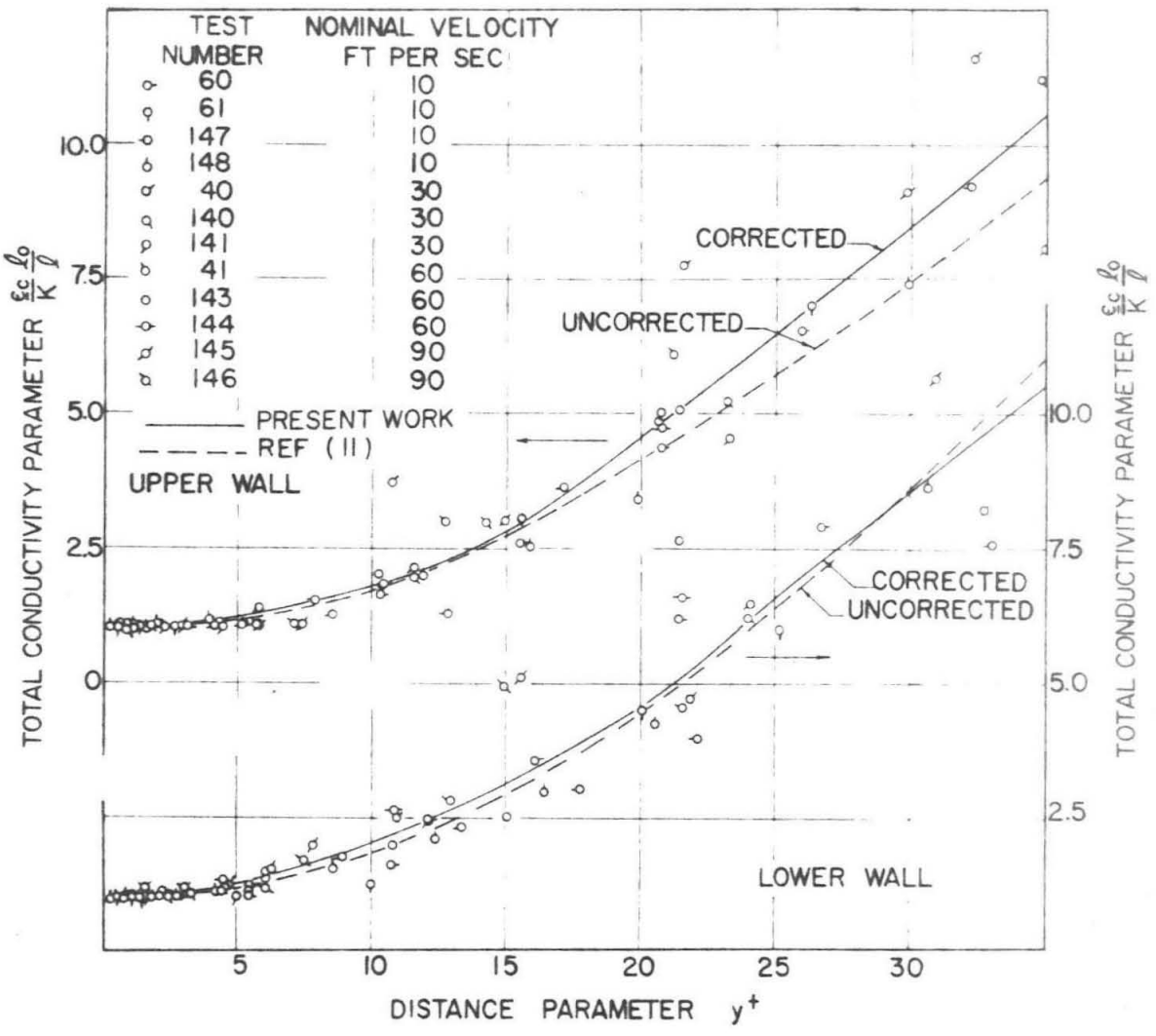

Figure 7: Total Conductivity Parameter Near the Upper and Lower Walls

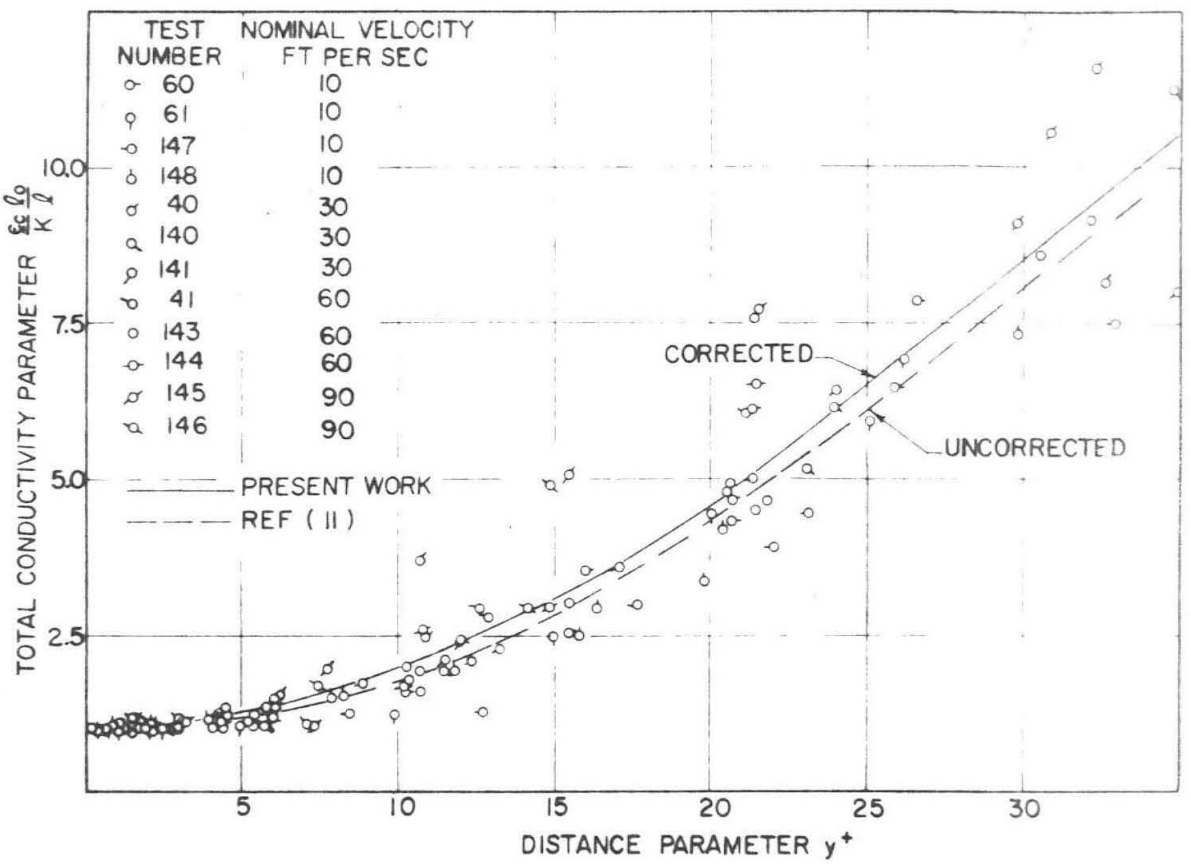

Figure 8: Total Conductivity Parameter Near a Wall

DISCUSSION OF RESULTS

Effect of the Correction on the Total Conductivity

The effect of the correction on the total conductivity can be seen most easily by comparing the two parts of fig. 9. The upper part of the figure shows results obtained at Reynolds number of about 54, 000 by neglecting the effect of dissipation on the heat flux. The total conductivity appears to be a function of temperature gradient as well as position, since the data at the average temperature gradients of 200 and 1000 ^{o}F/ft. differ by about 30%, which is larger than the experimental uncertainty of 7% estimated from uncertainties in the individual measurements (2, 3, 5, 6). The corrected values are shown in the lower part of the figure, in this case no clear relation exists between the total conductivity and the temperature gradient. Neither corrected nor uncorrected values of the total conductivity appear to be symmetric about the centerline of the channel, although the lack of symmetry is less marked for the corrected results.

In order to obtain a definite measure of the average temperature gradient on the values of the total conductivity, a complete variance analysis (24) would be desirable, but unfortunately the data available is not sufficient for such an analysis. Nonetheless, it is possible to obtain a measure of the significance of the trends by making some assumptions. Tests 196 and 197 are replicates of Tests 32 and 33, respectively, as regards to Reynolds numbers, and these four tests are at essentially the same average temperature gradient. These tests

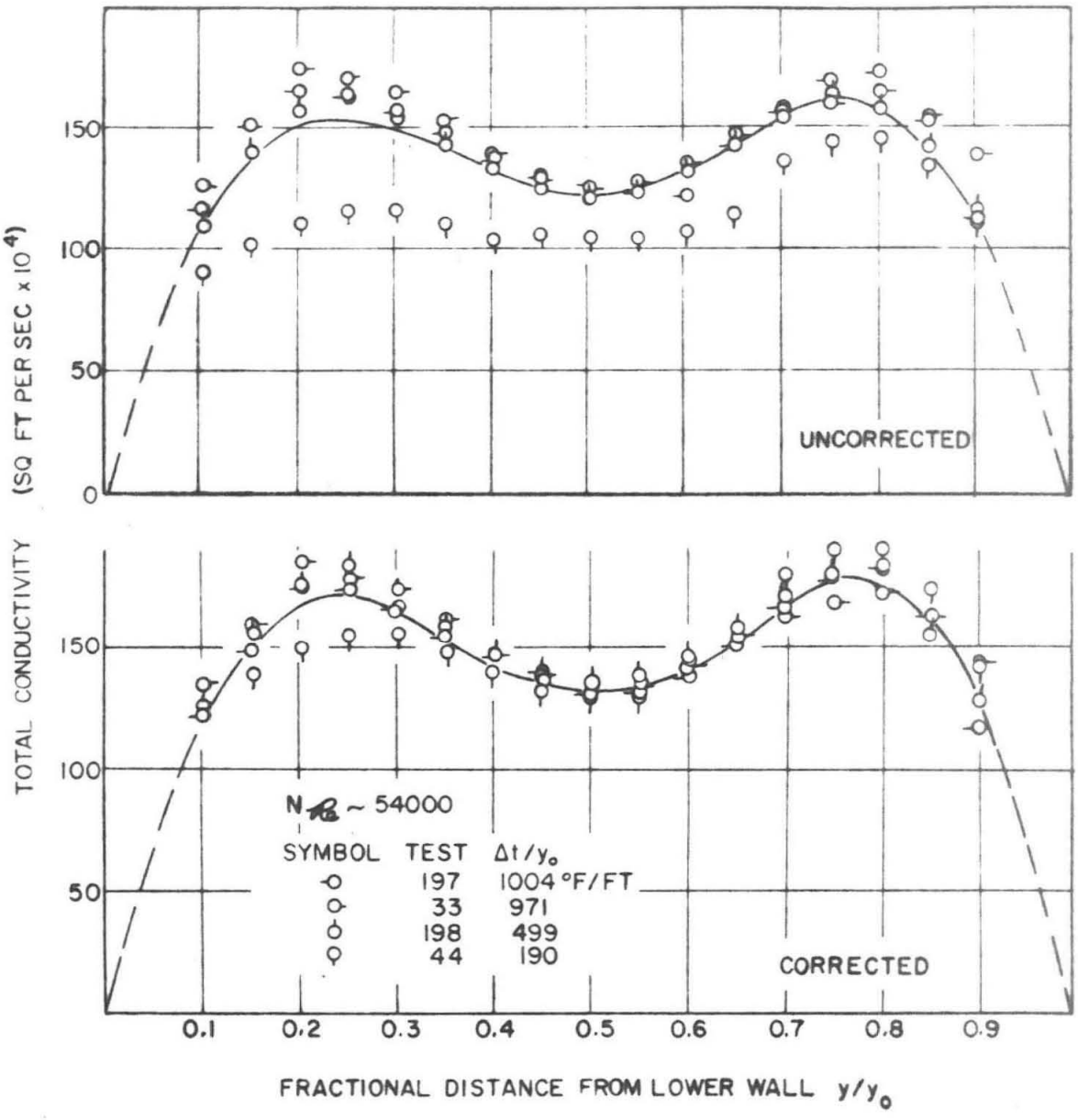

Figure 9: Typical Experimental Values of the Total Conductivity

were therefore used to determine the significance of asymmetry and it was found that at the temperature gradient of about 1000 ^{o}F/ft. the asymmetry was not significant for either corrected or uncorrected values of the total conductivity. The data, however, is not sufficient to establish whether this result is applicable at lower temperature gradients.

Since asymmetry is not significant at high temperature gradients, and since the previous analysis indicates that the correction is nearly constant near the center of the channel, it is reasonable to assume that this effect is absent near the center of the channel. Making this assumption, it is possible to obtain a variance analysis by considering values of the total conductivity at $y/y_o = 0.40$ and $y/y_o = 0.60$ as replicates. Such an analysis was performed, and it indicated that the effect of temperature gradient is significant about the 1% level in the uncorrected results, but is not significant in the corrected results. Thus the qualitative observations mentioned earlier are confirmed by this analysis.

In view of the foregoing discussion, it is of interest to eliminate the asymmetry from the smooth values reported. For this reason, Table VII and fig. 10, containing smooth, symmetrical values of the total conductivity corrected for viscous dissipations are included.

Comments on Reynolds' Analogy

It is of interest to determine the validity of Reynolds' analogy, as defined by equation 6, and of the modified Reynolds' analogy defined in equation 5 in view of the corrections for viscous dissipation. Figure 11

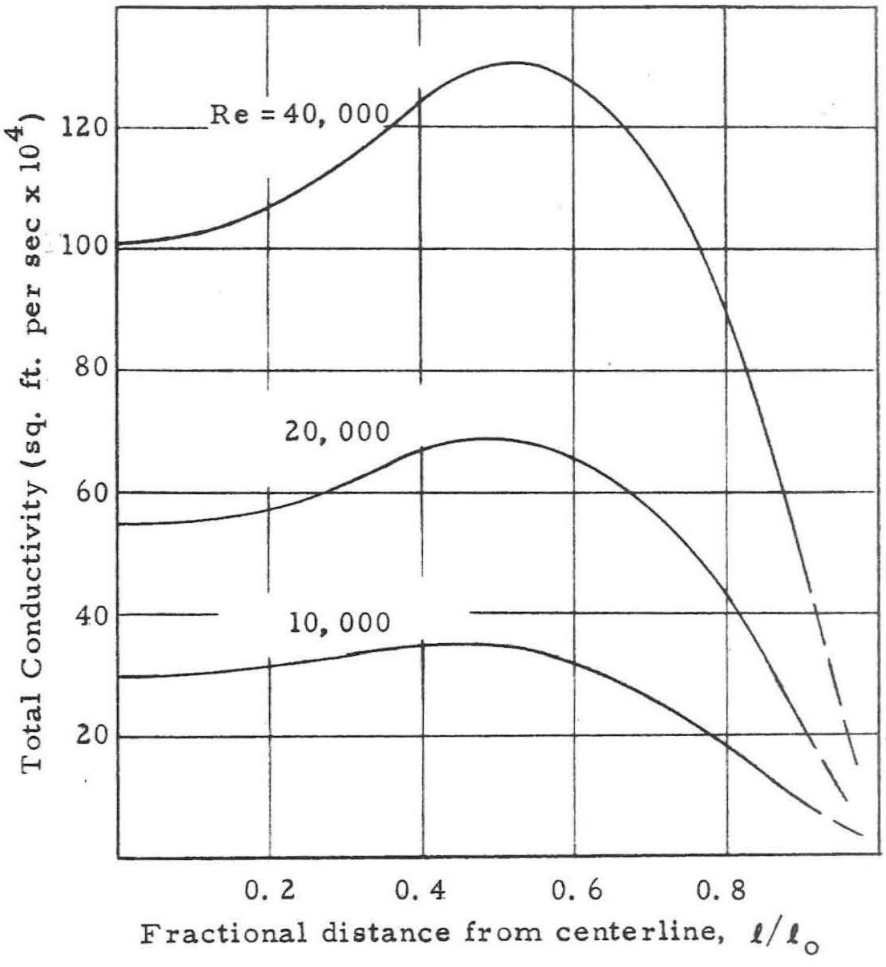

Figure 10: Smooth, Symmetrical Values of the Corrected Total Conductivity

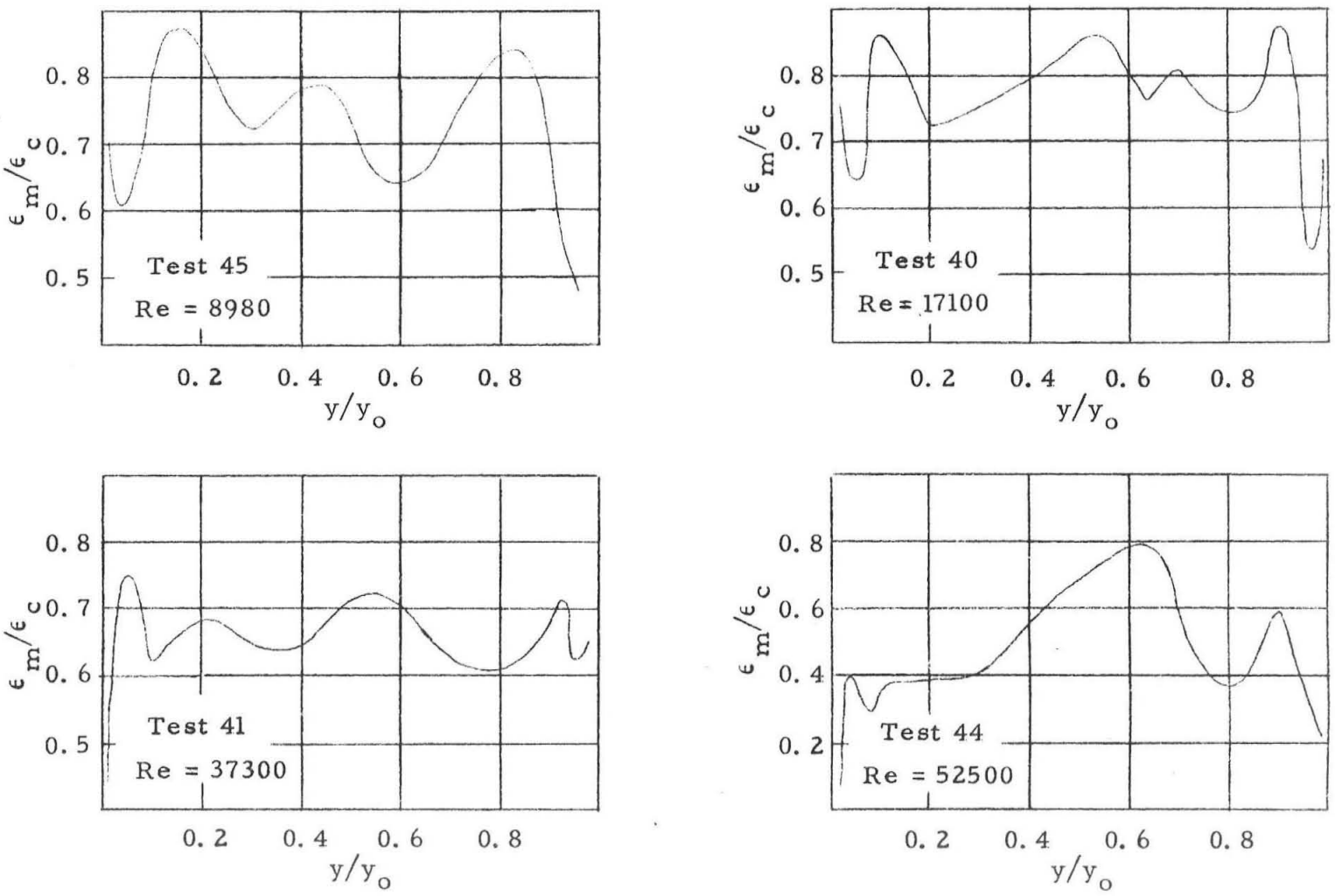

Figure 11: Dependence of the Eddy Prandtl Number on Reynolds Number and Position

depicts the ratio of the eddy viscosity to the eddy conductivity corrected for viscous dissipation, the ratio is given as a function of the position, for four Reynolds numbers, and at a temperature gradient of about 200 ^{o}F/ft. In the preparation of this figure data of Page (5) was used in addition to data presented in this work.

The eddy Prandtl number

$$Pr_{\epsilon} = \frac{\epsilon_m}{\epsilon_c} \tag{33}$$

varies appreciably with position, and appears to vary somewhat with Reynolds number. Figure 12 shows the average value of the eddy Prandtl number as a function of the reciprocal of the Reynolds number. This average was defined by the equation

$$(Pr_{\epsilon})_{ave} = \frac{1}{0.9} \int_{0.05}^{0.95} \frac{\epsilon_m}{\epsilon_c} \, d\left(\frac{y}{y_o}\right) \tag{34}$$

This somewhat arbitrary definition was necessary because the uncertainty in the ratio becomes very large as the walls are approached, and the ratio is indeterminate at the wall. This figure indicates that the eddy Prandtl number does not vary in a systematic way with Reynolds number, and for all the measurements considered is within 10% of the molecular Prandtl number. This is probably within the experimental uncertainty of the measurements.

It therefore appears that although the eddy Prandtl number varies with position in the channel, on the average it satisfies the equation

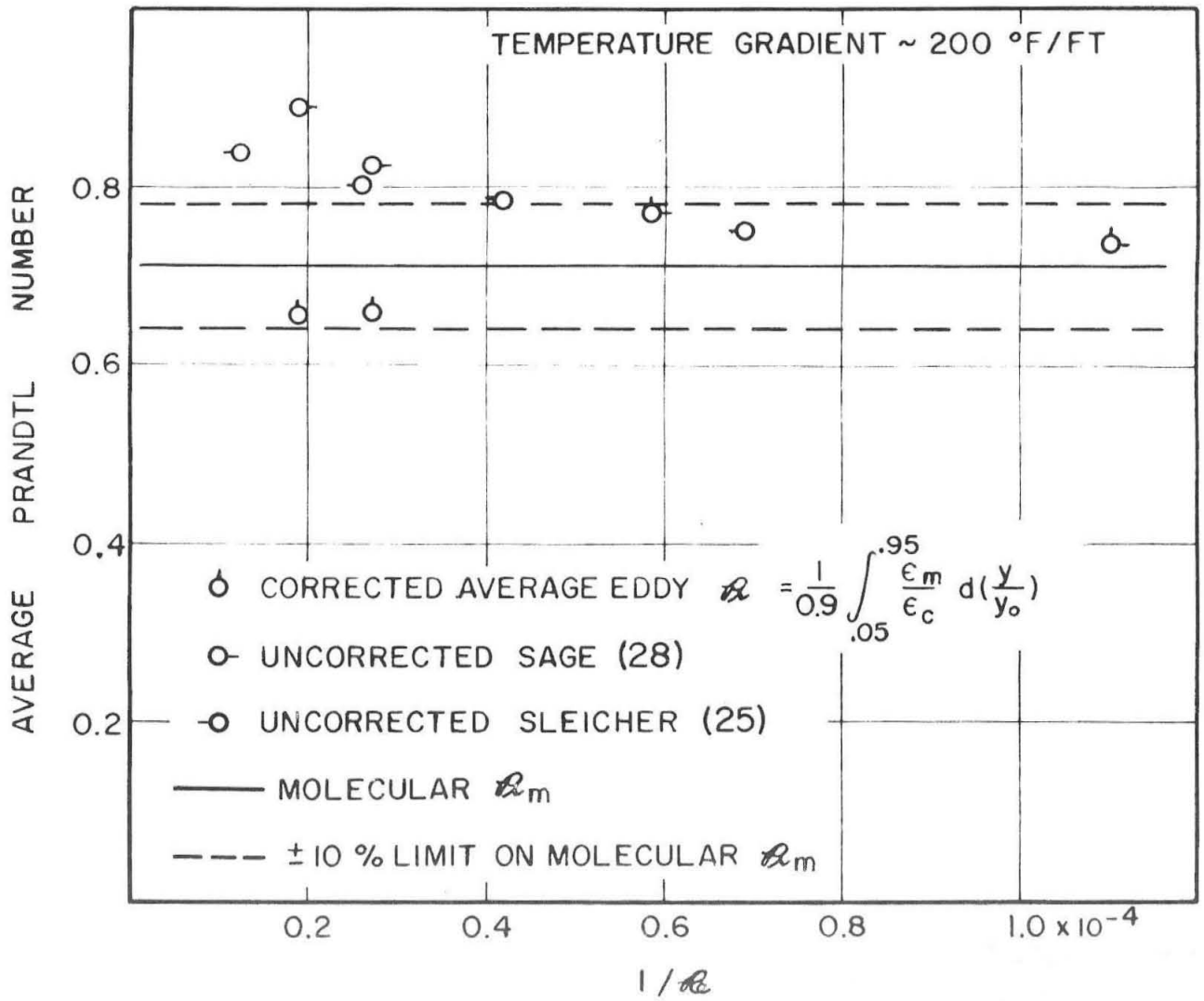

Figure 12: Effect of Reynolds Number on the Average Eddy Prandtl Number

$$(Pr_\epsilon)_{ave} = Pr_m \tag{35}$$

Approximate values of the average eddy Prandtl number obtained from the data of Sleicher (25) for flow of air through a pipe are also shown in fig. 12, and appear to contradict these conclusions. This discrepancy is probably due to the fact that Sleicher neglected the effect of viscous dissipation in calculating the eddy conductivity, this assumption leads to a calculated average eddy Prandtl number which increases with increasing Reynolds number (28).

Equation 35 is probably applicable to gases in general, but should not be applied to systems whose molecular Prandtl number differs appreciably from unity. The data of Isakoff and Drew (26) and of Brown, Amstead, and Short (27) indicates that for mercury at Reynolds numbers of the order of 500,000 the eddy Prandtl number decreases toward unity and is not independent of Reynolds number.

CONCLUSIONS

The total conductivity based on the local heat flux has been shown to be independent of the average temperature gradient, to within experimental error. On the other hand, the values of total conductivity obtained from the experimental data by neglecting the effect of viscous dissipation depend on the average temperature gradient.

In practical applications, therefore, the total conductivity may be considered as a function of position and of Reynolds number and the heat flux may be evaluated with due consideration to viscous dissipation. However, when temperature fields are to be calculated under conditions which closely resemble the experimental ones, it is probably easier to regard the heat flux as constant and to use values of the total conductivity computed without regard to viscous dissipation effects, but giving due consideration to the dependence of these values on the average temperature gradient.

At Reynolds numbers between 9, 000 and 50, 000, the data indicates that the eddy Prandtl number varies with position in the channel, but on the average this quantity is independent of Reynolds number to within 10%. Under these conditions, the average value of the eddy Prandtl number for air may be considered equal to the molecular Prandtl number to within experimental error.

REFERENCES

1. Corcoran, W. H., Roudebush, B., and Sage, B. H., Chem. Eng. Progr., 43, 135, (1947).

2. Billman, G. W., Ph. D. Thesis, California Institute of Technology, Pasadena (1948).

3. Corcoran, W. H., Ph. D. Thesis, California Institute of Technology, Pasadena (1948).

4. Mason, J. L., Ph. D. Thesis, California Institute of Technology, Pasadena (1950).

5. Page, F., Jr., Ph. D. Thesis, California Institute of Technology, Pasadena (1950).

6. Cavers, S. D., Ph. D. Thesis, California Institute of Technology, Pasadena (1951).

7. Corcoran, W. H., Page, F., Jr., Schlinger, W. G., and Sage, B. H., Ind. Eng. Chem., 44, 410 (1952).

8. Page, F., Jr., Corcoran, W. H., Schlinger, W. G., and Sage, B. H., Ind. Eng. Chem., 44, 419 (1952).

9. Page, F., Jr., Schlinger, W. G., Breaux, D. K. and Sage, B. H., Ind. Eng. Chem., 44, 424, (1952).

10. Schlinger, W. G., Hsu, N. T., Cavers, S. D., and Sage, B. H., Ind. Eng. Chem., 45, 864, (1953).

11. Cavers, S. D., Hsu, N. T., Schlinger, W. G., and Sage, B. H., Ind. Eng. Chem., 45, 2139, (1953).

12. Corcoran, W. H. and Sage, B. H., A. I. Ch. E. Journal, 2, 251, (1956).

13. Reynolds, O. S., Mem. Proc. Manchester Lit. and Phil. Soc., 14, 7, (1874).

14. Karman, Th. von, Trans. Am. Soc. Mech. Engrs., 61, 705, (1939).

15. Boelter, L. M. K., Martinelli, R. C., and Jonassen, F., Trans. Am. Soc. Mech. Engrs., 63, 447, (1941).

16. Martinelli, R. C., Trans. A. S. M. E., 69, 947, (1947).

17. Longwell, P. A., Mechanics of Fluid Flow, Department of Chemical Engineering, California Institute of Technology, Pasadena (1958).

18. Bird, R. B., Stewart, W. E., and Lightfoot, E. N., Transport Phenomena, John Wiley and Sons, New York, (1960).

19. Ferrari, C., "Turbolenza di Parete," in Corso sulla Teoria della Turbolenza, vol. 1, p. 171, Edizioni Cremonese, Roma, (1958).

20. Hinze, J. O., Turbulence, McGraw-Hill Book Co., Inc., New York (1959).

21. Laufer, J., N. A. C. A. Report 1053 (1951).

22. Laufer, J., N. A. C. A. Report 1174 (1954).

23. Townsend, A. A., The Structure of Turbulent Shear Flow, University Press, Cambridge (1956).

24. Mickley, H. S., Sherwood, T. K., and Reed, C. E., Applied Mathematics in Chemical Engineering, McGraw-Hill Book Co., Inc., New York (1957).

25. Sleicher, C. A., Jr., Trans. A. S. M. E., 80, 693, (1958).

26. Isakoff, S. E. and Drew, T. C., General Discussion of Heat Transfer, The Institution of Mechanical Engineers, (London), 405 (1951).

27. Brown, H. E., Amstead, B. H. and Short, B. E., Trans. A. S. M. E., 79, 279, (1957).

28. Schlinger, W. G., Berry, V. J., Jr., Mason, J. L., and Sage, B. H., Ind. Eng. Chem., 45, 662 (1953).

NOMENCLATURE

Roman Symbols

C_p	isobaric heat capacity, Btu/(lb.)(^oF)
f	a function
ℓ	distance from centerline, ft.
ℓ_o	distance from centerline to wall, ft.
N	number of experimental points
$\dot{q}$	thermal flux, Btu/(sq. ft.)(sec.)
$\dot{q}_j$	local thermal flux increase due to viscous dissipation, Btu/(sq. ft.)(sec.)
P	pressure, lb./sq. ft.
Pr_m	molecular Prandtl number = ν/κ
Pr_ϵ	eddy Prandtl number = ϵ_m/ϵ_c
$(Pr_\epsilon)_{avg}$	average eddy Prandtl number, defined in equation 34
Re	Reynolds number
t	temperature, ^oF
Δt	temperature difference between the plates, ^oF
u	instantaneous local velocity, ft./sec.
u_*	friction velocity = $(\tau_o/\rho)^{1/2}$
x	Cartesian coordinate along the axis of stream, ft.
y	Cartesian coordinate normal to wall, measured from the lower wall, ft.
y^+	distance parameter
y_o	separation between plates, ft.
z	Cartesian coordinate parallel to wall and normal to axis of stream, ft.

Greek Symbols

γ	a constant
ϵ_c	eddy conductivity, sq. ft./sec.
$\underline{\epsilon}_c$	total conductivity, sq. ft./sec.
ϵ_m	eddy viscosity, sq. ft./sec.
$\underline{\epsilon}_m$	total viscosity, sq. ft./sec.
η	molecular viscosity, lb. sec./ft.^{2}
κ	thermometric conductivity, sq. ft./sec.
ν	kinematic viscosity, sq. ft./sec.
ρ	density, lb. sec.^{2}/ft.^{4}
σ	specific weight, lb./cu. ft.
σ_e	standard error of estimate defined in equation
τ	shear stress, lb./ft.^{2}
τ_o	shear at the wall, lb./ft.^{2}
ϕ	dissipation function, Btu/(cu. ft.)(sec.)
ψ	turbulent energy transport function, defined in equation 11

Subscripts

a	at upper plate
b	at lower plate
exp	experimental value
i, k	dummy variables
sm	smooth value
x	in x direction
y	in y direction
z	in z direction

Superscripts

$\bar{}$	time-averaged value
$'$	fluctuating component, difference between instantaneous value and time-averaged value
$*$	value uncorrected for viscous dissipation

TABLE I. EXPERIMENTAL CONDITIONS

Quantity	Test Numbers			
	32	33	40	41
Distance between plates, ft.	0.0626	0.0618	0.0571	0.0568
Traverse location, ft	10.3	10.3	12.7	12.7
Incoming air temperature, ^{o}F.	100.0	100.0	100.0	100.0
Upper plate temperature, ^{o}F.	130.0	130.0	104.2	105.1
Lower plate temperature, ^{o}F.	70.0	70.0	95.0	94.6
Gross velocity, ft/sec.	54.2	79.2	28.13	60.96
Reynolds number	36400	52900	17100	37300
Thermal flux, Btu/(sq.ft.)(sec.)	0.0865	0.116	0.00732	0.0126
Weight fraction water	0.0088	0.0088	0.014	0.0081
Pressure at traverse location, lb./sq.in.	14.381	14.336	14.252	14.297
Pressure gradient, lb./cu.ft.	-0.59	-1.18	-0.227	-0.835
Average temperature gradient, ^{o}F/ft.	958	971	161	185

TABLE I. (Continued)

Quantity	Test Numbers			
	44	60	61	140
Distance between plates, ft.	0.0564	0.05725	0.05708	0.05758
Traverse location, ft.	12.7	12.5	12.5	8.1
Incoming air temperature, ^{o}F.	100.0	100.0	100.0	100.0
Upper plate temperature, ^{o}F.	105.1	114.98	85.29	114.96
Lower plate temperature, ^{o}F.	94.4	85.31	114.49	85.03
Gross velocity, ft./sec.	88.43	13.1	12.6	30.0
Reynolds number	52500	8122	7754	18578
Thermal flux, Btu/(sq. ft.)(sec.)	0.0156	0.0113	0.0107	0.0242
Weight fraction water	0.0139	0.0115	0.0145	0.0110
Pressure at traverse location, lb./sq. in.	14.108	14.374	14.308	14.260
Pressure gradient, lb./cu. ft.	-1.629	-0.0515	-0.0488	-0.2517
Average temperature gradient, ^{o}F/ft.	190	518	-512	520

TABLE I. (Continued)

Quantity	Test Numbers			
	141	143	144	145
Distance between plates, ft.	0.05825	0.05825	0.05750	0.05750
Traverse location, ft.	12.5	12.5	8.1	8.1
Incoming air temperature, ^{o}F.	100.0	100.0	100.0	100.0
Upper plate temperature, ^{o}F.	115.04	115.04	114.95	115.04
Lower plate temperature, ^{o}F.	84.82	84.85	85.03	85.15
Gross velocity, ft./sec.	30.0	57.6	60.2	91.3
Reynolds number	18821	36115	37528	56689
Thermal flux, Btu/(sq.ft.)(sec.)	0.0243	0.0411	0.0421	0.0558
Weight fraction water	0.0129	0.0095	0.0109	0.0110
Pressure at traverse location, lb./sq.in.	14.285	14.286	14.389	14.332
Pressure gradient, lb./cu.ft.	-0.2453	-0.7759	-0.8215	-1.685
Average temperature gradient, ^{o}F/ft.	519	518	520	520

TABLE I. (Continued)

Quantity	Test Numbers			
	146	147	148	195
Distance between plates, ft.	0.05815	0.05833	0.05833	0.05983
Traverse location, ft.	12.5	12.5	8.1	10.6
Incoming air temperature, ^{o}F.	100.0	100.0	100.0	100.0
Upper plate temperature, ^{o}F.	115.07	114.88	114.87	129.98
Lower plate temperature, ^{o}F.	85.53	85.04	85.10	70.02
Gross velocity, ft./sec.	86.8	10.4	9.8	27.6
Reynolds number	54680	6611	6069	17766
Thermal flux, Btu/(sq. ft.)(sec.)	0.0537	0.00934	0.00901	0.0438
Weight fraction water	0.0089	0.0087	0.0096	0.0094
Pressure at traverse location, lb./sq. in.	14.378	14.319	14.337	14.250
Pressure gradient, lb./cu. ft.	-1.514	-0.0331	-0.0293	-
Average temperature gradient, ^{o}F/ft.	508	512	510	1002

TABLE I. (Continued)

Quantity	Test Numbers			
	196	197	198	199
Distance between plates, ft.	0.06042	0.06000	0.06017	0.06042
Traverse location, ft.	10.6	10.6	10.6	10.6
Incoming air temperature, ^{o}F.	100.0	100.0	100.0	100.0
Upper plate temperature, ^{o}F.	130.02	130.24	115.00	115.00
Lower plate temperature, ^{o}F.	70.02	70.01	85.00	85.00
Gross velocity, ft./sec.	57.1	86.1	85.9	57.3
Reynolds number	37232	55657	55568	37476
Thermal flux, Btu/(sq. ft.)(sec.)	0.0767	0.1073	0.0525	0.0387
Weight fraction water	0.0103	0.0070	0.0080	0.0093
Pressure at traverse location, lb./sq. in.	14.270	14.252	14.243	14.319
Pressure gradient, lb./cu. ft.	-	-	-	-
Average temperature gradient, ^{o}F/ft.	993	1004	499	497

Table I. (Concluded)

Quantity	Test Numbers	
	200	201
Distance between plates, ft.	0.06050	0.05950
Traverse location, ft.	10.6	10.6
Incoming air temperature, °F.	100.0	100.0
Upper plate temperature, °F.	115.00	115.00
Lower plate temperature, °F.	85.00	85.00
Gross velocity, ft./sec.	28.2	9.5
Reynolds number	18342	6060
Thermal flux, Btu/(sq. ft.)(sec.)	0.0220	0.0085
Weight fraction water	0.0116	0.0120
Pressure at traverse location, lb./sq. in.	14.246	14.264
Pressure gradient, lb./cu. ft.	-	-
Average temperature gradient, °F/ft.	496	504

TABLE II. UNCORRECTED AND CORRECTED VALUES OF TOTAL CONDUCTIVITY

	Test 40			Test 200			Test 195		
y/y_o	$\underline{\epsilon}_c^* \times 10^4$ ft^2/sec	$1 + \frac{\dot{q}_j}{\dot{q}_a}$	$\underline{\epsilon}_c \times 10^4$ ft^2/sec	$\underline{\epsilon}_c^* \times 10^4$ ft^2/sec	$1 + \frac{\dot{q}_j}{\dot{q}_a}$	$\underline{\epsilon}_c \times 10^4$ ft^2/sec	$\underline{\epsilon}_c^* \times 10^4$ ft^2/sec	$1 + \frac{\dot{q}_j}{\dot{q}_a}$	$\underline{\epsilon}_c \times 10^4$ ft^2/sec
0.10	33.57	1.031	34.61	42.61	1.012	43.12	40.93	1.006	41.18
0.15	47.16	1.030	48.58	53.74	1.010	54.28	52.05	1.005	52.31
0.20	57.64	1.029	59.31	60.36	1.010	60.96	61.53	1.005	61.84
0.25	58.33	1.028	59.96	62.78	1.010	63.41	62.32	1.005	62.63
0.30	55.69	1.027	57.19	59.94	1.010	60.54	58.72	1.005	59.01
0.35	52.29	1.027	53.70	56.59	1.010	57.16	55.12	1.005	55.40
0.40	48.87	1.027	50.19	52.94	1.010	53.47	52.27	1.005	52.53
0.45	46.42	1.027	47.67	50.14	1.010	50.64	51.12	1.005	51.38
0.50	45.61	1.027	46.84	48.34	1.010	48.82	51.12	1.005	51.38
0.55	47.59	1.027	48.87	49.21	1.010	49.70	51.98	1.005	52.24
0.60	53.12	1.027	54.55	53.46	1.010	53.99	53.91	1.005	54.18
0.65	59.90	1.027	61.52	58.32	1.010	58.90	56.85	1.005	57.13
0.70	64.15	1.026	65.82	61.93	1.010	62.55	60.75	1.005	61.05
0.75	64.15	1.026	65.82	62.96	1.010	63.59	64.83	1.005	65.15
0.80	61.72	1.025	63.26	59.58	1.010	60.18	64.10	1.005	64.42
0.85	53.35	1.025	54.68	51.43	1.008	51.84	58.98	1.004	59.22
0.90	38.34	1.023	39.22	38.94	1.008	39.25	39.31	1.004	39.48

TABLE II. (Continued)

	Test 41			Test 199			Test 32		
y/y_o	$\epsilon_c^* \times 10^4$	$1 + \frac{\dot{q}_j}{\dot{q}_a}$	$\epsilon_c \times 10^4$	$\epsilon_c^* \times 10^4$	$1 + \frac{\dot{q}_j}{\dot{q}_a}$	$\epsilon_c \times 10^4$	$\epsilon_c^* \times 10^4$	$1 + \frac{\dot{q}_j}{\dot{q}_a}$	$\epsilon_c \times 10^4$
	ft^2/sec		ft^2/sec	ft^2/sec		ft^2/sec	ft^2/sec		ft^2/sec
0.10	70.38	1.161	81.71	70.32	1.056	74.26	92.41	1.026	94.80
0.15	87.05	1.153	100.4	99.07	1.053	104.3	103.16	1.025	105.7
0.20	93.67	1.149	107.6	110.14	1.051	115.8	114.80	1.024	117.6
0.25	94.58	1.146	108.4	114.67	1.050	120.4	129.00	1.023	132.0
0.30	91.62	1.143	104.7	112.06	1.050	117.7	117.49	1.023	120.2
0.35	88.30	1.142	100.8	103.08	1.049	108.1	112.37	1.023	115.0
0.40	86.51	1.141	98.71	95.06	1.049	99.7	98.86	1.023	101.1
0.45	85.95	1.141	98.03	90.19	1.049	94.6	88.03	1.023	90.0
0.50	86.27	1.141	98.43	89.09	1.049	93.5	94.94	1.023	97.1
0.55	87.90	1.141	100.3	90.10	1.049	94.5	98.67	1.023	100.9
0.60	90.50	1.141	103.3	92.74	1.049	97.3	104.04	1.023	106.4
0.65	94.51	1.140	107.7	98.18	1.048	102.9	107.18	1.022	109.5
0.70	98.67	1.139	109.8	110.07	1.048	115.4	111.52	1.022	114.0
0.75	100.96	1.136	114.7	120.95	1.047	126.60	146.20	1.022	149.4
0.80	99.84	1.133	113.1	116.81	1.046	122.2	124.10	1.021	126.7
0.85	93.67	1.128	105.6	105.53	1.044	110.2	117.47	1.021	119.9
0.90	71.91	1.121	80.61	86.60	1.042	90.2	92.98	1.019	94.75

TABLE II. (Continued)

	Test 196			Test 44			Test 198		
y/y_o	$\epsilon_c^* \times 10^4$ ft^2/sec	$1 + \frac{\dot{q}_j}{\dot{q}_a}$	$\epsilon_c \times 10^4$ ft^2/sec	$\epsilon_c^* \times 10^4$ ft^2/sec	$1 + \frac{\dot{q}_j}{\dot{q}_a}$	$\epsilon_c \times 10^4$ ft^2/sec	$\epsilon_c^* \times 10^4$ ft^2/sec	$1 + \frac{\dot{q}_j}{\dot{q}_a}$	$\epsilon_c \times 10^4$ ft^2/sec
0.10	75.34	1.028	77.4	90.06	1.369	123.3	110.02	1.117	122.9
0.15	98.27	1.027	100.9	102.22	1.354	138.4	140.29	1.112	156.0
0.20	109.72	1.026	112.6	110.67	1.344	148.7	158.17	1.109	175.4
0.25	115.54	1.025	118.4	115.72	1.338	154.8	164.15	1.107	181.7
0.30	111.81	1.025	114.6	116.41	1.334	155.3	155.38	1.106	171.8
0.35	101.78	1.025	104.3	110.55	1.331	147.1	142.84	1.105	157.8
0.40	95.82	1.025	98.2	104.56	1.330	139.1	132.75	1.104	146.6
0.45	92.47	1.024	94.7	105.69	1.330	140.6	125.52	1.104	138.6
0.50	90.78	1.024	93.0	104.91	1.330	139.5	122.26	1.104	135.0
0.55	90.77	1.024	93.0	104.56	1.329	139.0	124.59	1.104	137.6
0.60	92.73	1.024	95.0	108.11	1.328	143.6	132.06	1.104	145.8
0.65	98.28	1.024	100.6	114.62	1.327	152.1	143.29	1.103	158.0
0.70	108.44	1.024	111.0	135.88	1.324	179.9	154.64	1.103	170.6
0.75	116.72	1.024	119.5	143.77	1.319	189.6	162.73	1.101	179.2
0.80	116.27	1.023	118.9	144.98	1.312	190.2	158.04	1.099	173.7
0.85	109.69	1.022	112.1	133.57	1.301	173.8	141.64	1.095	155.10
0.90	80.57	1.021	82.26	111.27	1.284	142.9	117.05	1.090	127.6

TABLE II. (Concluded)

	Test 33			Test 197		
y/y_o	$\epsilon_c^* \times 10^4$ ft^2/sec	$1 + \frac{\dot{q}_j}{\dot{q}_a}$	$\epsilon_c \times 10^4$ ft^2/sec	$\epsilon_c^* \times 10^4$ ft^2/sec	$1 + \frac{\dot{q}_j}{\dot{q}_a}$	$\epsilon_c \times 10^4$ ft^2/sec
0.10	127.3	1.054	134.2	116.78	1.057	123.4
0.15	150.7	1.052	158.5	150.80	1.055	158.9
0.20	175.1	1.051	184.0	164.88	1.053	173.6
0.25	169.9	1.050	178.4	164.36	1.052	172.9
0.30	164.8	1.049	172.9	157.38	1.052	165.5
0.35	153.2	1.049	160.7	147.88	1.052	155.4
0.40	139.5	1.049	145.9	138.00	1.051	145.0
0.45	130.1	1.049	136.5	131.00	1.051	137.7
0.50	125.6	1.049	131.8	125.71	1.051	132.1
0.55	127.6	1.049	133.8	123.89	1.051	130.2
0.60	134.8	1.048	141.3	131.82	1.051	138.1
0.65	146.5	1.048	153.5	144.17	1.050	151.4
0.70	156.7	1.048	164.2	158.21	1.050	166.1
0.75	161.3	1.047	168.9	169.23	1.049	177.6
0.80	164.7	1.046	172.3	172.97	1.048	181.3
0.85	155.3	1.044	162.1	154.24	1.046	161.4
0.90	139.2	1.042	145.0	112.27	1.044	117.2

TABLE III. SMOOTH VALUES OF THE TOTAL CONDUCTIVITY[a] CORRECTED FOR VISCOUS DISSIPATION

y/y_o	Reynolds Number						
	10,000	15,000	20,000	30,000	40,000	50,000	60,000
0.10	18.4×10^{-4}	31.0×10^{-4}	43.4×10^{-4}	67.0×10^{-4}	90.0×10^{-4}	112.5×10^{-4}	134.9×10^{-4}
0.15	26.3	41.4	56.4	84.6	112.2	139.1	166.0
0.20	32.2	46.6	64.8	95.4	125.3	154.5	183.6
0.25	35.0	51.5	67.7	98.4	128.5	157.7	187.0
0.30	34.2	50.0	65.6	94.9	123.7	151.8	179.8
0.35	33.0	47.6	62.0	89.1	115.7	141.7	167.6
0.40	31.6	45.0	58.2	83.2	107.6	131.4	155.2
0.45	30.4	43.2	55.8	79.6	103.0	125.7	148.4
0.50	30.4	42.9	55.3	78.6	101.5	123.8	146.0
0.55	31.2	43.8	56.2	79.6	102.5	124.9	147.2
0.60	32.8	45.9	58.9	83.5	107.5	130.9	154.3
0.65	34.4	48.6	62.6	89.1	115.1	140.4	165.7
0.70	35.2	51.2	67.0	96.8	125.9	154.3	182.7
0.75	36.0	53.4	70.6	103.0	134.7	165.6	196.4
0.80	32.5	50.0	67.4	100.0	132.0	163.1	194.3
0.85	27.4	43.8	60.0	90.6	120.5	149.6	178.7
0.90	18.0	31.7	45.3	70.8	95.9	120.3	144.7

[a] Total conductivity expressed in sq. ft. /sec.

TABLE IV. STANDARD ERROR OF ESTIMATE OF THE DATA CORRECTED FOR VISCOUS DISSIPATION FROM THE SMOOTH RESULTS

Test	$\sigma_e \times 10^4$ ft^2/sec
40	4.14
200	2.23
195	2.30
41	10.92
199	6.12
32	8.40
196	7.14
44	11.15
198	7.12
33	3.25
197	6.48

TABLE V. CORRECTED VALUES OF THE TOTAL CONDUCTIVITY PARAMETER, $\frac{\epsilon_c}{\kappa}\frac{\ell_o}{\ell}$

	Upper Wall		Lower Wall	
	y^+	$\frac{\epsilon_c}{\kappa}\frac{\ell_o}{\ell}$	y^+	$\frac{\epsilon_c}{\kappa}\frac{\ell_o}{\ell}$
Test 60	0.25	1.00	0.27	1.00
	0.51	1.00	0.54	1.00
	0.76	1.01	0.81	1.01
	1.02	1.01	1.08	1.01
	1.27	1.01	1.35	1.01
	2.20	1.02	2.70	1.02
	5.10	1.05	5.38	1.04
	10.26	1.61	10.70	1.60
	15.46	2.56	16.00	3.52
	20.67	4.33	21.31	6.13
	25.87	6.48	26.60	7.86
Test 61	0.26	1.00	0.25	1.00
	0.52	1.00	0.49	1.00
	0.79	1.01	0.74	1.01
	1.05	1.01	0.98	1.01
	1.31	1.01	1.23	1.01
	2.61	1.02	2.46	1.02
	5.21	1.11	4.94	1.04
	10.36	1.78	9.93	1.24
	15.49	3.01	14.96	2.48
	20.62	4.95	20.00	4.46
	26.19	6.94	25.04	5.93

TABLE V. (Continued)

	Upper Wall		Lower Wall	
	y^+	$\frac{\epsilon_c}{K}\frac{\ell_o}{\ell}$	y^+	$\frac{\epsilon_c}{K}\frac{\ell_o}{\ell}$
Test 147	0.21	1.00	0.22	1.00
	0.40	1.00	0.43	1.00
	0.63	1.01	0.67	1.01
	0.84	1.01	0.89	1.02
	1.05	1.01	1.12	1.02
	2.10	1.02	2.23	1.08
	4.21	1.05	4.46	1.34
	8.47	1.24	8.87	1.73
	12.76	1.86	13.26	2.28
	17.05	3.60	17.64	2.96
	21.35	5.01	22.01	3.94
	32.13	9.19	32.90	7.50
Test 148	0.19	1.00	0.21	1.00
	0.38	1.00	0.40	1.00
	0.58	1.01	0.62	1.00
	0.78	1.01	0.83	1.01
	0.97	1.02	1.04	1.01
	1.95	1.06	2.07	1.02
	3.92	1.15	4.14	1.12
	7.85	1.50	8.25	1.53
	11.83	1.94	12.30	2.08
	15.80	2.50	16.36	2.93
	19.80	3.36	20.41	4.21
	29.80	7.35	30.52	8.59

TABLE V. (Continued)

	Upper Wall		Lower Wall	
	y^+	$\frac{\epsilon_c}{\kappa}\frac{\ell_o}{\ell}$	y^+	$\frac{\epsilon_c}{\kappa}\frac{\ell_o}{\ell}$
Test 40	10.72	3.71	10.88	2.49
	21.47	7.70	21.73	4.67
	32.24	11.59	32.60	8.16
Test 140	0.57	1.00	-	-
	1.14	1.01	1.21	1.01
	1.71	1.01	1.82	1.02
	2.28	1.01	2.42	1.03
	2.85	1.01	5.02	1.06
	5.72	1.05	6.03	1.49
	11.50	1.92	12.01	2.43
	23.10	5.19	23.92	6.15
	34.74	11.25	-	-
Test 141	0.57	1.00	0.61	1.01
	1.14	1.01	1.22	1.01
	1.71	1.01	1.82	1.02
	2.29	1.01	2.43	1.03
	2.86	1.01	3.04	1.07
	5.74	1.35	6.06	1.34
	11.52	2.10	12.06	2.36
	23.17	4.47	24.85	6.43
	34.85	8.02	-	-

TABLE V. (Continued)

	Upper Wall		Lower Wall	
	y^+	$\frac{\epsilon_c}{\kappa}\frac{\ell_o}{\ell}$	y^+	$\frac{\epsilon_c}{\kappa}\frac{\ell_o}{\ell}$
Test 41	12.66	2.94	12.86	2.77
	21.13	6.07	21.44	4.50
Test 143	1.01	1.01	1.08	1.08
	2.03	1.01	2.16	1.09
	3.05	1.03	3.24	1.09
	4.07	1.04	4.31	1.10
	5.10	1.06	5.39	1.12
	10.24	1.99	10.73	1.94
	20.57	4.81	21.36	7.58
Test 144	1.02	1.01	1.09	1.08
	2.04	1.01	2.17	1.09
	3.07	1.02	3.26	1.08
	4.10	1.04	4.34	1.10
	5.13	1.05	5.41	1.22
	10.31	1.73	10.79	2.60
	20.70	4.68	21.49	6.52

TABLE V. (Concluded)

	Upper Wall		Lower Wall	
	y^+	$\frac{\epsilon_c}{\kappa}\frac{\ell_o}{\ell}$	y^+	$\frac{\epsilon_c}{\kappa}\frac{\ell_o}{\ell}$
Test 145	1.46	1.01	1.56	1.18
	2.93	1.02	3.12	1.18
	4.41	1.03	4.67	1.23
	5.88	1.04	6.21	1.52
	7.36	1.06	7.75	1.96
	14.82	2.95	15.45	5.06
	29.74	9.11	30.82	10.58
Test 146	1.41	1.01	1.50	1.18
	2.82	1.02	3.00	1.18
	4.23	1.03	4.49	1.17
	5.65	1.04	5.98	1.19
	7.08	1.06	7.46	1.69
	14.15	2.94	14.87	4.92

TABLE VI. SMOOTH VALUES OF THE TOTAL CONDUCTIVITY PARAMETER, CORRECTED FOR VISCOUS DISSIPATION

Distance Parameter y^+	Total Conductivity Parameter		
	Upper Wall	Lower Wall	Mean
1.0	1.010	1.015	1.015
2.0	1.035	1.050	1.050
3.0	1.080	1.100	1.100
4.0	1.135	1.165	1.165
5.0	1.205	1.250	1.250
6.0	1.290	1.365	1.360
7.0	1.385	1.500	1.495
8.0	1.500	1.660	1.645
9.0	1.630	1.850	1.810
10.0	1.780	2.050	1.995
11.0	1.945	2.255	2.185
12.0	2.140	2.465	2.390
13.0	2.340	2.670	2.595
14.0	2.560	2.885	2.820
15.0	2.795	3.120	3.060
16.0	3.065	3.370	3.320
17.0	3.375	3.640	3.595
18.0	3.745	3.925	3.890
19.0	4.140	4.235	4.215
20.0	4.540	4.560	4.560
21.0	4.945	4.945	4.945
σ_e	0.5581	0.6021	0.5854

TABLE VII. SMOOTH, SYMMETRICAL VALUES OF THE TOTAL CONDUCTIVITY[a] CORRECTED FOR VISCOUS DISSIPATION

ℓ/ℓ_o	Reynolds Number						
	10,000	15,000	20,000	30,000	40,000	50,000	60,000
0.0	30.44×10^{-4}	42.94×10^{-4}	55.31×10^{-4}	78.65×10^{-4}	101.52×10^{-4}	123.77×10^{-4}	146.01×10^{-4}
0.1	30.82	43.48	56.00	79.62	102.76	125.28	147.78
0.2	32.18	45.46	58.57	83.34	107.60	131.20	154.80
0.3	33.68	48.07	62.30	89.14	115.40	141.04	166.62
0.4	34.72	50.58	66.26	95.84	124.84	153.04	181.23
0.5	35.54	52.44	69.14	100.69	131.59	161.65	191.71
0.6	32.40	49.34	66.09	97.70	128.68	158.80	188.94
0.7	26.88	42.62	58.19	87.58	116.36	144.36	172.36
0.8	18.17	31.34	44.35	68.92	92.98	116.39	139.80

[a]Total conductivity expressed in sq. ft. /sec.

PART II

THERMAL TRANSFER FROM SMALL WIRES IN THE BOUNDARY FLOW ABOUT A CYLINDER

INTRODUCTION

The problem of heat transfer from small wires is of particular interest because this transport phenomenon is the basis for the techniques of hot-wire anemometry (1, 2)*. The determination of temperature in regions of large temperature gradients also requires knowledge of the heat transfer from small wires (3, 4). Although the heat transfer from wires in boundary flows is of particular interest, no systematic research has been done on this problem, and it is usually assumed (1, 2) that the heat transfer from a wire is dependent only on the local velocity of the fluid stream.

It appears, however, that this assumption is not valid. Recent work on the boundary flow about spheres (3, 5) has indicated that such an assumption is not valid in three-dimensional flows, probably due to flow parallel to the wire axis induced by the three-dimensional gradients (3, 5). A mathematical model (6) predicts that in two-dimensional boundary flows the heat transfer from a wire will depend on the local velocity and on the ratio of the distance between the wire axis and the wall to the wire radius.

In order to gain some understanding of the phenomenon of heat transfer from small wires in boundary flows an investigation of the heat transfer from a 0.001-inch wire in the forward half of the boundary flow about a 1-inch diameter cylinder was undertaken. In this investigation the wire was maintained parallel to the axis of the cylinder, so as to

*Numbers in parentheses indicate references listed on page 120.

retain as much as possible the two-dimensional character of the flow. Furthermore, the cylinder was maintained at the same temperature as the air stream so the flow was nearly isothermal. It is hoped that the results of this study can serve as a basis for comparison for future work treating non-isothermal and three-dimensional flows, so that eventually some understanding of the problems involved may be obtained.

THEORY

The problem of convective heat transfer from bodies immersed in a fluid can be approached by considering the equations of continuity, momentum, and energy. These may be written respectively in the form:

$$\frac{D\sigma}{D\theta} = -\sigma \nabla \cdot \vec{u} \qquad (1)^*$$

$$\rho \frac{Du_i}{D\theta} = F_i - \frac{\partial P}{\partial x_i} + \sum_{j=1}^{3} \frac{\partial}{\partial x_i} \left[\eta \left(\frac{\partial u_i}{\partial x_j} + \frac{\partial u_j}{\partial x_i} - \frac{2}{3} \delta_{ij} \nabla \cdot \vec{u} \right) \right] \qquad (2)$$

$$i = 1, 2, 3$$

$$\sigma \left[\frac{DE}{D\theta} + P \frac{DV}{D\theta} \right] = - \nabla \cdot \dot{q} + \phi \qquad (3)$$

If these equations could be solved simultaneously for the boundary and initial conditions of the physical situation, and using the equations of state of the fluid under consideration, a complete description of heat transfer in boundary flows could be obtained. Solutions of this type are extremely difficult to obtain even when the differential equations are simplified and the properties of the fluid are expressed in terms of elementary functions of temperature and pressure.

It is possible, however, to obtain solutions to approximate equations of transport, and these are useful for purposes of comparison with experimental data. Since these solutions are discussed in detail in the literature, only the main results will be mentioned.

*Definitions of the symbols used are given on page 122.

Description of the Flow Field About a Cylinder

For Reynolds numbers large compared to unity it is customary to divide the flow field into two regions (7, 8), in the outer region or core the fluid is considered to undergo potential flow (9) whereas in the inner region it is assumed that the flow is governed by Prandtl's boundary layer equations (7, 8, 10) which are an approximation to equation 2. The solutions are well-known for the case of a cylinder in an infinite stream.

In the region of potential flow the tangential and radial velocity components are given respectively by the equations

$$u_{\psi p} = U_\infty\left(1 + \frac{r_o^2}{r^2}\right) \sin \psi \tag{4}$$

$$u_{rp} = U_\infty\left(1 - \frac{r_o^2}{r^2}\right) \cos \psi \tag{5}$$

From these equations the magnitude of the velocity is found to be

$$|u|_p = U_\infty\left(1 + \frac{r_o^4}{r^4} + \frac{2r_o^2}{r^2} \cos 2\psi\right)^{1/2} \tag{6}$$

In the boundary layer, the velocity components are expressed in terms of non-elementary functions:

$$u_{\psi b} = 2U_\infty\left(\psi \frac{df_1}{d\Omega} - \frac{4}{3!} \psi^3 \frac{df_3}{d\Omega} + \frac{6}{5!} \psi^5 \frac{df_5}{d\Omega} - \dots\right) \tag{7}$$

$$u_{rb} = \frac{2U_\infty}{(Re)^{1/2}} \left(f_1 - 2\psi^2 f_3 + \frac{1}{4} \psi^4 f_5 - \dots\right) \tag{8}$$

where

$$\Omega = \left(\frac{r}{r_o} - 1\right)(Re)^{1/2} \tag{9}$$

The functions f_i and $df_i/d\Omega$ are available in the literature (7, 8).

Heat Transfer From Wires at Low Reynolds Number

When the dissipation function, ϕ, is negligible and the fluid properties are constant, equation 3 may be written as

$$\vec{u} \cdot \nabla t = \frac{k}{C_p \sigma} \nabla^2 t \tag{10}$$

This equation can be solved in closed form if it is assumed that the velocity is constant in the flow field. This approximation, which corresponds to Oseen's approximation for the case of momentum transport (11), has been solved by Cole and Roshko (12). Under these conditions the Nusselt number is given by

$$Nu = 2 \sum_{n=0}^{\infty} (-1)^n \frac{I_n\left(\frac{Re_w Pr}{4}\right)}{K_n\left(\frac{Re_w Pr}{4}\right)} \tag{11}$$

Piercy, Richardson and Winny (6) have obtained a solution of equation 10 assuming the flow field is that of potential flow in a region bounded by an infinite flat plate and a cylinder, with the flow at infinity parallel to the plate. The temperature of the plate was the same as that of the approaching fluid. The solution to this problem is not expected to apply at values of the Peclet number, $Re_w Pr$, larger than unity, or when the distance between the wire and the plate is of the

order of one wire diameter. Within the limits of applicability, the solution agrees fairly well with experiment (6). Figure 1 shows the predicted dependence of the Nusselt number on the Peclet number and distance from the cylinder.

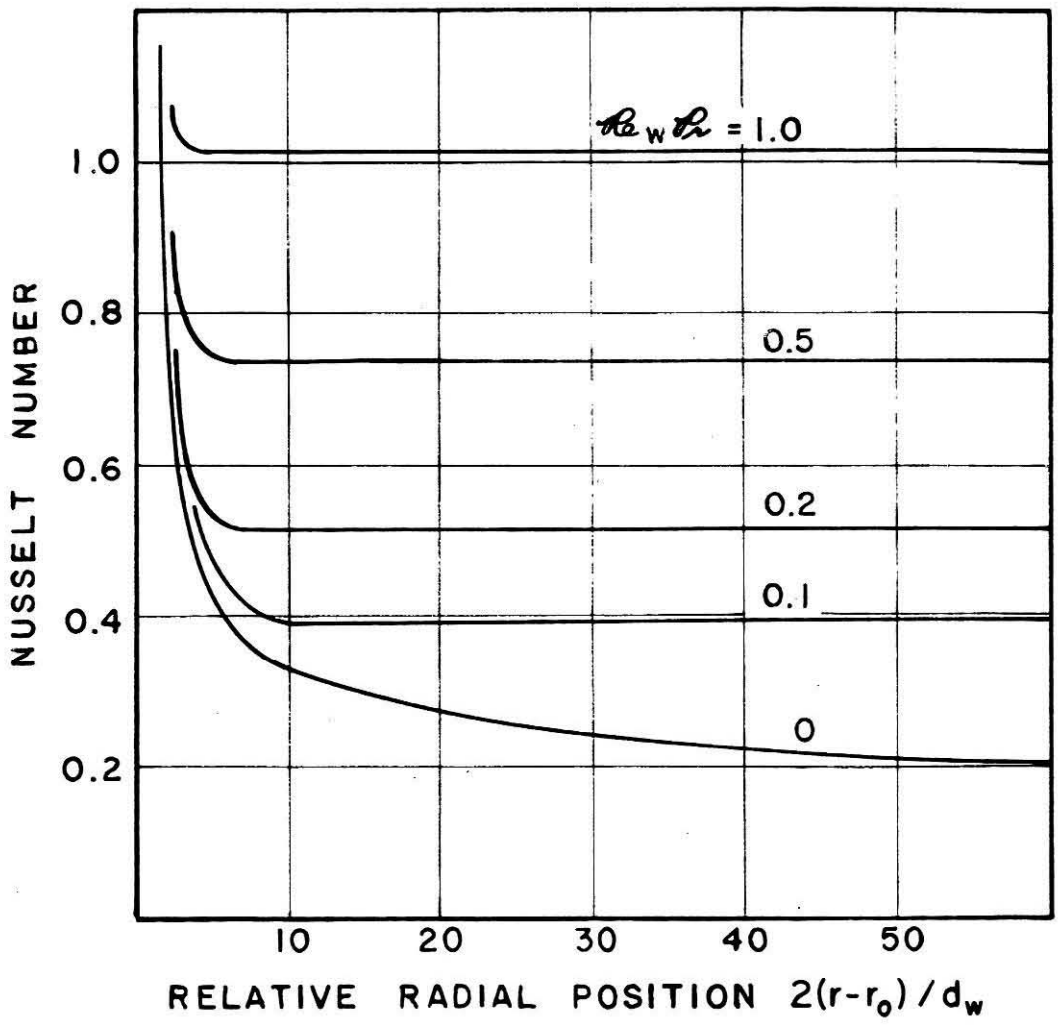

Figure 1: Nusselt Number for a Wire Near a Flat Plate (6)

SOME PRELIMINARY CONSIDERATIONS

Definitions of Reynolds Number

Many definitions of Reynolds number have been used in the literature (7, 8, 13, 14). In the present discussion the term "Reynolds number" is used to denote the Reynolds number based on cylinder diameter and free-stream conditions, as defined by the equation:

$$Re_{\infty} = \frac{2r_o U_{\infty} \rho_{\infty}}{\eta_{\infty}} \tag{12}$$

The Reynolds number based on wire diameter, local velocity, and properties of air at free-stream conditions is referred to as "wire Reynolds number." It is defined by the equation

$$Re_w = \frac{d_w u \rho_{\infty}}{\eta_{\infty}} \tag{13}$$

Definition of Heat Transfer Coefficient

The heat transfer coefficient is usually defined as the ratio of a heat flux to a temperature difference. For the present case it is defined specifically as the ratio of the electrical power dissipated in the wire, per unit area of wire surface, to the difference between the mean temperature of the wire as determined from the electrical resistance and the free-stream temperature:

$$h = \frac{\dot{q}_e}{(t_w - t_{\infty}) \pi d_w \ell} \tag{14}$$

Definitions of Nusselt Number

For any given conditions, a general definition of Nusselt number can be given in terms of the expression:

$$Nu_a = \frac{hd_w}{k_a} \tag{15}$$

The subscript a in equation 15 is used to indicate that the thermal conductivity of the fluid, k_a, is evaluated at a temperature t_a, which is a function of the temperatures t_w and t_∞ and is selected so that the Nusselt number defined by equation 15 depends on only one parameter. The use of such composite temperatures, t_a, results from the empirical observation that the Nusselt modulus based on free stream conditions depends not only on the wire Reynolds number but also on the temperature difference between the wire and the free stream. This dependence arises from the non-linearity of the equations which govern the transport.

The definition of t_a as a function of the variables t_w and t_∞ is not unique (13, 15) since it depends on the specific parameter used for purposes of correlation. Thus if it is desired to obtain a relation between the Nusselt number and the wire Reynolds number based on properties at the free-stream temperature the dependence of t_a on t_w and t_∞ will not be the same as that obtained by correlating the Nusselt number with a Reynolds number based on properties at some other temperature, such as the mean wire temperature.

In order to maintain a close correspondence between the quantities measured in the laboratory and the parameters derived from

them, the Nusselt number based on free stream conditions was used. This quantity is called "experimental Nusselt number," and is defined as

$$Nu_e = \frac{hd_w}{k_\infty} \tag{16}$$

Since, however, the experimental Nusselt number was found to vary with wire temperature, and "adjusted Nusselt number," Nu^*, was defined. This is the Nusselt number that would have been measured if the experimental conditions had been a wire temperature of $150^\circ F$. and a free stream temperature of $100\ ^\circ F$. The method used to obtain this quantity, is described in pages 84 to 87.

Various authors (1, 12, 16, 17) have indicated that the Nusselt number as calculated from the heat transfer coefficient defined by equation 16 is not useful for purposes of comparison among different wires. In order to obtain a value of the Nusselt number which is independent of the dimensions of the wire, two effects must be taken into account:

a) the effect of non-uniform wire temperature due to finite wire length (1, 12), which depends on the ratio of length to diameter of the wire, and

b) the effect of temperature jump at the air-wire interface (16, 17) due to molecular mean free paths of the general order of magnitude of the wire diameter, which depend on the ratio of molecular mean free path of the fluid to wire diameter.

For this reason a third definition of Nusselt number was used:

$$Nu_{\infty} = \xi Nu^{*} \tag{17}$$

The quantitative aspects involved in the determination of the correction factor ξ are summarized in Appendix I. Since this definition of the Nusselt modulus is the one of more general application, the unmodified term "Nusselt number" will be used to name it.

Discussion of Some Constants Used

The values of the properties of air used in the present work are given in Table I.* This data was obtained from a critical survey of the literature by Sage and co-workers (18), and from a recent publication of the National Bureau of Standards (19). The values of the properties of air given in these publications are in good agreement. These properties are defined in terms of a British thermal unit (Btu) of 0.947831×10^{-3} absolute joules (19), accordingly, this value of the conversion factor was used throughout.

Assumptions Made in the Analysis

In reducing the experimental data to obtain final results some assumptions were made. An estimate of the effect of these will be given in the following paragraphs.

One assumption was that the radiant transfer between the wire and the surroundings is negligible. Assuming that the surroundings are a black body at 90 $^{\circ}$F and that the emissivity of platinum is 0.04

*Tables are presented on page 126.

(13), the heat flux by radiation is found to be 0.0016 Btu/sq. ft. sec. for a wire temperature of 200 °F. This is consistent with a value measured by Short (5) of 0.0035 Btu/sq. ft. sec. at a wire temperature of 238 °F. Under the same temperature conditions, the lowest heat flux encountered was approximately 3.00 Btu/sq. ft. sec., so the error introduced by this assumption is less than 0.1%. Only at very low wire temperatures, when the transport by convection between the wire and the air stream was very small, would the assumption of negligible radiant transport introduce a significant error.

In calculating the difference in temperature between the wire and the air stream, it was assumed that the bridge current used in determining the resistance of the wire at free-stream conditions did not materially affect its temperature. The change in wire temperature calculated from the conditions under which measurements were taken was of 0.05 °F, if radiant transport was neglected. If radiant transport was taken into account this was reduced to about 0.02 °F, which is near the precision limit of the measurement of temperature by means of the wire.

Finally, it was assumed that, when significant oscillations occurred, time-averaged values of the measured quantities gave a good representation of steady-state conditions.

EQUIPMENT

The measurements of heat transfer coefficients from a small wire in the boundary flow about a cylinder were carried out in an air stream emerging from a rectangular jet. The equipment will be described in several sections, each pertaining to one part of the total equipment used.

Air Supply

Except for minor modifications, the air supply equipment used in the present investigation has been described by other workers (20, 21). The main difference between the system that they described and the one used is that the duct was redesigned to eliminate a bend close to the duct opening. Figure 2 shows a schematic diagram of the air supply equipment. It consisted of a blower, A, from which air was pumped, through a Venturi meter, B, into a system of 12 x 12 square ducts. The duct led from the blower to a jet opening, C, 3 inches wide and 12 inches long, preceded by a smooth converging section. In this way, a flat velocity profile was obtained at the duct opening as shown in fig. 3. The data used in the preparation of this figure are given in Table II, the values of the velocity were obtained from corresponding values of the Nusselt number by the correlation of Collis and Williams (16).

The duct and converging section were provided with heaters which could be regulated independently so as to control closely the temperature of the air stream. For finer control of this parameter, the duct

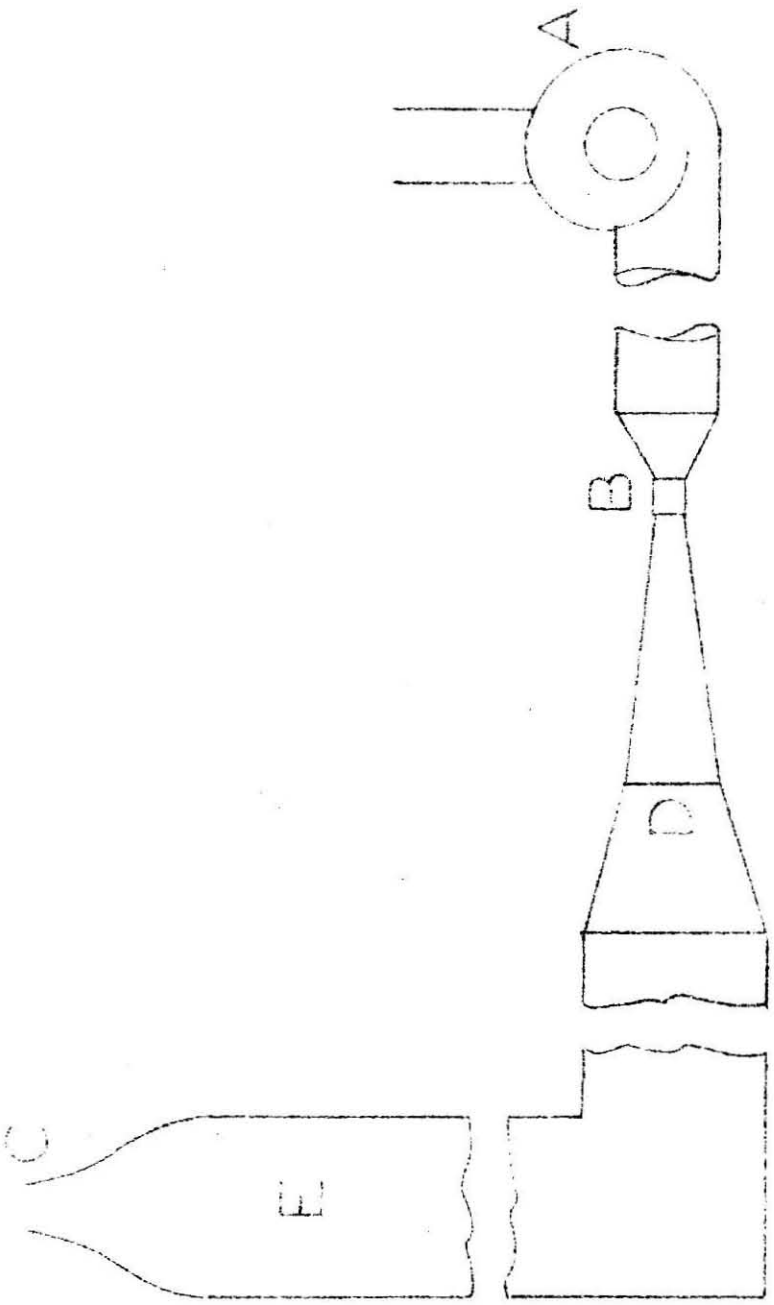

Figure 2: Schematic Diagram of Air Supply Equipment

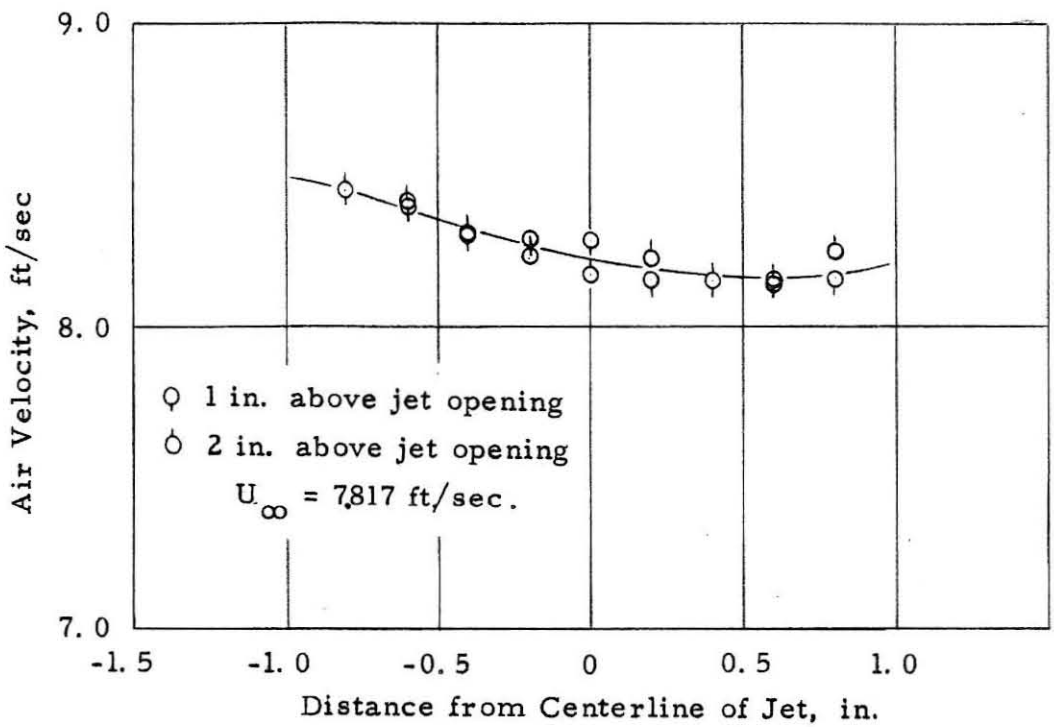

Figure 3: Velocity Profile of Unobstructed Jet

was provided with a control heater, operated through a thyratron circuit by a resistance thermometer. The details of this temperature control system have been described by Corcoran and co-workers (22). The temperature at eleven points in the duct could be determined by means of 40-gauge copper-constantan thermocouples; two copper constantan thermocouples, 0. 003 inches in diameter, were available for the measurement of duct temperature. The air temperature at the Venturi meter and upstream of the converging section could be determined by means of platinum resistance thermometers shown at D and E, respectively, in fig. 2.

Copper Cylinder

Figure 4 shows a diagram of the copper cylinder. The core, A, consisted of a 12-inch copper tube with a machined double-lead thread, B, 1/8 inch wide by 1/8 inch deep and of 1/4 inch pitch. Each lead of the thread was provided with a ribbon heating element, C, insulated electrically from the core by means of alundum insulation.

Three thermocouples were installed in thermocouple wells, D, located at the mid-point and two inches on either side of it. The thermocouple leads were insulated from the core by means of glass capillaries and were cemented so the thermocouple junction was flush with the outside of the core. The thermocouple leads were brought to the exterior through the hollow center of the tube.

The core was covered by a copper shell, E, 0. 030 inches thick and 1. 000 $\pm$ 0. 003 inches in external diameter. The core and shell were soft-soldered by tinning both, sliding the core into the shell and placing

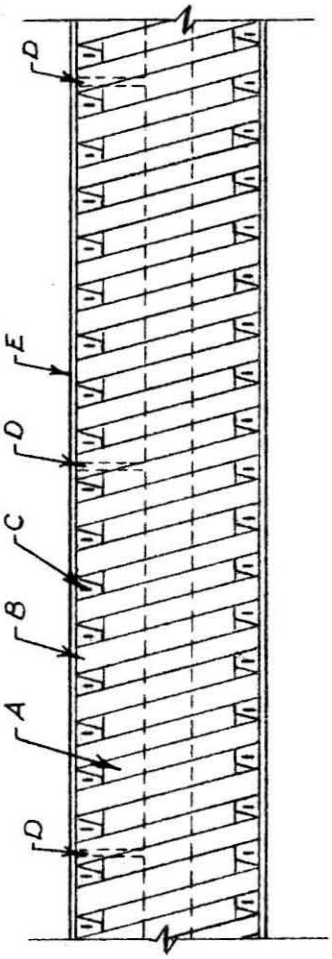

Figure 4: The Copper Cylinder

the assembly into an oven at 400 ^{o}F (23).

For purposes of support the copper section was continued at both ends by about 12 inches of bakelite tube of the same external dimensions. The electrical leads were passed through the opening in the bakelite and connected in a terminal box mounted on one end of the bakelite extension.

The cylinder assembly was mounted on machined aluminum clamps and aligned so that its axis coincided with the centerline of the jet. Alignment was accomplished by use of a depth probe mounted on a jeweler's milling attachment. A spirit level was used to ensure that the cylinder axis was parallel to the plane of the jet opening. The distance between the cylinder axis and the jet opening was approximately 2 inches.

Wire Assembly

The wire assembly consisted essentially of a supporting probe and a traversing gear. The probe, shown in fig. 5, consisted of two tapered platinum needles, A, of about 0.03 inch diameter at the base, attached through bakelite supports, B, to a steel head, C. The steel head was bolted to a 0.25 inch steel shaft, D, which could be secured to the traversing gear. The platinum needles were supplied with 30-gauge platinum wires, E, welded close to the base to provide current and potential terminals for measurements. These leads were fastened to the bakelite supports and extended about 6 inches along the supporting shaft, at which point they were connected to copper leads extending into a contact box near the duct.

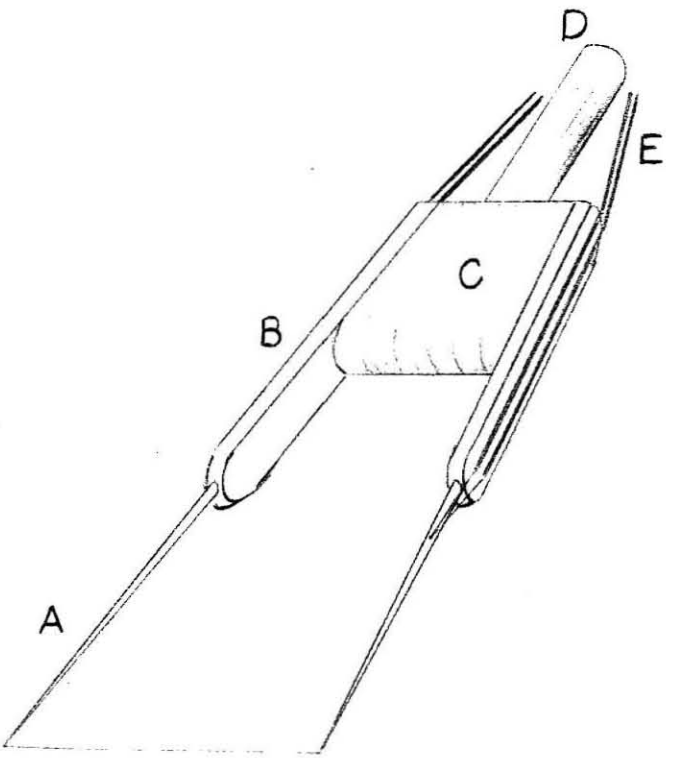

Figure 5: Diagram of the Probe

The wire itself was welded onto the tips of the needles. The wire used was pure platinum Wollaston wire 0.001 inch in diameter. A microphotograph of a section of wire is shown in fig. 6 together with a microphotograph of a calibrated scale taken at the same focal distance. Dimensions of the wire as determined from these photographs agreed to within experimental error with the nominal value quoted by the manufacturer. Throughout this investigation wires were obtained from the same spool.

The traversing gear used to position the wire consisted of three milling attachments such as are used by jewelers. The position in a plane perpendicular to the cylinder axis could be determined with precision by means of two dial gauges with 0.001-inch divisions. A photograph of the probe and traversing gear is shown in fig. 7.

Wire Measuring Circuit

A diagram of the measuring circuit used for determination of the heat transfer characteristics is shown in fig. 8. It consisted of a Wheatstone bridge with two adjacent arms composed of fixed resistors of 4 and 40 ohms. The arm adjacent to the 40 ohm resistor consisted of a variable resistor, R_v, which could be used to balance the galvanometer, G. The fourth arm was composed of two standard manganin resistors having nominal values of 0.5 and 0.05 ohms, and of the wire itself. The standard resistors were provided with potential terminals which could be connected to a White potentiometer or to a K-2 type potentiometer, for the determination of the potential difference across these elements.

Fig. 6a: Microphotograph of a Wire

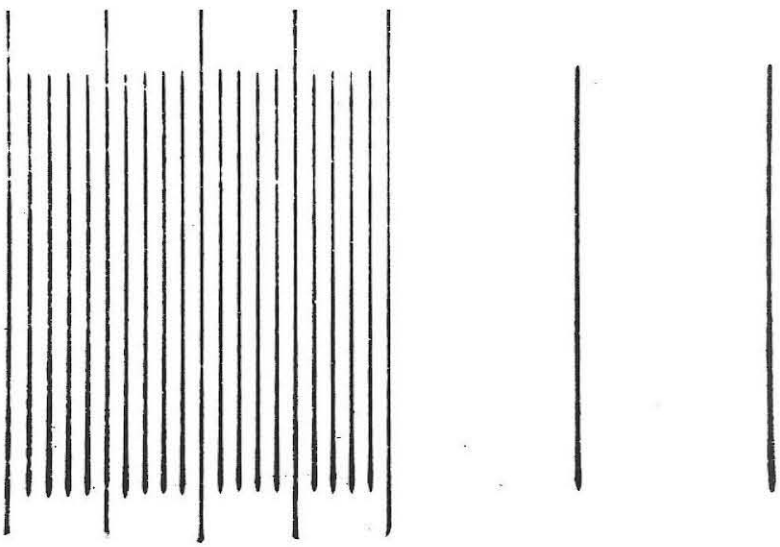

Fig. 6b: Microphotograph of a Calibrated Scale
(smallest division 1 micron)

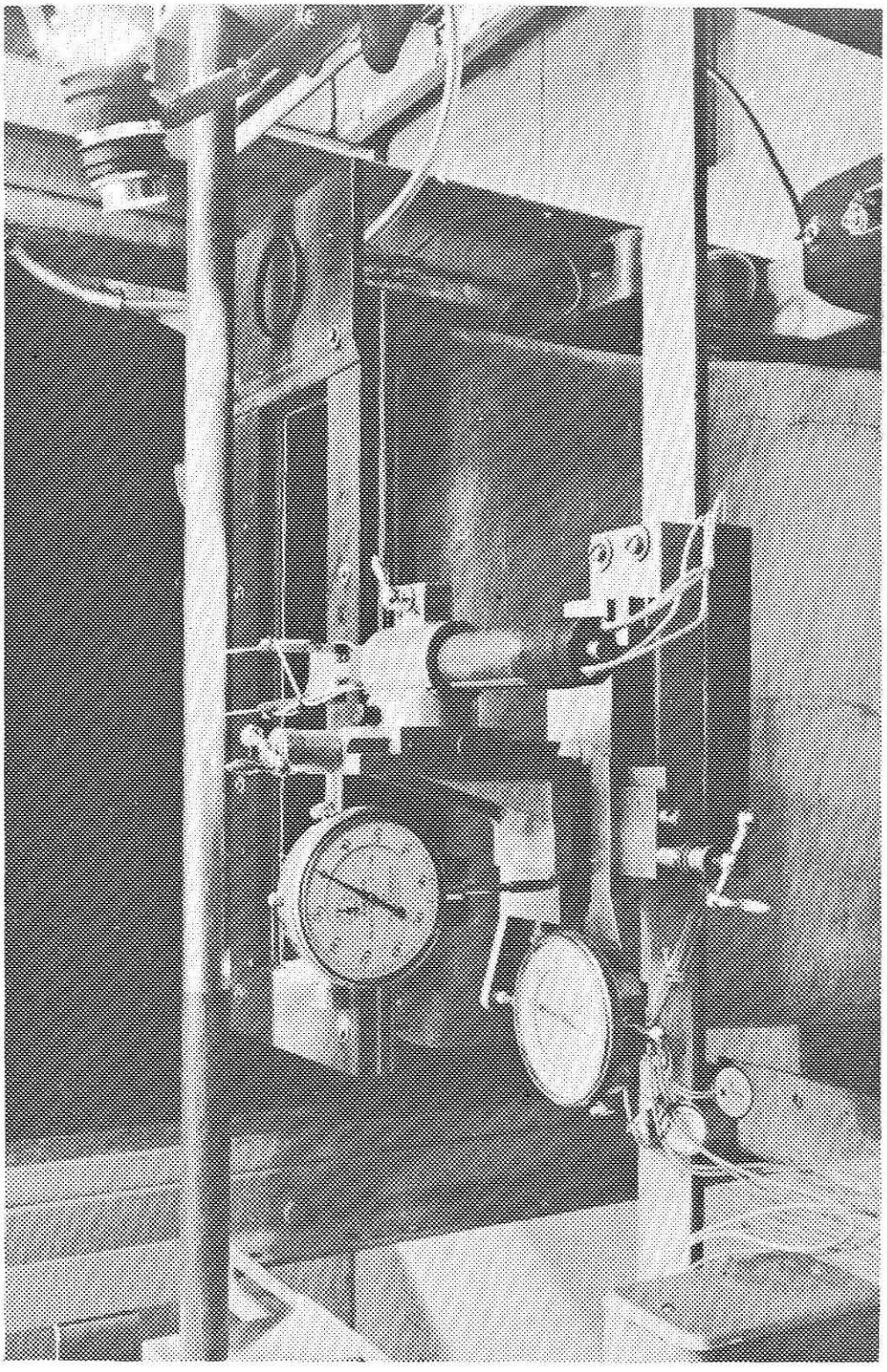

Figure 7: Photograph of the Traversing Gear and Probe

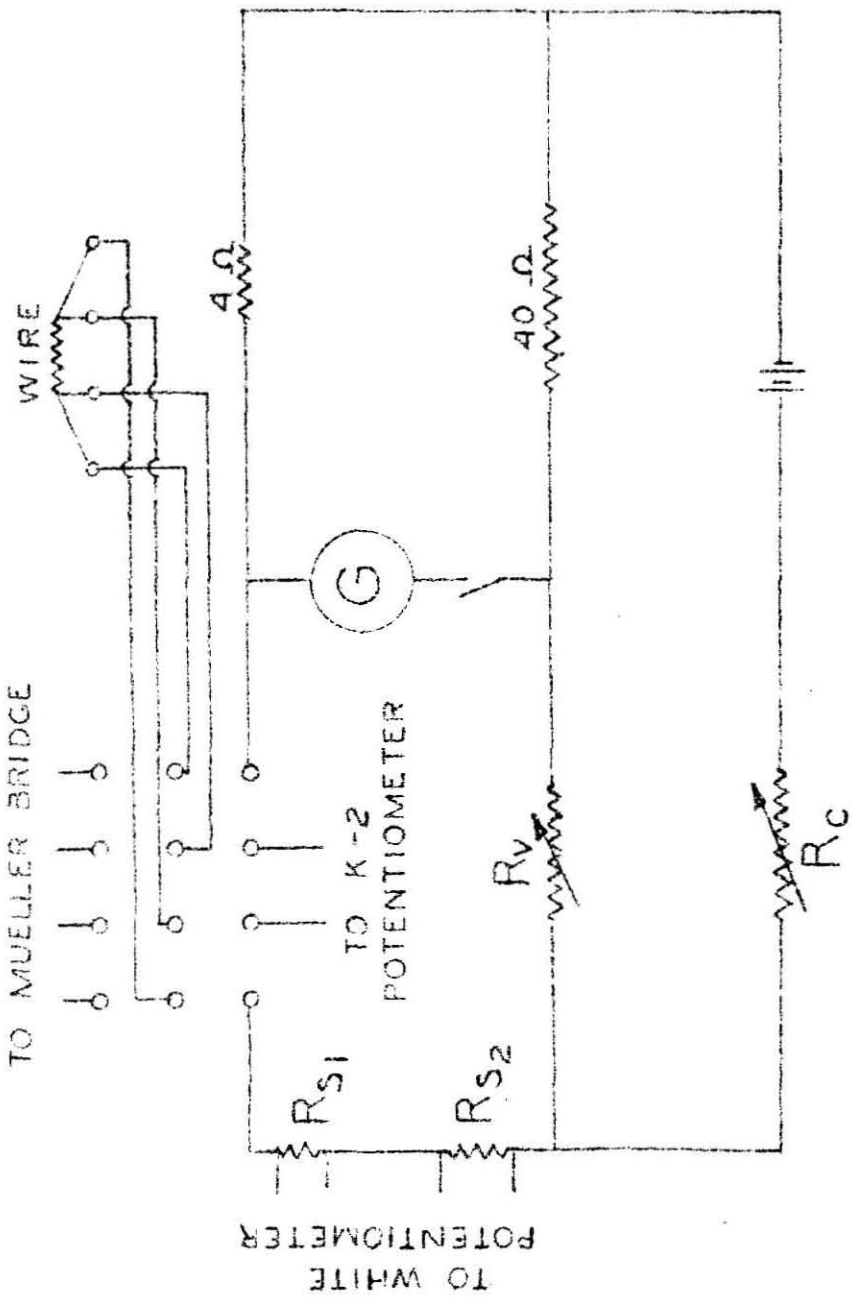

Figure 8: Circuit for Measurements

The current leads from the wire assembly could be connected into the Wheatstone bridge circuit by means of a commutator switch, and the potential leads could be connected to either of the potentiometers mentioned earlier. The power supply consisted of two 6-volt DC batteries connected to the bridge through a control resistor, R_c, which served to regulate the current through the bridge so that the wire resistance could be maintained at any given value as determined from the setting of the balancing resistor, R_v, and balance of the galvanometer.

The potentiometer connections then permitted the simultaneous measurement of potential difference across the hot wire and a standard resistor. In this way the resistance of the wire and the input of electrical energy to it could be determined accurately. The commutator switch connecting the wire to the bridge circuit could also be used to connect the wire to a G-1 type Mueller bridge, with which the resistance of the wire at the temperature of the air stream could be measured. When the wire was connected in this position, the bridge circuit was closed through a 7-ohm resistor so that current would be maintained through the bridge; in this fashion transient behavior of the batteries and bridge components was minimized.

EXPERIMENTAL MEASUREMENTS AND REDUCTION OF THE DATA

The purpose of the present section is to indicate briefly the experimental methods employed and the procedures used to calculate final results from the experimental data. Since the measurement of the heat transfer characteristics of a small wire in a boundary flow requires several auxiliary measurements, these also will be discussed. For the sake of clarity the experimental measurements and the reduction of the data will be divided into several sections: measurement of flow conditions, calibrations of the wires as temperature measuring devices, determination of the heat transfer coefficient, determination of a method for adjusting the heat transfer coefficient, and determination of the heat through characteristics in the boundary flow.

Measurement of Flow Conditions

During the course of experimental work, it was of importance to ensure that steady state operation of the equipment was obtained. For this purpose the equipment was started about 5 hours before the beginning of a test. During the stabilization period measurements of duct temperature at the 15 points at which this variable could be measured were obtained at frequent intervals. The temperature of the Venturi meter and duct resistance thermometers were followed closely. In addition, the pressure difference across the Venturi meter was observed in order to ensure that stable control of this variable had been attained. Similar measurements were taken before and after each test, and also at approximately 40-minute intervals during the period in which actual measure-

ments of the heat transfer from the wire were being made.

The data pertaining to conditions at the Venturi meter was sufficient to permit the determination of mass flow rates of air. From these, and the measured temperature and pressure at the duct opening, it was possible to compute the average velocity at the jet by the equation:

$$U_{\infty} = \frac{\dot{m}}{A} \cdot \frac{ZbT}{P} \qquad (18)$$

The average velocity thus obtained was used to calculate the Reynolds number by equation 12.

The temperature of the air at the jet opening was obtained from the readings of the resistance thermometer, as this instrument retains calibration for much longer periods than copper constantan thermocouples. However, the indications of the thermocouples in the duct were taken into consideration in determining whether steady state had been attained before the beginning of the test. Table III presents the conditions under which the experimental data was obtained.

Calibration of the Wires

In order to obtain accurate heat transfer data, the resistance of the wires must be known as a function of temperature. Ideally this information should be obtained by determining the resistance of the element at the three fixed points used in precision thermometry: the ice-point, the normal boiling point of water and the melting point of sulphur. However, since the wires were approximately 1. 25 inches long, immersion in baths would have required extensive insulation to eliminate appreciable gradients.

The procedure followed was to determine the resistance of the wire while in the air duct, using air temperatures of approximately 80°, 100°, and $120\ ^{\circ}F$; this variation represented the maximum temperature range obtainable with the equipment. The temperature of the air during these calibration tests was measured by means of a standard platinum resistance thermometer installed at the duct opening within a few inches of the wire under calibration.

Due to the relatively small range of temperatures that could be attained with the equipment the second derivative of resistance with respect to temperature could not be determined with precision. In order to obtain a significant quadratic fit for the resistance as a function of temperature, additional information was obtained from data on laboratory resistance thermometers (24). As shown in fig. 9 a plot of the derivative

$$\alpha = \frac{d(R/R_o)}{dt} \tag{19}$$

normalized to a value of unity at $100\ ^{\circ}F$, versus temperature indicates that the derivative of this quantity is constant:

$$\frac{d(\alpha/\alpha_{100})}{dt} = -\ 0.000169\ \ (^{\circ}F)^{-1} \tag{20}$$

A value of the derivative dR/dt at $100\ ^{\circ}F$ and an estimated value of the ice-point resistance were obtained by the method of least squares (25). From this data the value of α at $100\ ^{\circ}F$ could be estimated. With this information, each datum point could be used, in conjunction with equation 20, to obtain new approximations to the ice-point resistance.

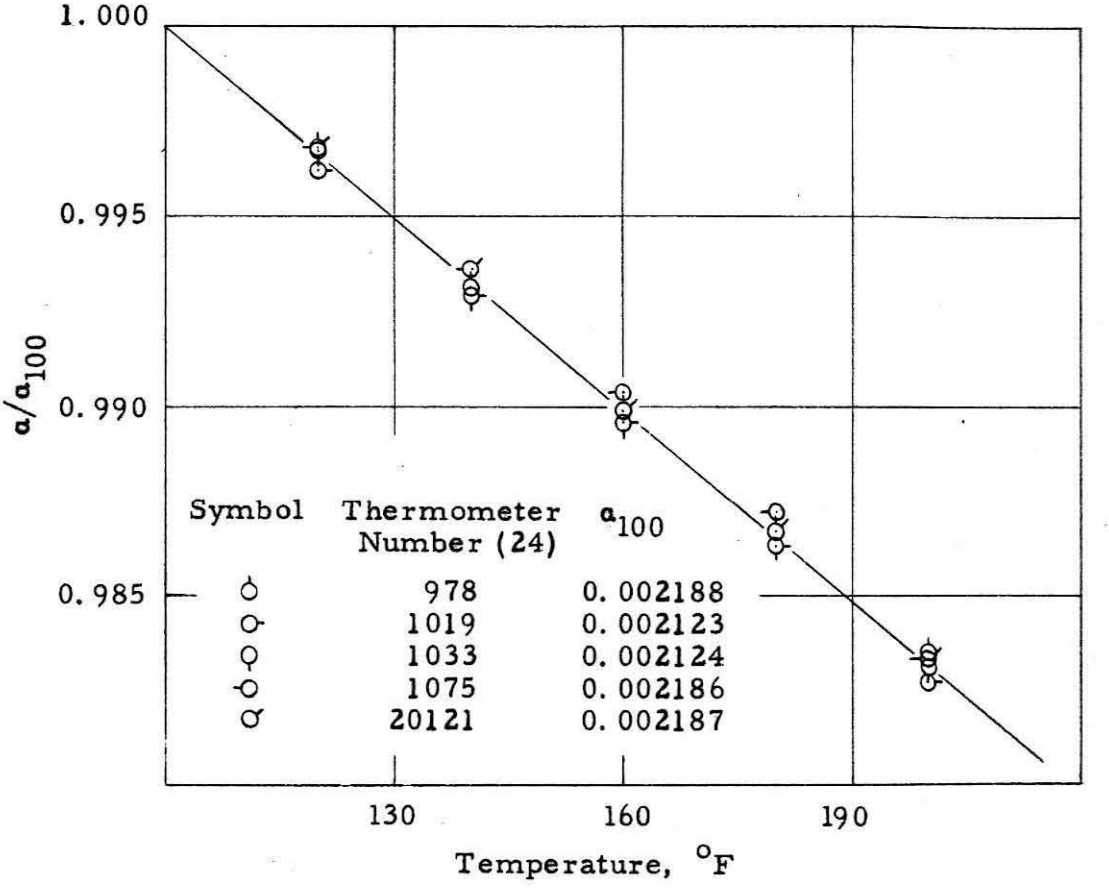

Figure 9: Dependence of a/a_{100} on Temperature

Successive approximations were made until consistent values were obtained in two consecutive trials.

The resistance was expressed as a function of temperature by the equation:

$$\frac{R}{R_o} = 1 + B_1 + B_2 t + B_3 t^2 \qquad (21)$$

Table IV presents the important properties of the wires used, as well as those of pure platinum calculated from data of Mueller (26) and of Wenner and Lindberg (27). The resistance per unit length for pure platinum was calculated by assuming that the wire was circular and 0.00100 inches in diameter. The agreement of the data obtained with that of pure platinum is good.

Determination of Heat Transfer Coefficients

Under steady conditions, the electrical energy dissipated in the wire per unit time is given by

$$\dot{q}_e = E_w I_w \qquad (22)$$

Since the current through the wire is equal to the current through the standard resistor, equation 22 may be expressed in the form

$$\dot{q}_e = E_w \frac{E_s}{R_s} \qquad (23)$$

Combining equations 14 and 23 it follows that

$$h = \frac{\dot{q}_e}{(t_w - t_\infty)\pi d_w \ell} = \left(\frac{1}{\pi d_w \ell} \frac{E_w E_s}{R_s}\right)/(t_w - t_\infty) \qquad (24)$$

In order to obtain data for the calculation of heat transfer coefficients, the potential difference across the wire, E_w, and across the standard resistor, E_s, were determined.

The potential differences measured, with the known resistance of the standard resistor, were used to calculate the resistance of the heated wire:

$$R_w = \frac{E_w}{E_s} R_s \qquad (25)$$

This value was used in conjunction with equation 21 to obtain the wire temperature, t_w, while the free stream temperature, t_∞, was calculated from equation 21 using the resistance of the wire as measured with a Mueller bridge.

Determination of the Adjusted Nusselt Number

As defined in page 64, the adjusted Nusselt number is the value of the experimental Nusselt number which would have been obtained if the measurements had been carried out with a wire temperature of 150 °F and a free stream temperature of 100 °F. In order to determine the relation between the adjusted Nusselt number and quantities measured in the laboratory, it was necessary to establish the dependence of experimental Nusselt number on temperature difference, wire Reynolds number, and position relative to the cylinder. Since the free stream temperature did not differ materially from 100 °F, it was not necessary to investigate this additional variable.

Tests 359, 376, and 377 were conducted with the purpose of establishing this dependence, by varying the pertinent parameters. The

data obtained indicated that the change of experimental Nusselt number with temperature difference was of the order of 0.0005 per degree, and that the effect of other variables was of a smaller order of magnitude. Since the variation of experimental Nusselt number with temperature was found to be essentially linear, as shown by some typical results in fig. 10, it was found convenient to account for this dependence by determining an "average" temperature at which the thermal conductivity could be evaluated to give a Nusselt number independent of the temperature difference between the wire and the free stream. This was found to be

$$t_{1/4} = t_\infty + \frac{1}{4}\Delta t \tag{26}$$

Hence the adjusted Nusselt number was defined as

$$Nu^* = Nu_e \left(\frac{k_\infty}{k_{1/4}}\right)\left(\frac{k_{112.5}}{k_{100}}\right) \tag{27}$$

In order to obtain a quantitative measure of the success of equation 27 in determining a value of the Nusselt parameter at reference conditions, the derivative $d(Nu^*)/d(\Delta t)$ was obtained by the method of least squares (25) for all the points obtained. The results, which are presented in Table V, indicate that the variation of the adjusted Nusselt number is of the order of 0.00005 per degree. The dependence of adjusted Nusselt number with temperature is illustrated in fig. 10.

The results appear to indicate a slight variation of adjusted Nusselt number with temperature difference, but this is too small to determine with any certainty. Furthermore, since the difference between adjusted and experimental values of the Nusselt modulus is of the order of 0.5%,

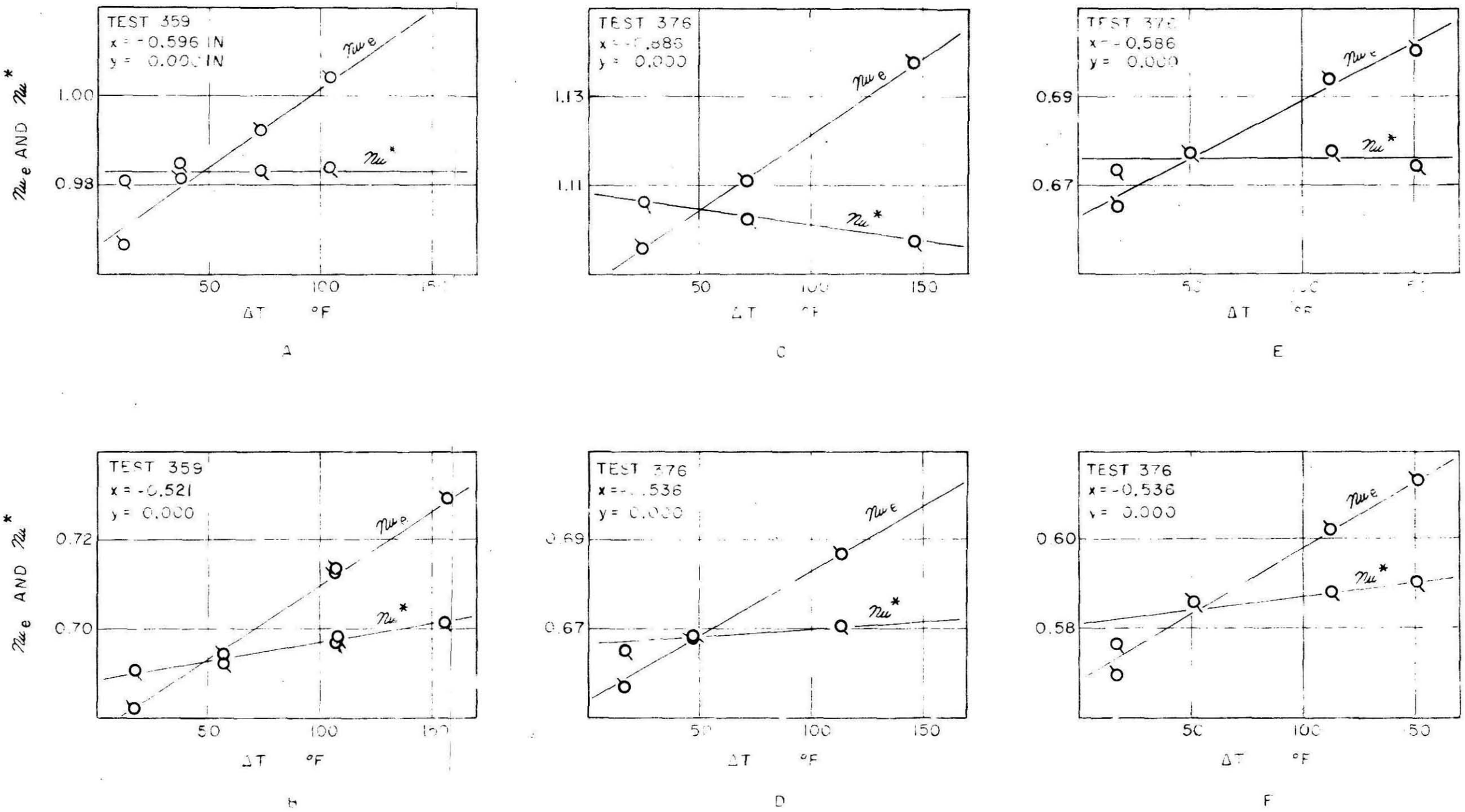

Figure 10: Dependence of Experimental and Adjusted Nusselt Number on Temperature Difference

even a moderate error in the method of interpolation would introduce only insignificant error in the final result. For these reasons it was decided that no further study of the relationship between these two parameters was necessary.

Determination of the Heat Transfer Characteristics from Wires in the Boundary Flow

a) Determination of the cylinder coordinates relative to the wire coordinates. - An accurate description of the dependence of Nusselt number on the position of the wire in the boundary flow, requires that the position of the wire relative to the cylinder be known. In order to obtain this information, the traversing gear was moved slowly to bring the wire toward the cylinder along a horizontal line. When the wire was close to the cylinder, a small light source was directed toward the expected point of contact so as to be nearly tangential to the cylinder. The traversing gear was then carefully moved until the tips of the platinum needles, their reflection in the cylinder, and their shadow along the cylinder surface coincided. Similar information was also obtained for vertical approach of the wire to the cylinder. This technique was found to give a sensitive indication of position, and results obtained in this way were reproducible to within 0.002 inch, which is the same magnitude as the variation in cylinder diameter as obtained from micrometer measurements. It should also be noted that both probe needles were observed, so the uncertainty mentioned gives a measure of the lack of alignment between the wire and the cylinder axis.

b) Determination of the Nusselt number field. - In order to determine the Nusselt number field in the forward part of the boundary flow, coefficient of thermal transfer from the wire was determined at several points along horizontal and vertical traverse lines. Approximately 10 traverses, five horizontal and five vertical, were completed for each of three Reynolds number, so that the heat transfer coefficient was known at about 200 points for each Reynolds number. The experimental results are listed in Table VI.

Typical results for nominal Reynolds numbers of 7100, 3500, and 1750 are shown in figs. 11, 12, and 13 respectively. From the results obtained, through large-scale graphical methods, the distribution of Nusselt numbers in the boundary flows were obtained. The complete fields for the three nominal Reynolds numbers mentioned above are presented in figs. 14, 15, and 16 respectively.

From these figures, in turn, the variation of Nusselt number with radial position was determined. This dependence is given in Table VII, and shown in figs. 17, 18, 19, and 20, for angles of 0°, 30°, 60°, and 90° from stagnation. The standard error of estimate of the experimental data from the smooth curves, defined as

$$\sigma_e = \left[\frac{\sum_{i=1}^{N} (Nu_i - Nu_{si})^2}{N - 1} \right]^{1/2} \qquad (28)$$

is given in Table VIII.

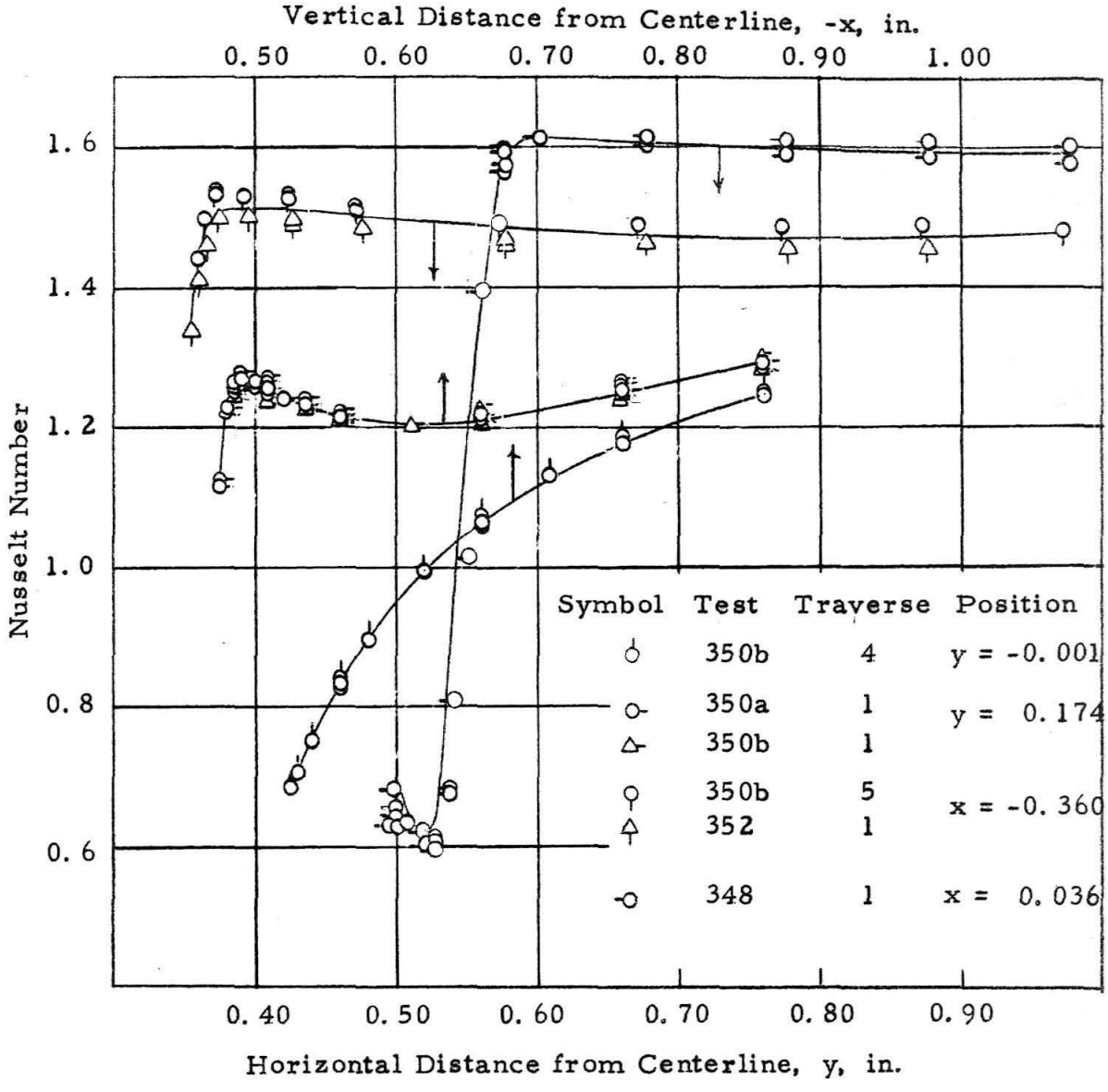

Figure 11: Typical Experimental Results at a Nominal Reynolds Number of 7100

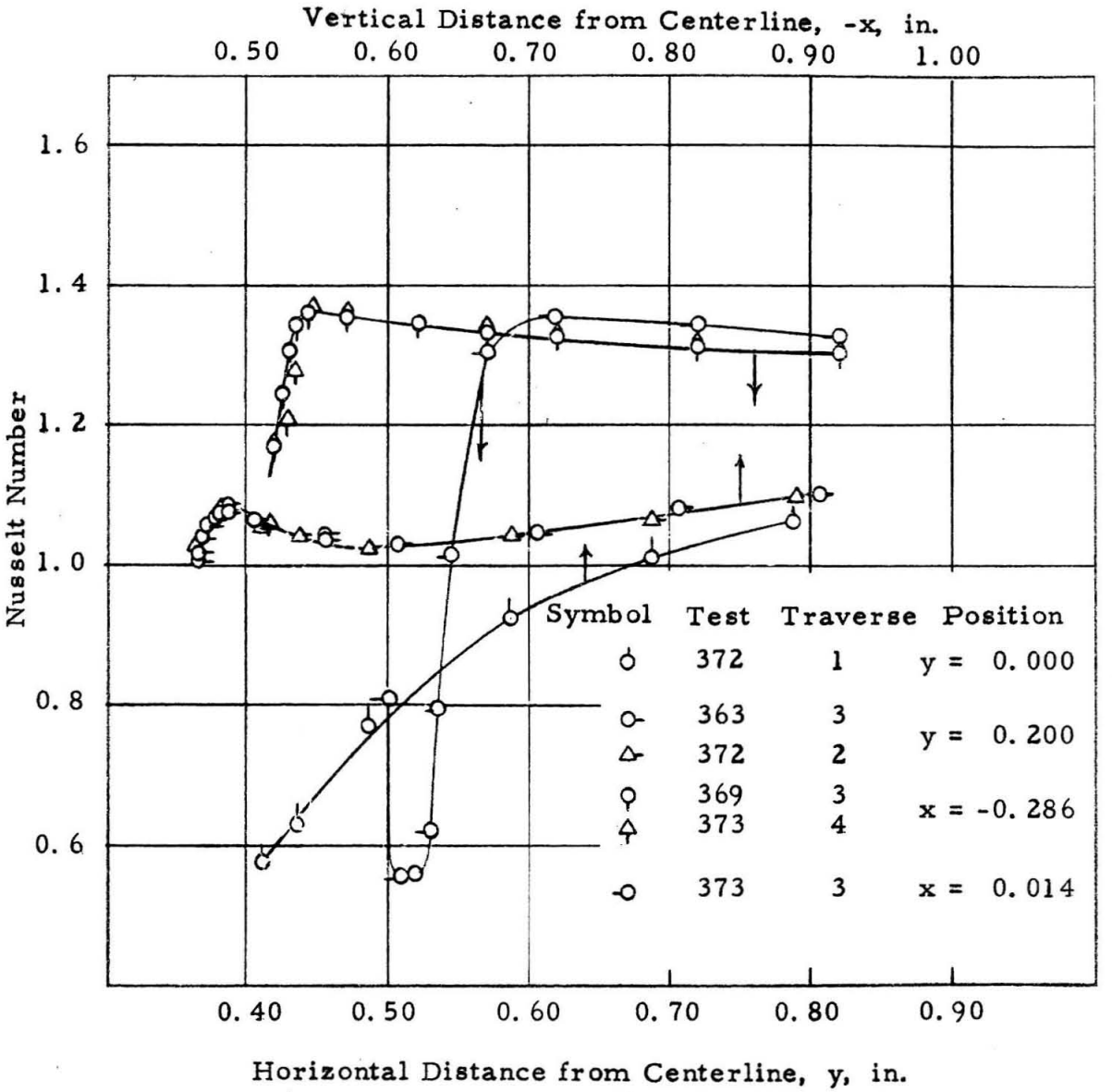

Figure 12: Typical Experimental Results at a Nominal Reynolds Number of 3500

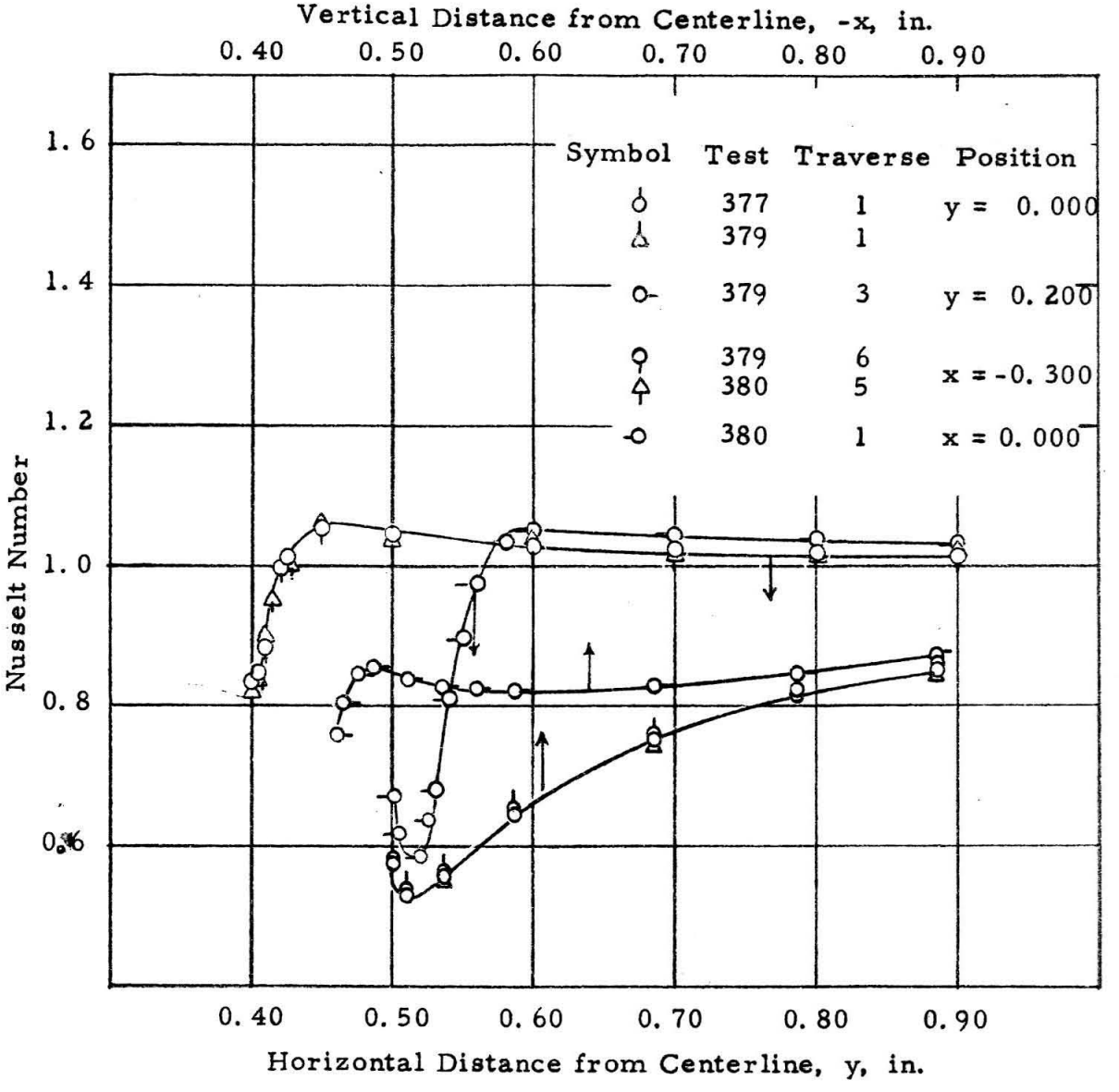

Figure 13: Typical Experimental Results at a Nominal Reynolds Number of 1750

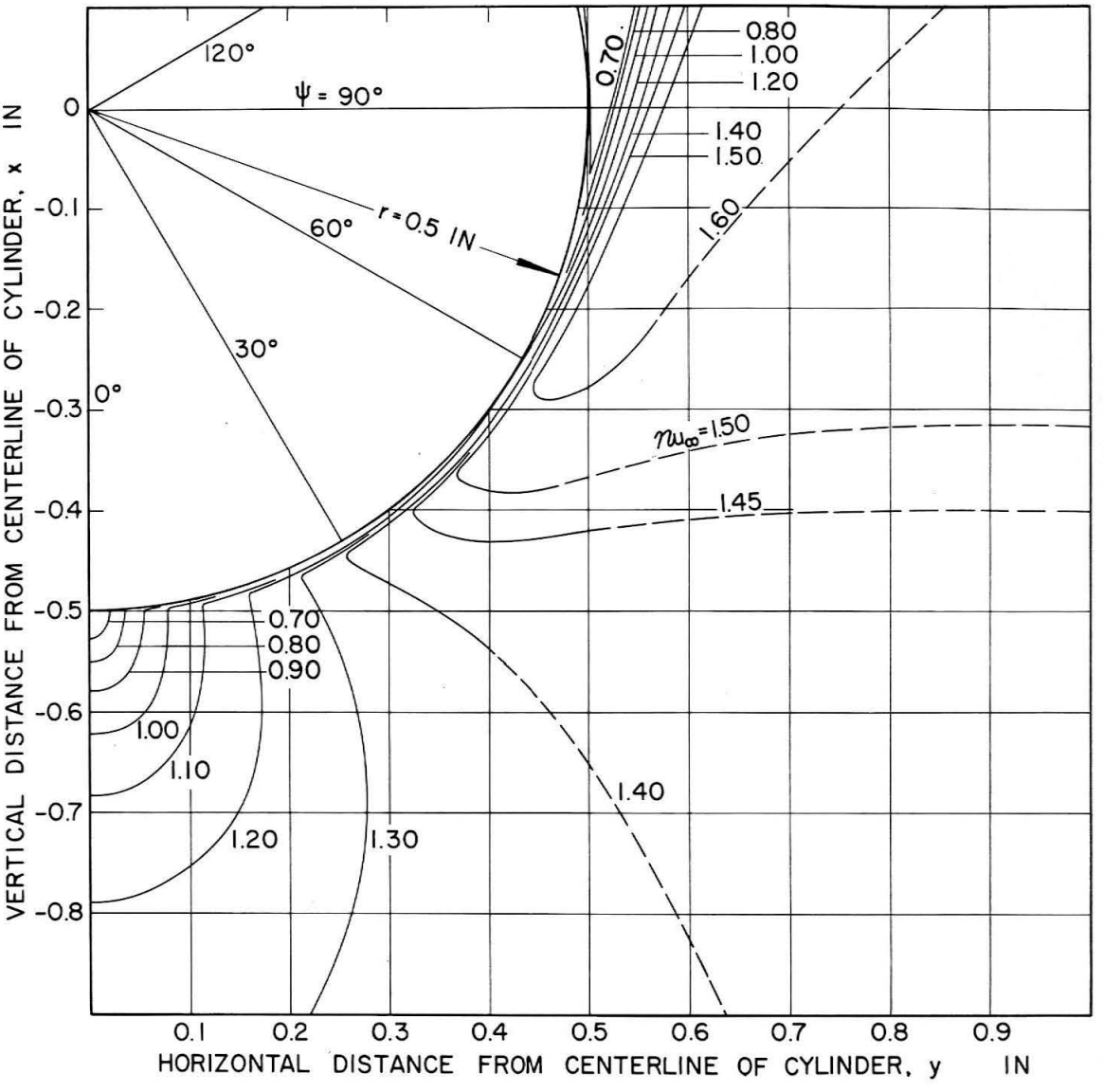

Figure 14: Nusselt Number Distribution in the Boundary Flow at a Reynolds Number of 7098

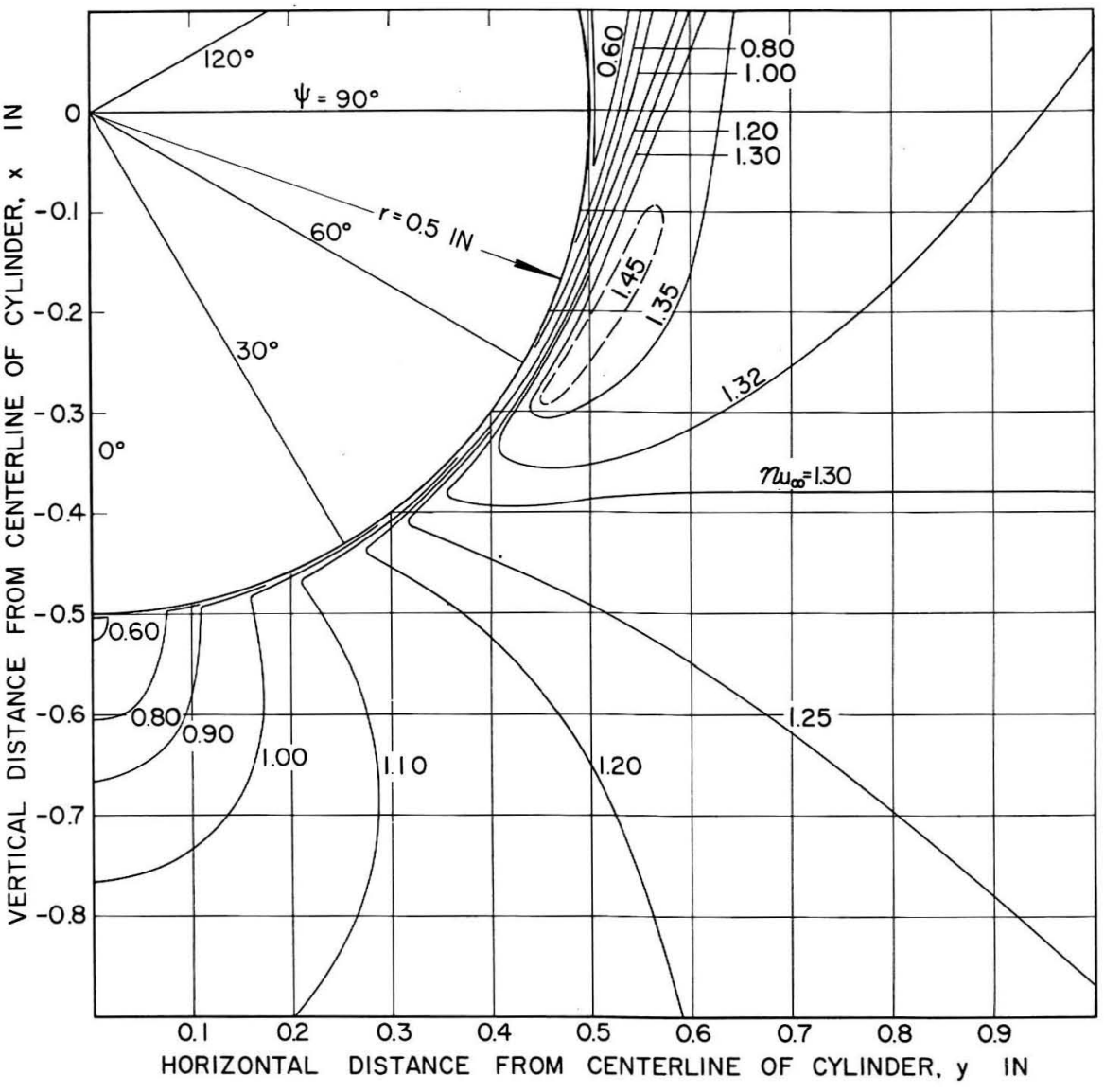

Figure 15: Nusselt Number Distribution in the Boundary Flow at a Reynolds Number of 3526

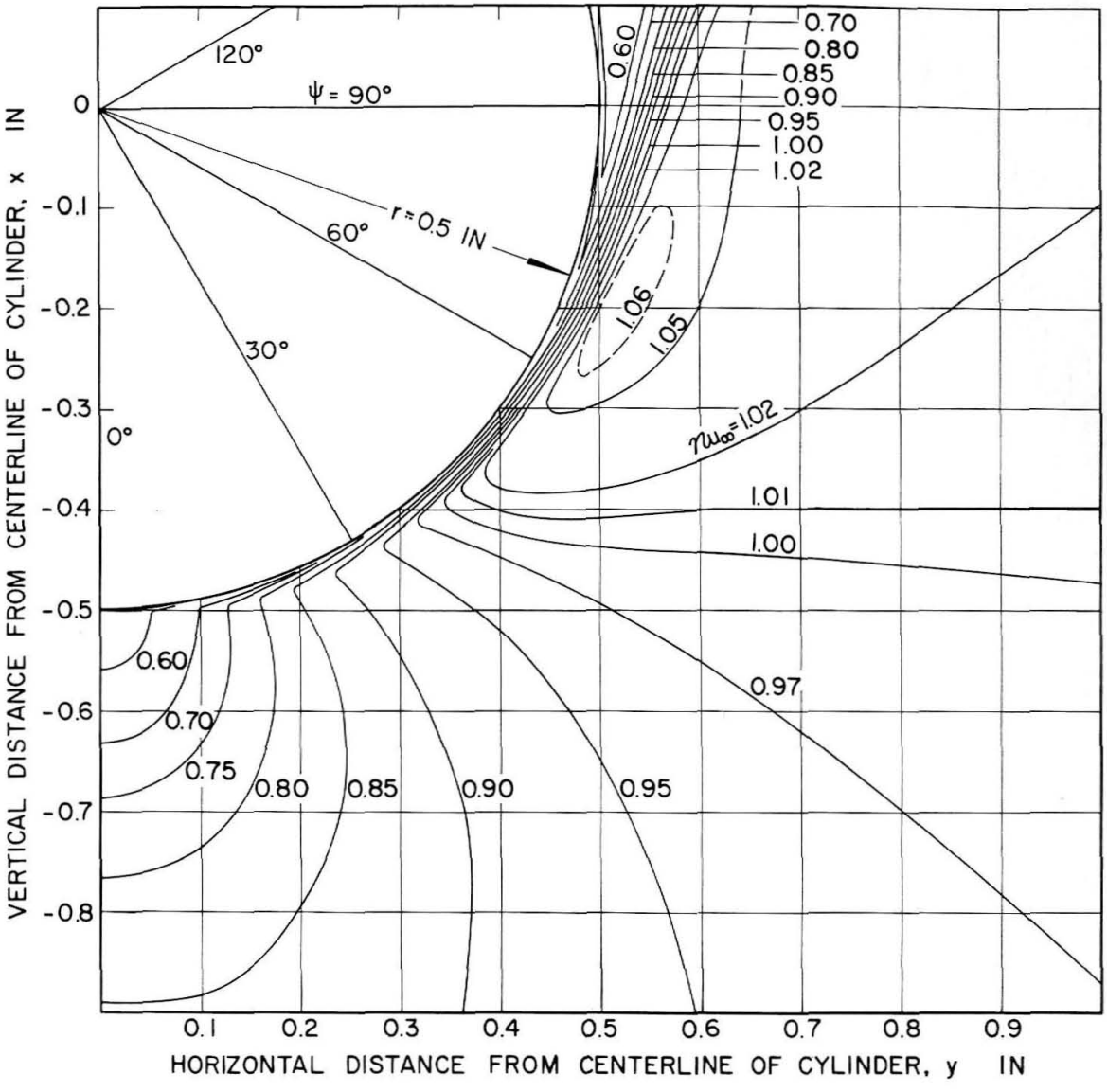

Figure 16: Nusselt Number Distribution in the Boundary Flow at a Reynolds Number of 1757

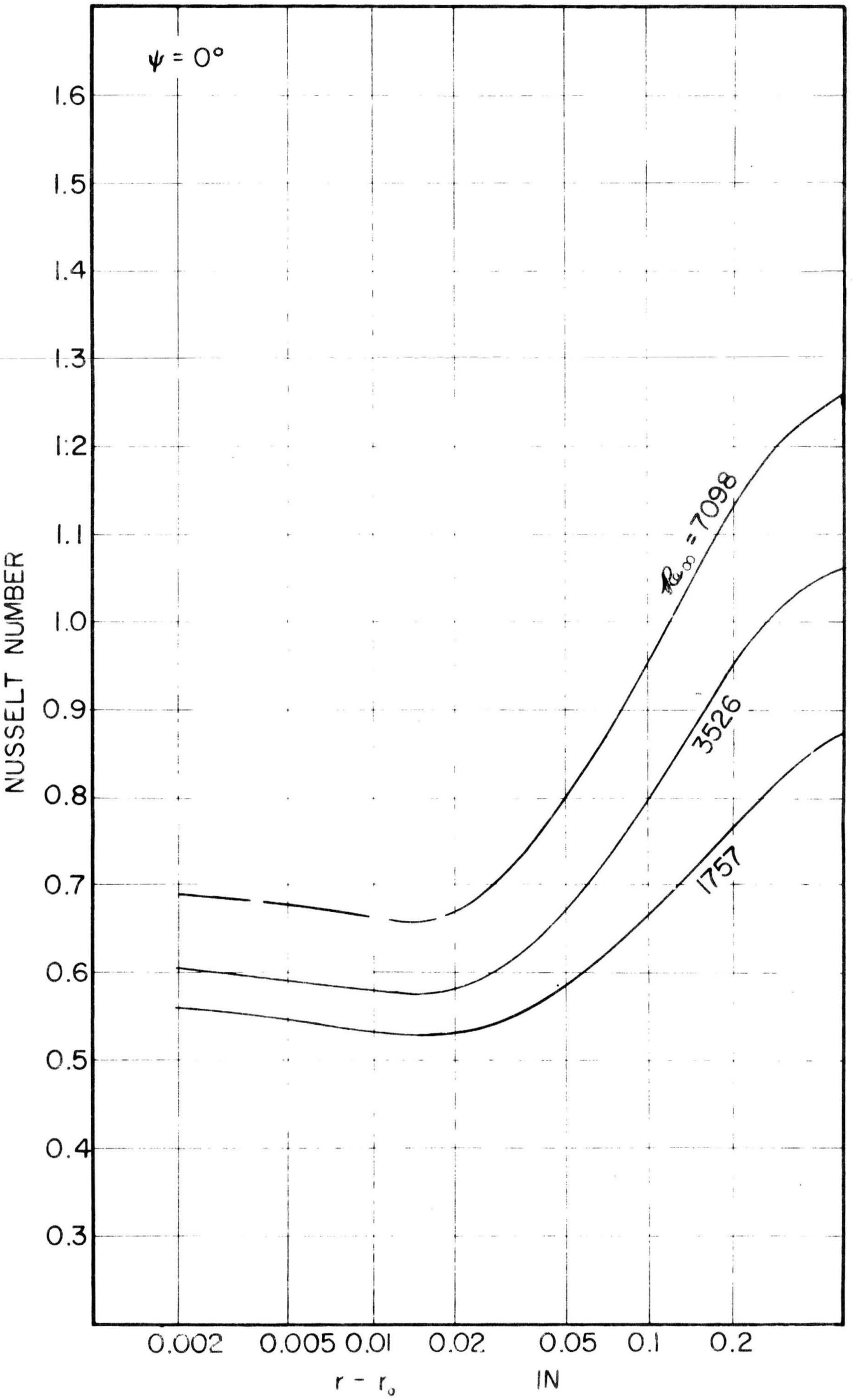

Figure 17: Dependence of Nusselt Number on Radial Distance from Cylinder Wall at Stagnation

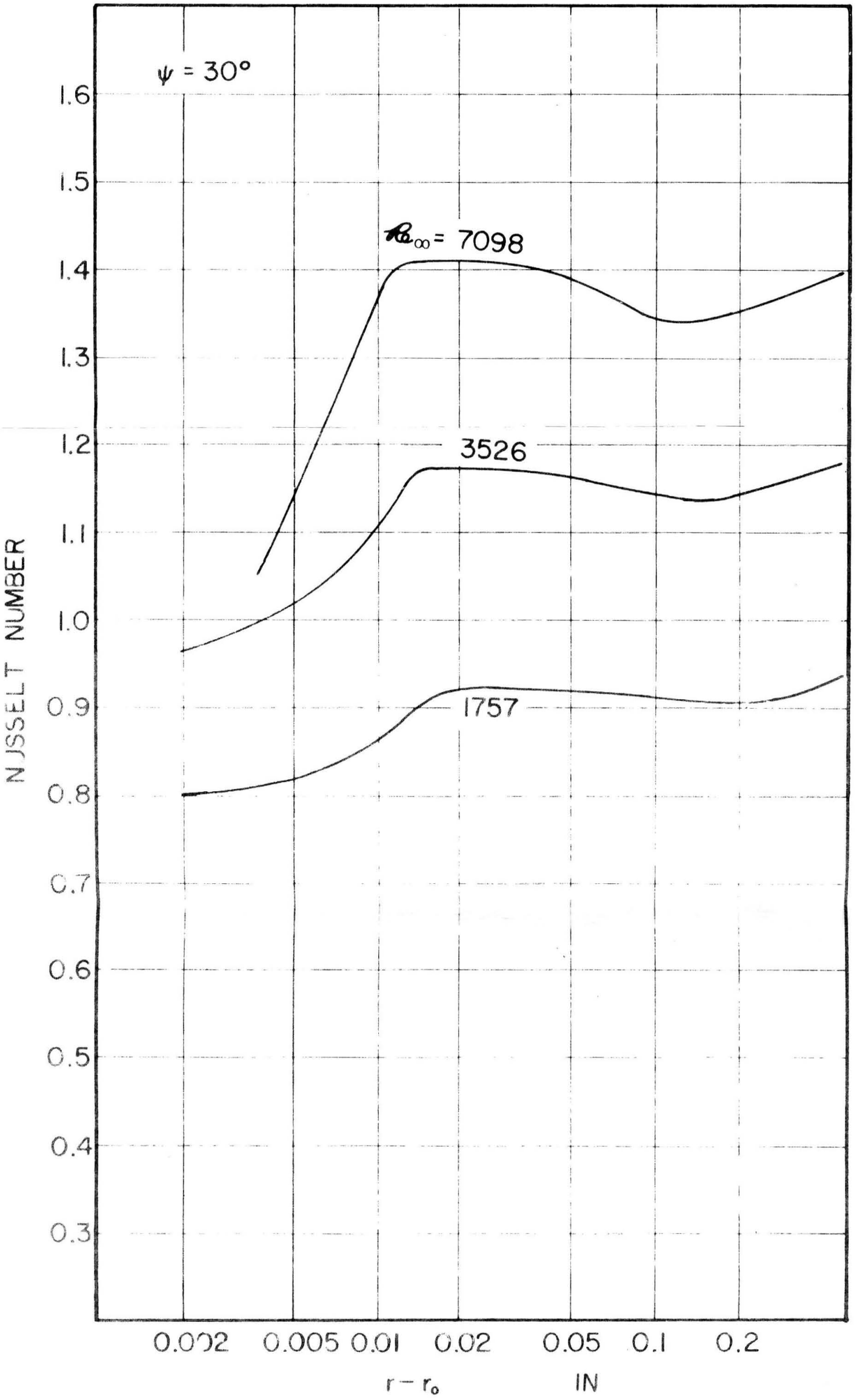

Figure 18: Dependence of Nusselt Number on Radial Distance from Cylinder Wall at 30° from Stagnation

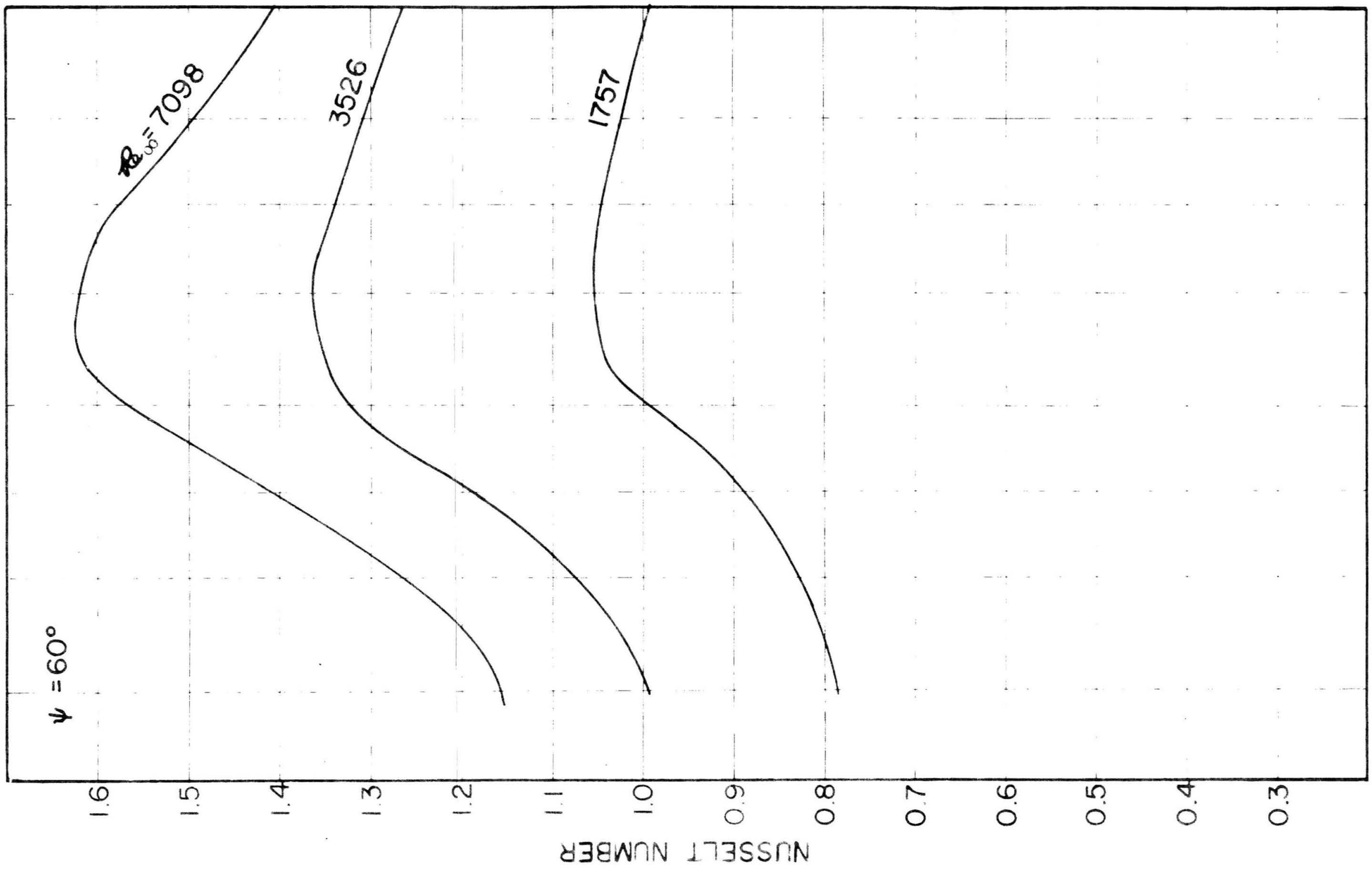

Figure 19: Dependence of Nusselt Number on Radial Distance from Cylinder Wall at 60° from Stagnation

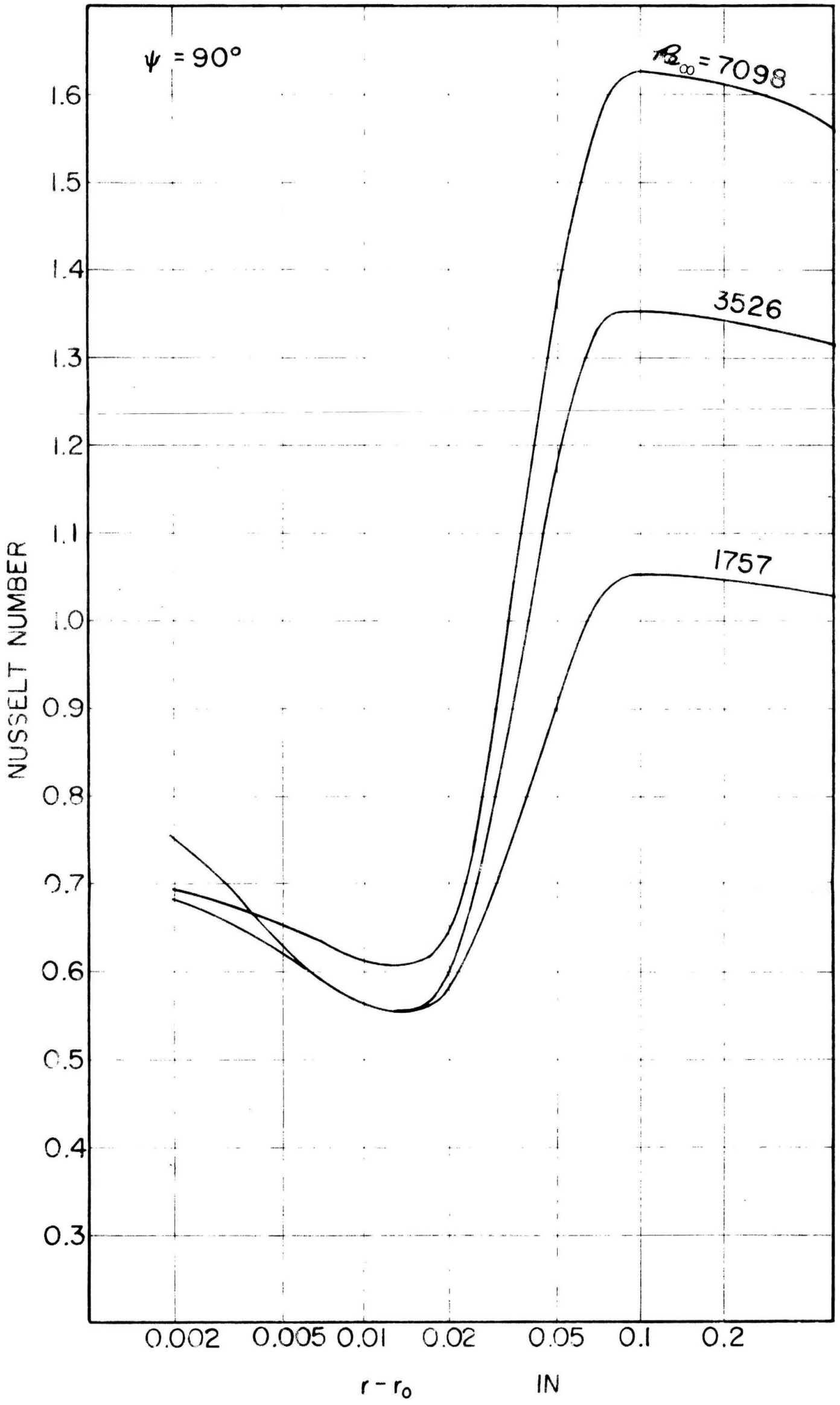

Figure 20: Dependence of Nusselt Number on Radial Distance from Cylinder Wall at 90° from Stagnation

DISCUSSION OF RESULTS

Accuracy of the Measurements

Because of the complexity of the measurements, an estimate of the accuracy of the results cannot be made conveniently without recourse to assumptions or empirical observation. Thus the error in the determination of temperature difference depends not only on the accuracy with which resistance measurements were made, but also on the accuracy of the calibration of the wire as a temperature measuring device, and on the relative accuracy of the instruments used to determine the resistance of the wire.

The relative accuracy of the Mueller bridge and the K-2 type and White potentiometers was determined by measuring the resistance of several precision resistors by two methods, one using the Mueller bridge and one using the two potentiometers. In this way it was established that the instruments were consistent to within 0.03%. Hence this value may be assumed to be the error involved in the difference in resistance of the wire as measured by the two methods. The error in a single resistor measurement with the Mueller bridge may be determined from the data presented in Table IV as about 0.0007 ohm absolute.

The derivative of resistance with respect to temperature was determined from measurements by means of the Mueller bridge in the range of 80 to 120 ^{o}F. In this interval the change in resistance was of about 0.52 ohms, so the maximum error in this difference was

0.3%. The error in temperature difference is of the order of 0.05%, so the error in the derivative may be as large as 0.35%. However, since the derivative of resistance with respect to temperature was established from more than two points, the error in this quantity may be taken as 0.10%.

From this data, the error in the temperature difference between the wire and the free stream was about 0.2 °F. This constitutes an error of 0.4% of the nominal temperature difference of 50 °F used in the determination of the Nusselt number field, but in some of the measurements used in establishing the dependence of experimental Nusselt number with conditions the error may be 4%.

The error in the measurement of power input to the wire may be estimated as 0.1%, so that the error in the electrical measurements may be expected to be 0.5%.

The largest uncertainties are those in the dimensions of the wire, since the length and the diameter were known only to within 1%. On this basis, the calculated heat transfer coefficients are known to within 2.5%, and the Nusselt numbers to within 1.5%. It should be remarked, however, that the consistency of the calculated resistances at the ice-point per unit length indicates that the errors in the dimensions may have been, fortuitously, lower than estimated.

Besides the errors in the quantities immediately relevant to the calculation of the Nusselt number, error in auxiliary measurements also affect the uncertainty with which the distribution of Nusselt number is determined. The error in the determination of position of the wire relative to the cylinder may be considered as 0.003 in. if the variation

of cylinder diameter is taken into consideration as well as the reproducibility of the point of contact.

The error in determining the Reynolds number is small compared to the variation of Reynolds number from test to test. This variation will be considered in the next section.

Reproducibility of Results

In general, the results were found to be reproducible to within experimental error. Values of the Nusselt number obtained at a given position during the same test, on different tests, and even with different wires, agreed to within the estimated error for most of the conditions investigated.

Values obtained at a nominal Reynolds number of 7100 at angles from stagnation greater than 45° constitute an exception to this generalization. In this region differences in the Nusselt number determined at a given position in different tests were of the order of 5%, as may be seen in the data for $x = -0.360$ in fig. 11.

In contrast to this behavior, the data closer to stagnation at a nominal Reynolds number of 7100, as well as all results at the lower Reynolds numbers, were considerably more reproducible. This may be seen by comparing the curves in figs. 11, 12, and 13 which contain duplicate sets of points, and is also evident from a comparison of the standard errors of estimate given in Table VIII.

The variations in Reynolds number from test to test do not, by themselves, account for this lack of reproducibility. This may be inferred from the dependence of Nusselt number on Reynolds number (12,

13,16) and from the fact that, with comparable variations in Reynolds number, the results are reproducible under all other conditions. It therefore seems reasonable to ascribe the variation of Nusselt number to variation of the flow field in this region caused by the slight changes in Reynolds number.

Characteristics of the Nusselt Number Field

The Nusselt number fields shown in figs. 14, 15, and 16 may be divided into two regions. Close to the cylinder the Nusselt number increases rapidly with radial distance, and curves of constant Nusselt number are roughly parallel to the cylinder wall. At larger distances from the cylinder, the variation of Nusselt number with radial position is relatively small.

The region close to the wall may further be subdivided. For angles between 0 and 70°, the lines of constant Nusselt number in this region intersect lines of constant angle only once; at larger angles, however, lines of constant Nusselt number have two intersections with lines of constant angle. This behavior indicates that the Nusselt number is rapidly increasing in the immediate vicinity of the wall. This effect, which may be seen from the traverse curves illustrated in figs. 11, 12, and 13, is not confined to this region, but also occurs in the outer region at small angles from stagnation. It is believed that this behavior is due to convection from the wire to the cylinder wall.

The appearance of the Nusselt number field in the vicinity of the

wall is indicated in figs. 21, 22, and 23 for the three Reynolds numbers studied. The use of logarithmic coordinates for the radial distance from the cylinder wall allows a clearer picture of the field to be given. The lines of constant Nusselt number, for values of this parameter lower than about 0.75, appear to consist of two detached segments, one in the region upstream of 30° and one in the region downstream of 70°. As mentioned earlier, the second segment intersects lines of constant angle twice. This behavior implies that the forward segment of this curve terminates at the cylinder wall or, more rigorously, one wire radius away from the wall.

For the higher Nusselt numbers shown in figs. 21, 22, and 23, the curves consist of a continuous segment over the region investigated. At intermediate values of the parameter the curves may be continuous or consist of distinct segments, however this cannot be decided on the basis of the experimental data; more accurate determination of the distance between the wire and the cylinder would be required to establish the behavior of these lines.

Comparison of the Results With Theory

The Nusselt number at any point in the flow field may be calculated from equation 6 or from equations 7 and 8, by making use of available correlations for Nusselt number as a function of Reynolds number. The correlation used in this work is that obtained by Collis and Williams (16). Values obtained in this way will be referred to as theoretical.

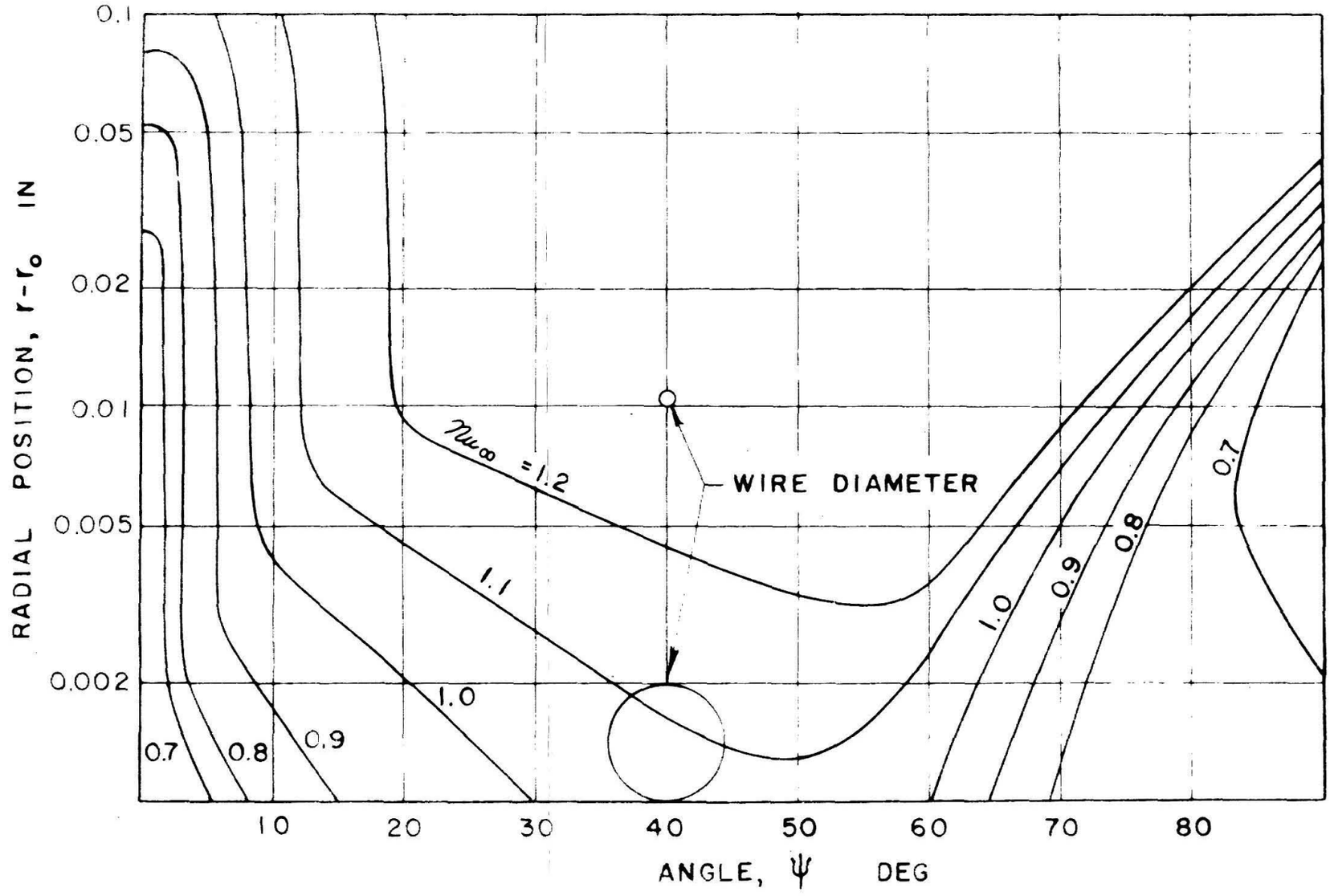

Figure 21: Nusselt Number Field Close to Cylinder at Re_{∞} = 7098

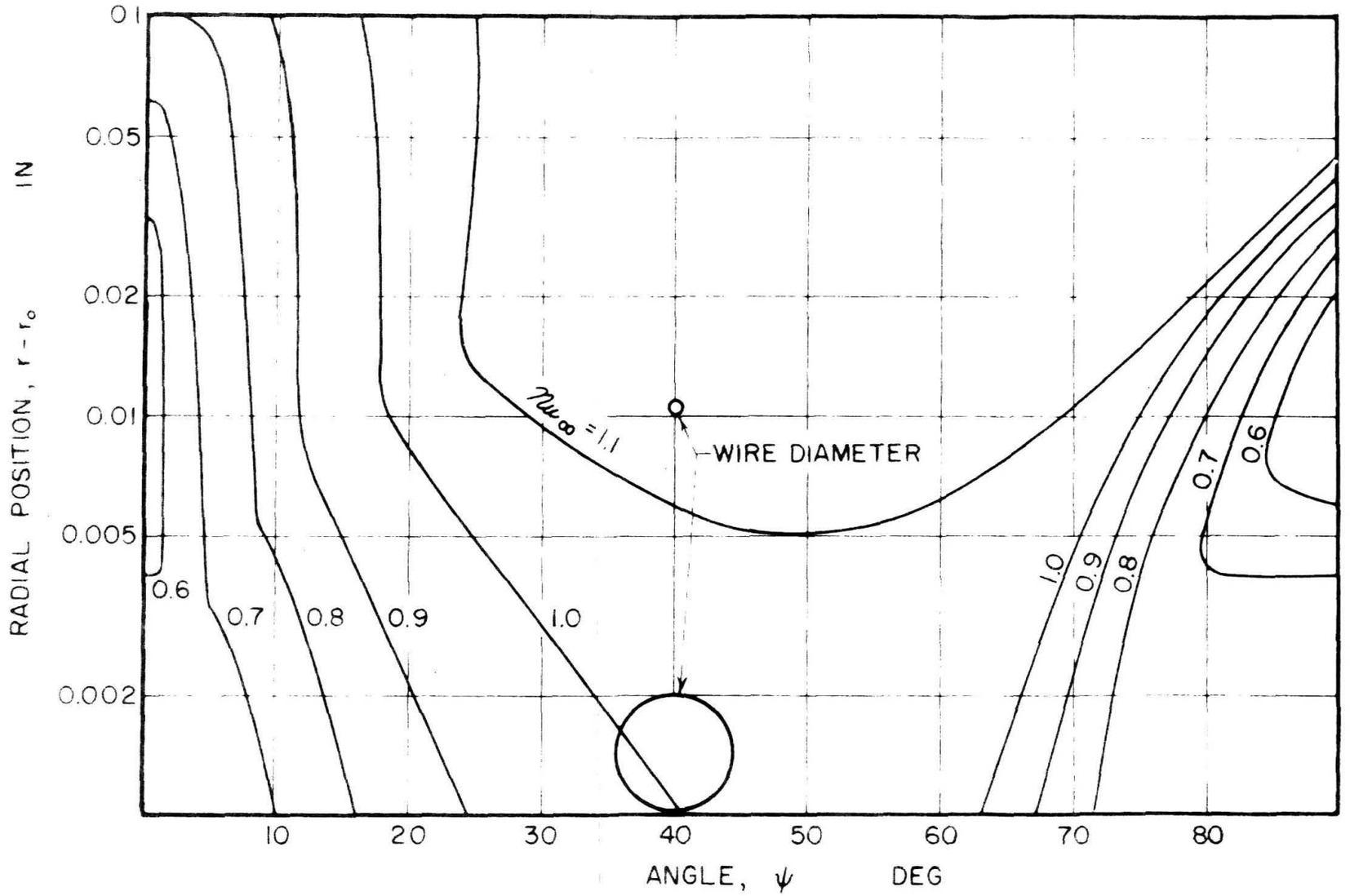

Figure 22: Nusselt Number Field Close to Cylinder at $Re_\infty = 3526$

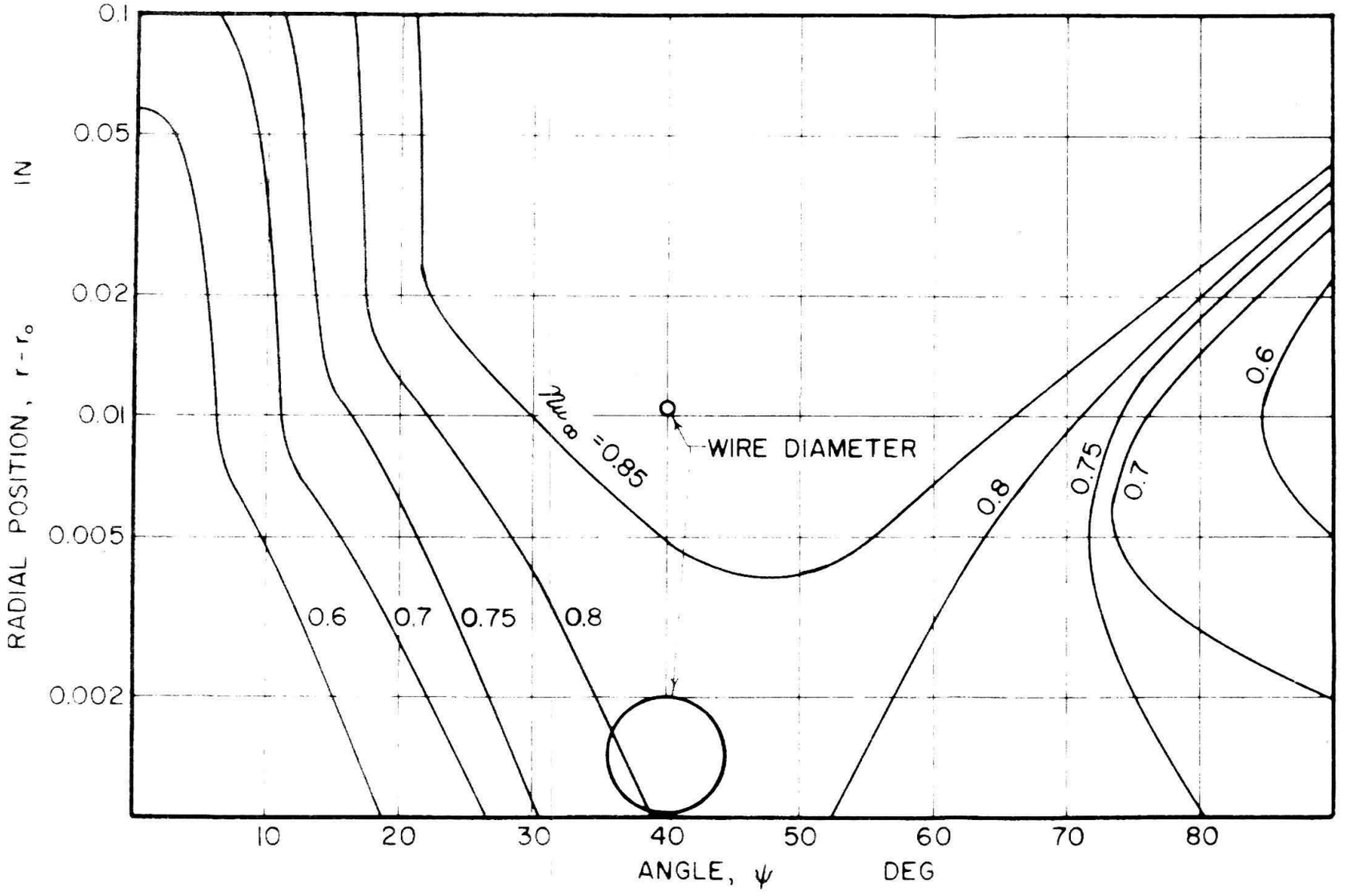

Figure 23: Nusselt Number Field Close to Cylinder at Re_∞ = 1757

The theoretical description of the Nusselt number distribution is subject to several limitations, these will be summarized before a quantitative comparison of experimental and predicted results is presented.

The velocity distributions described by equations 4, 5, 7, and 8 correspond to a cylinder in an infinite flow field. Thus they do not correspond closely to experimental conditions, in which the projected area of the cylinder was one-third of the area of the jet. Nevertheless, it is expected that reasonable agreement would be obtained in the region of stagnation.

A second limitation is that the boundary layer description is essentially an asymptotic solution for large Reynolds numbers (7,10). The Reynolds numbers used in this investigation are in the moderate range, so that the terms neglected in solving the equations of motion of the fluid are of the order of 1 to 5% of the terms retained (7).

The theoretical predictions obtained in this way correspond to the physical situation only in as much as the assumption made in hot-wire anemometry, that the Nusselt number depends only on the wire Reynolds number, is valid. Such predictions for the Nusselt number as function of radial distance are shown in figs. 24 and 25 for angles of 0 and 30° from stagnation. The results computed from potential flow theory are in fair agreement with experimental results. The curves obtained from boundary layer theory are not in agreement with the experimental results and, if the curve for a Reynolds number of 7098 at 30° from stagnation is excepted, the trends of the predicted

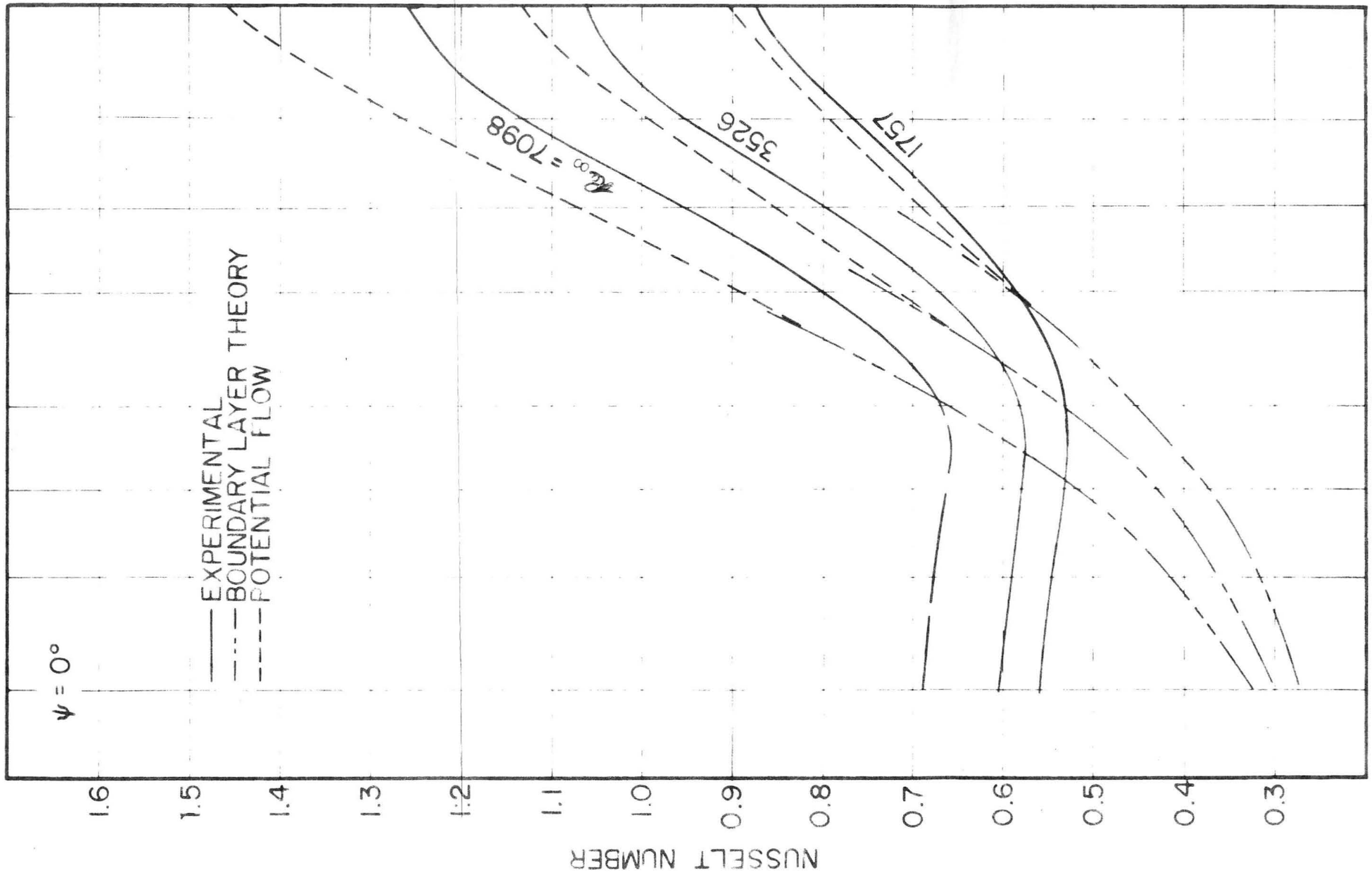

Figure 24: Comparison of Experimental Results at Stagnation with Theory

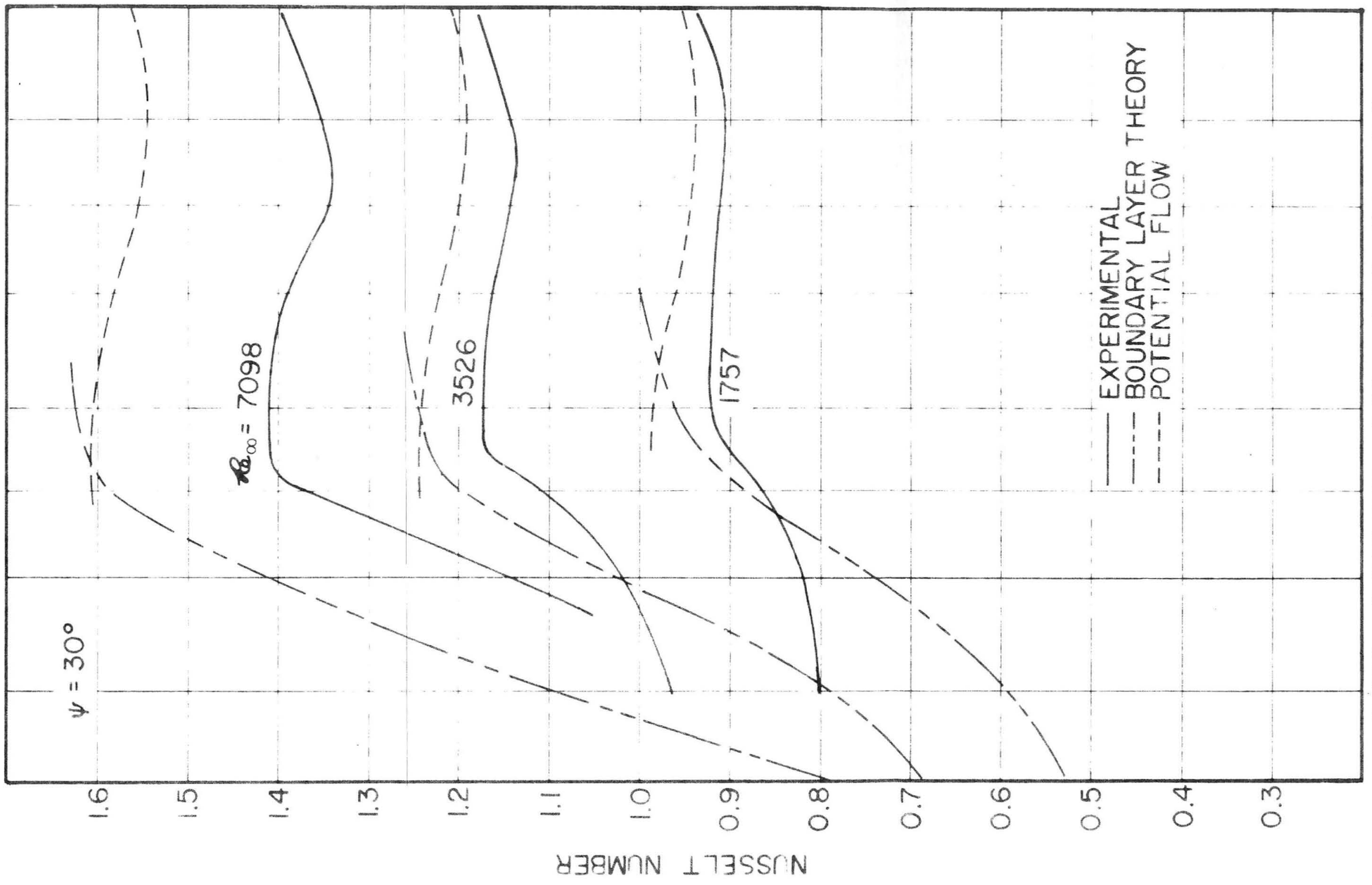

Figure 25: Comparison of Experimental Results at 30^{o} from Stagnation with Theory

and experimental curves differ appreciably. For the particular curve mentioned, the agreement is not good, but the trend of the experimental curve is very similar to that of the theoretical one.

The lack of agreement in the vicinity of the cylinder wall cannot be ascribed wholly to limitations in the theoretical description of the flow field. Regardless of the detailed description, it is well established that the fluid velocity tends to zero at the wall and, under such conditions, the Nusselt number should be monotonically increasing with radial distance if a one-to-one correspondence between Nusselt number and wire Reynolds number exists. The experimental data shown in fig. 24, as well as that presented in figs. 11, 12, 13, and 20, indicates that the curves are not all monotonic increasing in this region. Thus, by implication, the assumption that for a given wire Reynolds number there is one Nusselt number is not valid near the cylinder wall.

Two reasons may be advanced to account for these discrepancies. Firstly, as shown by Piercy, Richardson, and Winny (16) convection to the wall tends to increase the Nusselt number above that which would be obtained in the absence of a wall at the same wire Reynolds number. Secondly, thermal transport by natural convection becomes appreciable in the immediate vicinity of the wall (6,16) and tends to raise further the Nusselt number.

CONCLUSIONS

Experimental data on the heat transfer characteristics of a 0.001-in. wire in the boundary flow about a one-inch copper cylinder indicates that the Nusselt number may be considerably different from that predicted by using calculated velocity fields and correlations from the literature. These differences, which are most pronounced near the cylinder wall appear to be due to the increased importance of convection to the wall and of natural convection.

The experimental data obtained does not allow the formulation of conclusions as to the relative importance of these two effects. Data for this purpose could be obtained in several ways, such as by performing similar experiments using a cylinder constructed of material of low thermal conductivity. Under such circumstances the relative importance of convection to the cylinder wall would be greatly decreased, and the effect of natural convection could be determined.

In applying the results that have been presented it should be remembered that they were obtained with a cylinder temperature essentially equal to the free stream temperature. It is expected that if the temperature of the cylinder differs appreciably from the free stream temperature the relative importance of convection to the wall will significantly alter the heat transfer from the wire at small radial distances.

APPENDIX

The purpose of this appendix is to discuss briefly the nature of the corrections applied to the adjusted Nusselt number, and to summarize the quantitative aspects of these corrections.

The adjusted Nusselt number was defined in terms of the electrical power addition to the wire and the temperature difference between the wire and the air stream. This definition would apply rigorously if the ratio of the length of the wire to its diameter were infinite, if there were no radiation losses, and if the fluid were a continuum.

In the laboratory, however, these conditions are not obtained, and suitable corrections must be applied in order to obtain a value of the Nusselt number which will be independent of the geometrical dimensions of the wire.

The effect of radiation has been discussed, and it was shown that the largest errors involved in neglecting the transfer by this mechanism were of the order of 0.1%. The following discussion will therefore deal with effects of finite wire length and non-zero mean free path of the fluid molecules. In the course of this analysis it will be assumed that the fluid properties are constant, and that all properties of the wire, except its resistance, do not vary with temperature. These assumptions are justifiable because the corrections are small, so that the second order corrections which would arise from a more rigorous treatment are negligible. It will also be assumed that the convective heat flux from the wire is the same at all points on the wire surface.

Effect of Finite Length

Consider a wire such as that shown in fig. A1. If the resistance of the wire is assumed linear in temperature, then

$$R = R_{\infty}[1 + \alpha(t - t_{\infty})] \tag{A1}$$

If the temperature varies along the axis of the wire, the mean resistance is given by

$$R_w = \frac{R_{\infty}}{\ell} \int_{-\ell/2}^{\ell/2} [1 + \alpha(t - t_{\infty})]\, dz \tag{A2}$$

and for constant heat capacity and density, the mean temperature is given by

$$t_w = \frac{1}{\ell} \int_{-\ell/2}^{\ell/2} t\, dz \tag{A3}$$

Combining equations A2 and A3, there is obtained

$$R_w = R_{\infty}[1 + \alpha(t_w - t_{\infty})] \tag{A4}$$

The input of electrical energy to the wire is

$$\dot{q}_e = I^2 R_{\infty}[1 + \alpha(t_w - t_{\infty})] \tag{A5}$$

So the adjusted Nusselt number is given by

$$Nu^* = \frac{I^2 R_{\infty}[1 + \alpha(t_w - t_{\infty})]}{\pi \ell k_{\infty}(t_w - t_{\infty})} \tag{A6}$$

assuming that the measurements were carried out with a mean wire temperature of 150 °F and an air temperature of 100 °F.

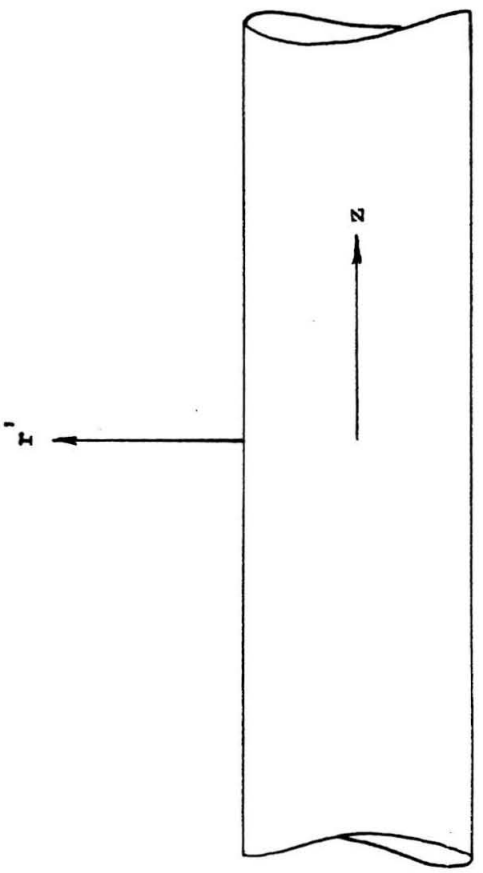

Figure A1: Diagram of Wire

If radiation is neglected, the energy equation for the wire may be written as (1, 4, 5)

$$\frac{d^2(t-t_\infty)}{dz^2} - \frac{4k_\infty}{d_w^2 k_s}\left(Nu_\ell - \frac{I^2 R_\infty \alpha}{\ell \pi k_\infty}\right)(t - t_\infty) = -\frac{4I^2 R_\infty}{\pi d_w^2 \ell k_s} \qquad (A7)$$

In equation A7 the parameter Nu_ℓ is the Nusselt number based on the convective heat flux. If the measurements had been made with an infinite wire carrying the same current and at a constant temperature t_ℓ, the Nusselt number Nu_ℓ could have been determined from the equation

$$Nu_\ell = \frac{I^2\left(\frac{R_\infty}{\ell}\right)[1 + \alpha(t_\ell - t_\infty)]}{\pi k_\infty (t_\ell - t_\infty)} \qquad (A8)$$

Combining equations A6 and A8 there results

$$Nu_\ell = Nu^* \frac{\beta_w}{\beta_\ell} \frac{1 + \beta_\ell}{1 + \beta_w} \qquad (A9)$$

where

$$\beta_w = \alpha(t_w - t_\infty) \qquad (A10)$$

and

$$\beta_\ell = \alpha(t_\ell - t_\infty) \qquad (A11)$$

If equation A7 is solved (28), and the results are combined with equations A8, A10, and A11, a description of the variation of temperature difference along the wire is obtained (1):

$$t - t_a = (t_\ell - t_a)\left[\, 1 - \frac{\cosh \frac{2z}{\ell}\,\frac{1}{s}\,(\beta_w/\beta_\ell)^{1/2}}{\cosh \frac{1}{s}\,(\beta_w/\beta_\ell)^{1/2}} \,\right] \qquad \text{(A12)}$$

where

$$s = \frac{d_w}{\ell}\left(\frac{1+\beta_w}{Nu_\ell}\right)^{1/2}\left(\frac{k_s}{k_\infty}\right)^{1/2} \qquad \text{(A13)}$$

Combining equations A3 and A12, there results

$$\frac{\beta_w}{\beta_\ell} = 1 - s(\beta_\ell/\beta_w)^{1/2}\tanh[1/s(\beta_w/\beta_\ell)^{1/2}] \qquad \text{(A14)}$$

Equation A14 implicitly defines a function such that

$$\frac{\beta_w}{\beta_\ell} = f(s) \qquad \text{(A15)}$$

For small values of s, a good approximation of this function is given by (1):

$$f(s) = 1 - 1.1s \qquad \text{(A16)}$$

If the parameter s were known, the ratio β_w/β_ℓ could then be found, and from a knowledge of the wire characteristics and its mean temperature, the value of the Nusselt number Nu_ℓ could be obtained by equation A9. In general successive approximations must be made because s, as defined by equation A13, involves the parameter Nu_ℓ. However, if the correction is small, the error introduced by using the adjusted Nusselt number in the calculation of s is extremely small.

Effect of Temperature Jump

When a surface at a temperature t_w is immersed in a gas, the temperature of the gas at the interface, t_{ai}, may be determined by the equation (29):

$$t_{ai} = t_w - g\left(\frac{\partial t_a}{\partial r'}\right)_{r'=0} \tag{A17}$$

where

$$g = \frac{2-a}{a}\ \frac{4c\gamma}{\gamma+1}\ \frac{\lambda}{Pr} \tag{A18}$$

In equation A18, a is the accomodation coefficient, γ is the ratio of the isobaric to the isochoric specific heat, λ is the mean free path of the gas molecules, Pr is the Prandtl number of the gas, and c is a constant which depends on the kinetic model used for the gas, but differs only slightly from 0.50. For platinum in air, the value of g is very nearly twice the mean free path of the molecules (16,17) so the temperature of air at an air platinum interface is given approximately by

$$t_{ai} = t_w - 2\lambda\left(\frac{\partial t}{\partial r'}\right)_{r'=0} \tag{A19}$$

The convective flux is given by

$$\dot{q}_c = Nu_\ell (t_w - t_\infty)\ \frac{k_\infty}{d_w} \tag{A20}$$

if the temperature difference between the wire and the free stream is considered as the driving force. However, if the driving force is taken as the difference in temperature between the air at the interface and the

air at free stream conditions, the heat flux may be expressed as

$$\dot{q}_c = Nu_{\ell,\lambda}(t_{ai} - t_\infty) \frac{k_\infty}{d_w} \tag{A21}$$

Combining equations A20 and A21 there results

$$Nu_{\ell,\lambda} = Nu_\ell \frac{t_w - t_\infty}{t_{ai} - t_\infty} \tag{A22}$$

Finally, combining equations A19 with A22, there results

$$Nu_{\ell,\lambda} = \frac{Nu_\ell}{1 - 2\frac{\lambda}{d_w} Nu_\ell} \tag{A23}$$

Experimental results (16) have shown that the parameter $Nu_{\ell,\lambda}$ is independent of wire dimensions, whereas the parameter Nu_ℓ is not, thus supporting the hypothesis that the difference in temperature between the air at the interface and the air in the free stream should be considered as the driving force for convective heat transfer. Equation A22 has also been derived from the differential equations of transport (17).

Determination of the Correction Factor

In view of the experimental support (16) for the validity of the correction for temperature jump, the parameter $Nu_{\ell,\lambda}$ is the Nusselt number of greatest interest. Accordingly, the values of the Nusselt number used in this report are corrected for both finite length and temperature jump, that is

$$Nu_\infty \equiv Nu_{\ell,\lambda} \tag{A24}$$

In the text, the Nusselt number, Nu_{∞}, was defined by equation 17 as:

$$Nu_{\infty} = \xi Nu_{\ell,\lambda} \tag{A25}$$

Combining equations A9, A23, A24, and A25, the correction factor, ξ, is given by

$$\xi = \frac{\frac{\beta_w}{\beta_\ell} \frac{1+\beta_\ell}{1+\beta_w}}{1 - 2 \frac{\lambda}{d_w} Nu^* \frac{\beta_w}{\beta_\ell} \cdot \frac{1+\beta_\ell}{1+\beta_w}} \tag{A26}$$

Equation A26 thus describes the factor ξ in terms of quantities which can be calculated from experimental data.

REFERENCES

1. Kovasznay, L. S. G., "Turbulence Measurements," in Physical Measurements in Gas Dynamics and Combustion, R. W. Ladenburg, ed., Princeton University Press, Princeton (1954).

2. Kinze, J. O., Turbulence, McGraw-Hill Book Co., Inc., New York (1959).

3. Short, W. W. and Sage, B. H., A. I. Ch. E. Journal, 6, 163 (1960).

4. Smith, L. E., Trans. A. S. M. E., 72, 70 (1950).

5. Short, W. W., Ph. D. Thesis, California Institute of Technology, Pasadena (1958).

6. Piercy, N. A. V., Richardson, E. G., and Winny, H. F., Proc. Phys. Soc., 69, 731 (1956).

7. Schlichting, H., Boundary Layer Theory, McGraw-Hill Book Co., Inc., New York (1955).

8. Corcoran, W. H., Opfell, J. B., and Sage, B. H., Momentum Transfer in Fluids, Academic Press, New York (1956).

9. Streeter, V. L., Fluid Dynamics, McGraw-Hill Book Co., Inc., New York (1948).

10. Prandtl, L., Proc. III Intern. Math. Congr., Heidelberg (1904).

11. Oseen, C. W., Arkiv fur Mathematik, astronomi och fysik, 6, No. 29 (1910).

12. Cole, J., and Roshko, A., "1954 Heat Transfer and Fluid Mechanics Institute," California Book Co., Ltd., Berkeley (1954).

13. McAdams, W. H., Heat Transmission, McGraw-Hill Book Co., Inc., New York (1954).

14. Coulson, J. M., and Richardson, J. F., Chemical Engineering, McGraw-Hill Book Co., Inc., New York (1956).

15. Smith, J. C., Can. J. Chem. Eng., 39, 106 (1961).

16. Collis, D. C., and Williams, M. J., J. Fluid Mech., 6, 357 (1959).

17. Levey, H. C., J. Fluid Mech., 6, 385 (1959).

18. Sage, B. H., Ms. 2852, Department of Chemical Engineering, California InstituteofTe chnology, Pasadena (1958).

19. National Bureau of Standards, Circular 564, Tables of Thermal Properties of Gases, U. S. Dept. of Commerce, Washington (1955).

20. Sato, K., Ph. D. Thesis, California Institute of Technology, Pasadena (1955).

21. Hsu, N. T., Ph. D. Thesis, California Institute of Technology, Pasadena (1956).

22. Corcoran, W. H., Page, F., Jr., Schlinger, W. G., and Sage, B. H., Ind. Eng. Chem., 44, 410 (1952).

23. Brown, R. A. S., Student Report 742, Department of Chemical Engineering, California Institute of Technology, Pasadena (1957).

24. Ms. 2580, Department of Chemical Engineering, California Institute of Technology, Pasadena (1953).

25. Mickley, H. S., Sherwood, T. K., and Reed, C. E., Applied Mathematics in Chemical Engineering, McGraw-Hill Book Co., Inc., New York (1957).

26. Mueller, E. F., private communcation to the editors of "International Critical Tables," reported in International Critical Tables, Vol. VI, p. 136, McGraw-Hill Book Co., Inc., New York (1929).

27. Wenner, and Lindberg, private communication to the editors of "International Critical Tables," reported in International Critical Tables, Vol. VI, p. 136, McGraw-Hill Book Co., Inc., New York (1929).

28. Carslaw, H. S., and Jaeger, J. C., Conduction of Heat in Solids, Oxford University Press, Oxford (1959).

29. Kennard, E. H., Kinetic Theory of Gases, McGraw-Hill Book Co., Inc., New York (1938).

NOMENCLATURE

Roman

a	accommodation coefficient
A	area of jet opening, sq. ft.
b	specific gas constant
B_1, B_2, B_3	constants in equation 21
c	constant in equation A18
C_p	isobaric heat capacity, Btu/lb. $^{\circ}F$
C_v	isochoric heat capacity, Btu/lb. $^{\circ}F$
d	diameter, ft.
D	substantial derivative operator, $\frac{\partial}{\partial \theta} + \vec{u} \cdot \nabla$, sec.$^{-1}$
E	internal energy, Btu/lb.
E_s	potential difference across standard resistor, volt absolute
E_w	potential difference across wire, vote absolute
f	a function
F	body force, lb./cu. ft.
h	heat transfer coefficient, Btu/sq. ft. sec. $^{\circ}F$
I	current, amperes absolute
I_n	modified Bessel function of the first kind of order n
k	thermal conductivity of the fluid, Btu/sq. ft. sec. ($^{\circ}F$/ft.)
k_w	thermal conductivity of wire, Btu/sq. ft. sec. ($^{\circ}F$/ft.)
K_n	modified Bessel function of the second kind of order n
ℓ	length of wire, ft.
$\dot{m}$	total material flux, lb./sec.
Nu	Nusselt number

Nu_e	experimental Nusselt number
Nu_s	smooth value of Nusselt number
P	pressure, lb./sq. ft.
Pr	Prandtl number
$\dot{q}$	heat flux, Btu/sq. ft. sec.
$\dot{q}_c$	convective heat flux, Btu/sq. ft. sec.
$\dot{q}_e$	total electrical power input, Btu/sec.
r	radial distance from centerline of cylinder, ft. or in.
r_o	radius of cylinder, ft. or in.
r'	radial distance from wire surface, ft.
R	resistance of wire, ohm absolute
R_o	resistance of wire at ice-point, ohm absolute
R_s	resistance of standard resistor, ohm absolute
Re	Reynolds number
s	parameter defined in equation A13
t	temperature, ^oF
t_a	arbitrary average temperature, ^oF
$t_{1/4}$	average temperature defined in equation 26
T	absolute temperature, ^oF
u	local velocity, ft./sec.
U	bulk velocity, ft./sec.
V	specific volume, cu. ft./lb.
x	Cartesian coordinate in direction of flow, measured from cylinder axis, ft. or in.
y	Cartesian coordinate in horizontal direction, measured from cylinder axis, ft. or in.

z	Cartesian coordinate parallel to cylinder axis, measured from the centerline of the wire, ft.
Z	compressibility factor

Greek

α	derivative of normalized resistance with respect to temperature, $d(R/R_o)/dt$, $(^oF)^{-1}$
β_ℓ, β_w	parameters defined in equations A11 and A10 respectively
γ	ratio of heat capacities, C_p/C_v
δ_{ij}	Kronecker delta
η	viscosity of fluid, lb./ft. sec.
θ	time, sec.
λ	mean free path of gas molecules, ft.
ξ	correction factor
ρ	density, lb. $sec.^2/ft.^4$
σ	specific weight, lb./cu. ft.
σ_e	standard error of estimate
σ_v	sample estimate of population variance
ϕ	dissipation function, Btu/cu. ft./sec.
ψ	angle from stagnation, degrees or radians
Ω	distance parameter defined in equation 9

Superscripts

$\rightarrow$	vector
*	adjusted to reference conditions

Subscripts

a	air
ai	air at air-solid interface
b	boundary layer
i, j	dummy variables
ℓ	corrected for finite length
n	index
p	potential flow
r	radial component
s	platinum
w	wire
α	evaluated at t_α
λ	corrected for mean free path effects
ψ	tangential component
1/4	evaluated at $t_{1/4}$
100	evaluated at $100^\circ F$
112.5	evaluated at $112.5^\circ F$
∞	evaluated at free-stream conditions

TABLE I

PROPERTIES OF AIR

Temperature ^{o}F	Thermal Conductivity Btu/sec. ft^2 (^{o}F/ft)	Absolute Viscosity lb. sec. /ft^2
100	4.347×10^{-6}	3.98×10^{-7}
120	4.480	4.09
140	4.614	4.29
160	4.747	4.30
180	4.881	4.40
200	5.014	4.50

TABLE II

VELOCITY DISTRIBUTION IN AIR STREAM

Distance From Jet Centerline in.	Distance Above Jet Opening: 1 in. Nu_∞	1 in. u ft/sec	2 in. Nu_∞	2 in. u ft/sec
0.800	1.2766	8.170	1.2808	8.245
0.600	1.2762	8.165	1.2750	8.140
0.400	1.2762	8.165	1.2761	8.165
0.200	1.2760	8.160	1.2801	8.235
0.000	1.2835	8.295	1.2769	8.175
-0.200	1.2834	8.295	1.2802	8.235
-0.400	1.2845	8.310	1.2831	8.290
-0.600	1.2907	8.425	1.2889	8.390
-0.800	1.2924	8.455	1.2920	8.450

TABLE III

EXPERIMENTAL CONDITIONS

Test	Date	Wire No.	Number of Traverse	Pressure psia	Weight Fraction Water	Air Temp. °F	Cyl. Temp. °F	Gross Air Vel. ft/sec	Re_∞
348	12/15/60	1	5	14.455	0.0063	100.28	99.98	15.752	7122
350a	12/20/60	1	1	14.449	0.0043	100.34	99.97	15.780	7135
350b	12/21/60	1	5	14.364	0.0045	100.32	99.95	15.776	7133
352	12/22/60	1	6	14.349	0.0047	100.32	99.93	15.772	7131
359	1/27/61	1	4	14.424	0.0068	100.44	99.90	15.413	6969
363	2/6/61	1	6	14.356	0.0068	100.58	100.04	7.832	3548
369	2/13/61	2	3	14.375	0.0086	100.34	100.06	7.805	3529
372	2/16/61	2	4	14.276	0.0094	100.49	100.08	7.822	3537
373	2/20/61	2	5	14.417	0.0062	100.41	99.98	7.851	3550
376	2/22/61	2	4	14.305	0.0058	100.46	100.00	7.678	3472
377	2/23/61	2	2	14.359	0.0053	100.37	99.95	3.874	1752
379	2/27/61	3	6	14.414	0.0044	100.48	99.98	3.892	1760
380	3/1/61	3	6	14.396	0.0053	100.43	99.98	3.893	1760
382	3/8/61	4	2[a]	14.395	0.0045	100.42	--	7.817	3535

[a] These two traverses are given in Table II.

TABLE IV

CHARACTERISTICS OF PLATINUM WIRES

Wire Number	R_o ohm abs.	$B_1 \times 10^2$	$B_2 \times 10^3$ $(^oF)^{-1}$	$B_3 \times 10^7$ $(^oF)^{-2}$	R_o/ℓ $\frac{\text{ohm abs.}}{\text{ft.}}$	N	σ_v [a] ohm abs.
1	6.3890	-6.871	2.153	-1.79	59.0	12	0.0009
2	6.1009	-6.866	2.152	-1.79	59.0	3	0.0005
3	6.0661	-6.866	2.152	-1.79	58.7	-	-
4	6.3933	-6.811	2.134	-1.77	59.0	9	0.0009
Pure Pt	-	-7.095	2.213	-1.81	59.1	-	-

a) $$\sigma_v = \left[\frac{\sum_{i=1}^{N} (R_{oi} - \overline{R}_o)^2}{N - 1} \right]^{1/2}$$

TABLE V

VARIATION OF THE ADJUSTED NUSSELT NUMBER WITH TEMPERATURE DIFFERENCE

Test	Traverse	Position		Number of Points	$\frac{dNu^*}{d\Delta t} \times 10^4$
		-x in.	y in.		$(^oF)^{-1}$
359	1	0.896	0.000	5	-1.05
359	1	0.696	0.000	5	-1.90
359	2	0.596	0.000	4	0.14
359	2	0.546	0.000	4	-0.22
359	2	0.521	0.000	5	1.33
359	3	0.000	0.857	3	9.57
359	3	0.000	0.757	3	8.88
359	3	0.000	0.657	3	2.87
359	4	0.000	0.557	3	-4.59
359	4	0.000	0.507	3	-0.18
376	1	0.886	0.000	4	0.00
376	1	0.686	0.000	4	-0.22
376	1	0.536	0.000	3	0.54
376	2	0.866	0.200	3	-1.34
376	2	0.686	0.200	3	-0.95
376	2	0.486	0.200	3	-2.00
376	2	0.461	0.200	3	-7.16
376	3	0.286	0.919	3	-11.17
376	3	0.286	0.719	3	-1.46
376	3	0.286	0.519	2	-0.74
376	3	0.286	0.449	2	2.32
376	3	0.286	0.429	3	-11.03
377	1, 2	0.886	0.000	4	-0.99
377	1, 2	0.786	0.000	4	-0.58
377	1, 2	0.686	0.000	4	-0.27
377	1, 2	0.586	0.000	4	0.06
377	1, 2	0.536	0.000	4	0.93
377	1, 2	0.511	0.000	4	1.30
377	1, 2	0.501	0.000	4	1.08
Average					-0.57

TABLE VI. EXPERIMENTAL RESULTS
A) $Re_\infty = 7098$

-x in.	y in.	Δt ^oF	$h \times 10^2$ Btu/sec.ft^2 ^oF	Nu_e	Nu^*	Nu_∞
		Test 348		Traverse 1		
-0.036	0.978	67.06	8.481	1.6293	1.6186	1.5824
-0.036	0.878	66.97	8.517	1.6362	1.6256	1.5893
-0.036	0.778	66.94	8.534	1.6394	1.6288	1.5926
-0.036	0.678	66.93	8.582	1.6486	1.6380	1.6017
-0.036	0.578	66.91	8.454	1.6242	1.6137	1.5774
-0.036	0.528	66.86	3.313	0.6365	0.6324	0.6037
-0.036	0.508	66.90	3.482	0.6690	0.6647	0.6353
-0.036	0.503	66.93	3.512	0.6747	0.6703	0.6409
-0.036	0.500	66.95	3.721	0.7147	0.7101	0.6800
-0.036	0.501	66.98	3.571	0.6860	0.6816	0.6519
-0.036	0.498	67.00	3.443	0.6614	0.6571	0.6278
-0.036	0.528	67.04	3.291	0.6323	0.6282	0.5995
-0.036	0.523	67.07	3.336	0.6409	0.6367	0.6079
-0.036	0.538	67.11	3.702	0.7111	0.7065	0.6764
-0.036	0.563	59.74	7.465	1.4341	1.4287	1.3926
-0.036	0.603	59.23	8.629	1.6578	1.6518	1.6156
-0.036	0.778	59.00	8.543	1.6411	1.6354	1.5992
-0.036	0.878	58.96	8.523	1.6373	1.6317	1.5954
-0.036	0.978	57.99	8.558	1.6441	1.6390	1.6027
-0.036	0.778	57.96	8.604	1.6529	1.6478	1.6116
-0.036	0.578	57.94	8.512	1.6353	1.6302	1.5940
-0.036	0.528	57.90	3.298	0.6335	0.6316	0.6028
-0.036	0.508	57.86	3.464	0.6655	0.6634	0.6341
-0.036	0.518	57.84	3.429	0.6588	0.6568	0.6276
-0.036	0.538	57.82	3.726	0.7158	0.7136	0.6835
-0.036	0.553	57.77	6.219	1.1947	1.1910	1.1558
-0.036	0.543	57.73	4.419	0.8489	0.8464	0.8143
-0.036	0.578	57.68	8.513	1.6354	1.6305	1.5943
-0.036	0.678	57.51	8.630	1.6579	1.6531	1.6169
-0.036	0.878	57.59	8.589	1.6500	1.6451	1.6089

TABLE VI. (Continued)
A) $Re_\infty = 7098$

-x in.	y in.	Δt °F	$h \times 10^2$ Btu/sec. ft^2 °F	Nu_e	Nu^*	Nu_∞
		Test 348		Traverse 2		
0.064	0.978	57.91	8.511	1.6351	1.6301	1.5938
0.064	0.878	58.12	8.511	1.6351	1.6299	1.5937
0.064	0.778	58.39	8.526	1.6380	1.6326	1.5964
0.064	0.678	58.59	8.550	1.6424	1.6370	1.6007
0.064	0.578	58.88	8.555	1.6436	1.6379	1.6017
0.064	0.528	58.85	7.839	1.5059	1.5007	1.4645
0.064	0.508	58.82	4.187	0.8044	0.8016	0.7702
0.064	0.498	58.79	3.709	0.7125	0.7101	0.6800
0.064	0.518	58.76	6.325	1.2151	1.2110	1.1756
0.064	0.553	58.72	8.548	1.6421	1.6365	1.6003
0.064	0.513	58.33	5.330	1.0239	1.0206	0.9867
0.064	0.578	58.22	8.572	1.6467	1.6415	1.6053
0.064	0.678	57.83	8.545	1.6415	1.6365	1.6003
0.064	0.778	57.48	8.532	1.6391	1.6343	1.5981
		Test 348		Traverse 3		
0.164	0.978	51.86	8.254	1.5857	1.5844	1.5481
0.164	0.878	51.83	8.258	1.5865	1.5853	1.5490
0.164	0.778	51.82	8.290	1.5926	1.5914	1.5551
0.164	0.678	51.79	8.338	1.6018	1.6006	1.5643
0.164	0.578	51.76	8.435	1.6204	1.6191	1.5829
0.164	0.528	51.75	8.502	1.6332	1.6320	1.5958
0.164	0.503	51.74	8.503	1.6336	1.6324	1.5961
0.164	0.488	51.72	7.748	1.4885	1.4874	1.4512
0.164	0.478	51.69	5.598	1.0754	1.0746	1.0402
0.164	0.473	51.68	5.498	1.0563	1.0555	1.0213
0.164	0.498	51.65	8.421	1.6177	1.6165	1.5803
0.164	0.552	51.63	8.494	1.6317	1.6306	1.5944
0.164	0.628	51.89	8.381	1.6100	1.6087	1.5724

TABLE VI. (Continued)
A) $Re_\infty = 7098$

-x in.	y in.	Δt ^oF	$h \times 10^2$ Btu/sec. ft^2 ^oF	Nu_e	Nu^*	Nu_∞
		Test 348		Traverse 4		
0.264	0.978	53.11	8.270	1.5888	1.5868	1.5505
0.264	0.878	53.28	8.243	1.5835	1.5814	1.5451
0.264	0.778	53.20	8.283	1.5912	1.5892	1.5529
0.264	0.678	53.13	8.323	1.5990	1.5970	1.5607
0.264	0.578	52.75	8.469	1.6270	1.6252	1.5890
0.264	0.478	52.91	8.576	1.6476	1.6456	1.6094
0.264	0.438	52.87	7.750	1.4889	1.4872	1.4510
0.264	0.428	52.79	6.786	1.3036	1.3021	1.2664
0.264	0.468	52.70	8.587	1.6496	1.6478	1.6116
0.264	0.528	52.65	8.461	1.6254	1.6236	1.5874
0.264	0.628	52.63	8.344	1.6030	1.6012	1.5650
		Test 348		Traverse 5		
0.364	0.778	52.55	8.203	1.5758	1.5741	1.5379
0.364	0.678	52.53	8.218	1.5787	1.5771	1.5408
0.364	0.578	52.53	8.254	1.5857	1.5841	1.5478
0.364	0.478	52.51	8.336	1.6014	1.5997	1.5635
0.364	0.378	52.48	8.426	1.6187	1.6171	1.5809
0.364	0.358	52.46	7.543	1.4492	1.4477	1.4115
0.364	0.368	52.45	8.243	1.5835	1.5819	1.5456
0.364	0.363	52.44	7.977	1.5324	1.5309	1.4946
0.364	0.353	52.43	6.855	1.3169	1.3156	1.2798
0.364	0.478	52.42	8.285	1.5916	1.5900	1.5537

TABLE VI. (Continued)
A) $Re_\infty = 7098$

-x in.	y in.	Δt ^oF	$h \times 10^2$ Btu/sec. ft^2 ^oF	Nu_e	Nu^*	Nu_∞
		Test 350a		Traverse 1		
0.860	0.174	75.14	6.966	1.3382	1.3254	1.2895
0.760	0.174	74.60	6.785	1.3034	1.2912	1.2555
0.660	0.174	74.35	6.592	1.2662	1.2545	1.2190
0.560	0.174	73.84	6.598	1.2675	1.2560	1.2204
0.510	0.174	73.73	6.776	1.3016	1.2898	1.2541
0.485	0.174	73.61	6.808	1.3077	1.2959	1.2602
0.475	0.174	73.19	6.067	1.1655	1.1552	1.1202
0.480	0.174	64.66	6.615	1.2707	1.2636	1.2280
0.485	0.174	64.56	6.827	1.3113	1.3040	1.2682
0.490	0.174	64.46	6.863	1.3184	1.3111	1.2752
0.500	0.174	64.46	6.811	1.3084	1.3011	1.2653
0.510	0.174	64.56	6.747	1.2916	1.2888	1.2531
0.535	0.174	64.41	6.648	1.2771	1.2700	1.2344
0.860	0.174	64.16	6.957	1.3365	1.3292	1.2933
0.760	0.174	64.23	6.746	1.2959	1.2888	1.2531
0.660	0.174	64.11	6.572	1.2625	1.2557	1.2201
0.560	0.174	64.15	6.561	1.2603	1.2534	1.2179
0.535	0.174	64.05	6.640	1.2755	1.2686	1.2330
0.520	0.174	64.14	6.682	1.2836	1.2766	1.2409
0.510	0.174	64.14	6.747	1.2960	1.2889	1.2532
0.500	0.174	64.01	6.807	1.3075	1.3005	1.2647
0.490	0.174	63.96	6.856	1.3170	1.3099	1.2741
0.485	0.174	64.03	6.813	1.3088	1.3017	1.2660
0.480	0.174	63.80	6.624	1.2724	1.2656	1.2300
0.475	0.174	64.05	6.036	1.1595	1.1533	1.1183
0.510	0.174	63.80	6.756	1.2977	1.2909	1.2551
0.760	0.174	63.89	6.754	1.2973	1.2904	1.2547

TABLE VI. (Continued)
A) $Re_\infty = 7098$

-x in.	y in.	Δt ^oF	$h \times 10^2$ Btu/sec. ft^2 ^oF	Nu_e	Nu^*	Nu_∞
		Test 350b		Traverse 1		
0.860	0.174	66.74	6.914	1.3284	1.3199	1.2840
0.760	0.174	66.49	6.737	1.2943	1.2861	1.2504
0.660	0.174	66.54	6.556	1.2595	1.2515	1.2160
0.560	0.174	66.38	6.550	1.2583	1.2504	1.2149
0.510	0.174	66.44	6.720	1.2911	1.2830	1.2473
0.485	0.174	66.27	6.773	1.3012	1.2931	1.2574
0.495	0.174	66.19	6.828	1.3118	1.3037	1.2679
0.535	0.174	65.93	6.631	1.2739	1.2662	1.2305
0.610	0.174	65.96	6.513	1.2513	1.2437	1.2082
0.660	0.174	65.81	6.568	1.2618	1.2542	1.2186
0.760	0.174	65.73	6.731	1.2932	1.2854	1.2497
0.860	0.174	65.69	6.910	1.3276	1.3196	1.2838
		Test 350b		Traverse 2		
0.860	0.174	65.63	7.095	1.3631	1.3549	1.3189
0.760	0.174	65.69	7.020	1.3486	1.3405	1.3046
0.760	0.174	65.95	6.989	1.3426	1.3344	1.2985
0.660	0.174	65.92	6.985	1.3420	1.3338	1.2979
0.610	0.174	65.90	7.035	1.3516	1.3434	1.3074
0.560	0.174	65.91	7.145	1.3727	1.3643	1.3283
0.520	0.174	66.03	7.283	1.3992	1.3907	1.3546
0.500	0.174	66.00	7.367	1.4154	1.4067	1.3706
0.480	0.174	66.05	7.467	1.4345	1.4256	1.3895
0.460	0.174	66.12	7.591	1.4583	1.4493	1.4131
0.440	0.174	66.25	7.680	1.4755	1.4664	1.4302
0.430	0.174	66.23	7.414	1.4244	1.4155	1.3794
0.425	0.174	66.38	6.768	1.3002	1.2920	1.2563
0.435	0.174	72.68	7.652	1.4701	1.4575	1.4212
0.435	0.174	69.05	7.660	1.4717	1.4610	1.4247
0.435	0.174	68.63	7.641	1.4679	1.4575	1.4212
0.435	0.174	68.46	7.630	1.4658	1.4555	1.4193
0.440	0.174	68.01	7.690	1.4774	1.4672	1.4310
0.450	0.174	67.54	7.663	1.4721	1.4622	1.4260
0.460	0.174	67.30	7.589	1.4580	1.4484	1.4122

TABLE VI. (Continued)
A) $Re_\infty = 7098$

-x in.	y in.	Δt ^oF	$h \times 10^2$ Btu/sec. ft^2 ^oF	Nu_e	Nu^*	Nu_∞
		Test 350b		Traverse 3		
0.860	0.074	66.24	6.774	1.3013	1.2932	1.2575
0.760	0.074	66.30	6.458	1.2407	1.2329	1.1975
0.660	0.074	66.08	6.021	1.1567	1.1496	1.1146
0.560	0.074	66.16	5.462	1.0494	1.0429	1.0088
0.540	0.074	66.11	5.401	1.0377	1.0313	0.9972
0.530	0.074	66.12	5.399	1.0372	1.0308	0.9968
0.525	0.074	66.19	5.399	1.0373	1.0308	0.9968
0.520	0.074	66.20	5.398	1.0371	1.0307	0.9966
0.515	0.074	66.26	5.390	1.0356	1.0291	0.9951
0.510	0.074	67.01	5.280	1.0143	1.0077	0.9739
0.560	0.074	66.82	5.411	1.0395	1.0328	0.9988
0.610	0.074	66.86	5.671	1.0894	1.0824	1.0479
0.660	0.074	66.90	5.942	1.1415	1.1341	1.0993
		Test 350b		Traverse 4		
0.860	-0.001	65.95	6.724	1.2917	1.2838	1.2481
0.760	-0.001	65.90	6.363	1.2225	1.2151	1.1797
0.660	-0.001	65.83	5.767	1.1079	1.1012	1.0665
0.560	-0.001	65.72	4.535	0.8712	0.8659	0.8336
0.860	-0.001	67.88	6.744	1.2956	1.2867	1.2510
0.760	-0.001	68.26	6.360	1.2218	1.2133	1.1779
0.710	-0.001	68.25	6.108	1.1734	1.1653	1.1302
0.660	-0.001	68.31	5.763	1.1071	1.0993	1.0647
0.620	-0.001	68.33	5.380	1.0336	1.0264	0.9924
0.580	-0.001	68.43	4.863	0.9343	0.9277	0.8947
0.560	-0.001	68.31	4.537	0.8717	0.8656	0.8333
0.540	-0.001	68.25	4.105	0.7887	0.7832	0.7520
0.530	-0.001	67.69	3.877	0.7448	0.7398	0.7092
0.525	-0.001	67.88	3.755	0.7214	0.7165	0.6863
0.560	-0.001	67.76	4.540	0.8721	0.7662	0.8339
0.660	-0.001	67.58	5.774	1.1093	1.1019	1.0673

TABLE VI. (Continued)
A) $Re_\infty = 7098$

-x in.	y in.	Δt ^oF	$h \times 10^2$ Btu/sec. ft^2 ^oF	Nu_e	Nu^*	Nu_∞
		Test 350b		Traverse 5		
0.360	0.974	56.37	7.939	1.5252	1.5214	1.4851
0.360	0.874	56.25	7.969	1.5310	1.5273	1.4910
0.360	0.774	56.46	7.952	1.5276	1.5238	1.4875
0.360	0.674	56.44	7.971	1.5314	1.5275	1.4912
0.360	0.574	56.56	7.995	1.5359	1.5320	1.4957
0.360	0.474	56.48	8.085	1.5533	1.5493	1.5131
0.360	0.424	56.37	8.151	1.5659	1.5620	1.5258
0.360	0.394	56.71	8.172	1.5699	1.5658	1.5295
0.360	0.374	56.63	8.183	1.5720	1.5680	1.5317
0.360	0.364	56.62	8.009	1.5387	1.5347	1.4984
0.360	0.359	56.65	7.742	1.4873	1.4835	1.4472
0.360	0.374	56.76	8.178	1.5711	1.5669	1.5307
0.360	0.474	56.75	8.084	1.5531	1.5490	1.5127
		Test 352		Traverse 2		
0.060	0.876	58.70	7.945	1.5262	1.5211	1.4848
0.060	0.776	58.64	7.983	1.5335	1.5284	1.4921
0.060	0.676	58.52	8.041	1.5447	1.5396	1.5033
0.060	0.576	58.52	8.084	1.5530	1.5479	1.5116
0.060	0.526	58.61	7.540	1.4483	1.4435	1.4073
0.060	0.516	58.13	6.546	1.2574	1.2535	1.2179
0.060	0.546	58.44	8.063	1.5488	1.5438	1.5075
0.060	0.536	58.45	7.954	1.5280	1.5229	1.4867
0.060	0.531	58.09	7.830	1.5042	1.4994	1.4632
0.060	0.576	58.40	8.068	1.5499	1.5449	1.5086
0.060	0.876	58.32	7.946	1.5265	1.5216	1.4853

TABLE VI. (Continued)
A) $Re_\infty = 7098$

-x in.	y in.	Δt ^oF	$h \times 10^2$ Btu/sec. ft^2 ^oF	Nu_e	Nu^*	Nu_∞
		Test 352		Traverse 3		
-0.040	0.876	58.28	7.976	1.5321	1.5272	1.4909
-0.040	0.776	58.23	8.016	1.5398	1.5349	1.4986
-0.040	0.676	58.15	8.054	1.5471	1.5422	1.5060
-0.040	0.606	58.29	8.065	1.5493	1.5444	1.5081
-0.040	0.576	58.21	7.979	1.5328	1.5279	1.4916
-0.040	0.556	57.56	6.977	1.3403	1.3364	1.3005
-0.040	0.536	58.59	4.115	0.7904	0.7878	0.7566
-0.040	0.546	56.47	5.795	1.1132	1.1104	1.0757
-0.040	0.526	57.93	3.330	0.6397	0.6377	0.6089
-0.040	0.516	58.40	3.343	0.6421	0.6400	0.6111
-0.040	0.506	58.09	3.441	0.6610	0.6589	0.6297
-0.040	0.496	57.89	3.924	0.7538	0.7514	0.7207
-0.040	0.576	58.09	7.970	1.5310	1.5262	1.4900
		Test 352		Traverse 4		
0.860	0.176	50.98	6.778	1.3020	1.3014	1.2656
0.760	0.176	51.09	6.587	1.2653	1.2647	1.2291
0.660	0.176	50.88	6.448	1.2387	1.2382	1.2027
0.560	0.176	51.50	6.378	1.2251	1.2243	1.1889
0.510	0.176	51.03	6.626	1.2728	1.2722	1.2365
0.485	0.176	50.97	6.679	1.2830	1.2825	1.2468
0.480	0.176	51.06	6.462	1.2414	1.2408	1.2053
0.510	0.176	51.03	6.624	1.2724	1.2718	1.2362
0.660	0.176	50.97	6.443	1.2377	1.2371	1.2017

TABLE VI. (Continued)
A) $Re_\infty = 7098$

-x in.	y in.	Δt ^oF	$h \times 10^2$ Btu/sec. ft^2 ^oF	Nu_e	Nu^*	Nu_∞
		Test 352		Traverse 5		
0.860	0.376	51.10	7.091	1.3621	1.3614	1.3254
0.760	0.376	51.11	7.081	1.3603	1.3596	1.3236
0.660	0.376	51.04	7.145	1.3725	1.3719	1.3359
0.560	0.376	51.07	7.308	1.4038	1.4032	1.3671
0.510	0.376	51.10	7.441	1.4295	1.4287	1.3926
0.460	0.376	51.09	7.615	1.4628	1.4620	1.4258
0.410	0.376	51.13	7.814	1.5010	1.5002	1.4640
0.360	0.376	51.07	8.011	1.5388	1.5381	1.5018
0.340	0.376	51.16	7.354	1.4127	1.4120	1.3759
0.335	0.376	51.26	6.823	1.3106	1.3099	1.2741
0.360	0.376	51.05	8.036	1.5436	1.5429	1.5066
0.560	0.376	51.15	7.309	1.4041	1.4034	1.3673
		Test 352		Traverse 6		
0.860	0.026	51.07	6.616	1.2709	1.2703	1.2347
0.760	0.026	51.04	6.286	1.2075	1.2070	1.1717
0.660	0.026	51.00	5.755	1.1055	1.1050	1.0703
0.560	0.026	51.05	4.725	0.9077	0.9073	0.8745
0.535	0.026	51.20	4.350	0.8356	0.8351	0.8032
0.525	0.026	51.37	4.204	0.8076	0.8071	0.7756
0.520	0.026	51.07	4.170	0.8010	0.8006	0.7692
0.660	0.026	51.09	5.742	1.1029	1.1024	1.0678

TABLE VI. (Continued)
A) Re_∞ = 7098

-x in.	y in.	Δt ^oF	h x 10^2 Btu/sec. ft^2 ^oF	Nu_e	Nu^*	Nu_∞
		Test 359		Traverse 1		
0.896	0.000	55.98	6.984	1.3416	1.3384	1.3025
0.896	0.000	76.69	7.025	1.3494	1.3358	1.2999
0.896	0.000	38.13	6.923	1.3297	1.3356	1.2997
0.896	0.000	24.48	6.838	1.3135	1.3263	1.2904
0.896	0.000	13.62	6.937	1.3324	1.3510	1.3151
0.696	0.000	13.60	6.053	1.1628	1.1790	1.1439
0.696	0.000	25.94	6.135	1.1784	1.1892	1.1540
0.696	0.000	40.99	6.127	1.1769	1.1809	1.1457
0.696	0.000	60.89	6.136	1.1786	1.1736	1.1385
0.696	0.000	85.61	6.182	1.1875	1.1716	1.1365
		Test 359		Traverse 2		
0.596	0.000	104.25	5.229	1.0044	0.9840	0.9504
0.596	0.000	73.84	5.168	0.9927	0.9837	0.9501
0.596	0.000	39.70	5.108	0.9812	0.9850	0.9514
0.596	0.000	11.84	5.032	0.9666	0.9808	0.9472
0.546	0.000	14.28	4.191	0.8051	0.8161	0.7845
0.546	0.000	48.91	4.212	0.8090	0.8093	0.7778
0.546	0.000	91.47	4.290	0.8241	0.8112	0.7796
0.546	0.000	131.44	4.364	0.8382	0.8130	0.7814
0.521	0.000	156.37	3.799	0.7298	0.7014	0.6714
0.521	0.000	108.61	3.710	0.7126	0.6970	0.6671
0.521	0.000	108.41	3.716	0.7137	0.6982	0.6682
0.521	0.000	57.85	3.615	0.6943	0.6922	0.6624
0.521	0.000	16.93	3.552	0.6823	0.6909	0.6612

TABLE VI. (Continued)
A) $Re_\infty = 7098$

-x in.	y in.	Δt ^oF	$h \times 10^2$ Btu/sec. ft^2 ^oF	Nu_e	Nu^*	Nu_∞
		Test 359		Traverse 3		
0.000	0.857	23.75	8.306	1.5953	1.6113	1.5751
0.000	0.857	43.37	8.366	1.6069	1.6108	1.5746
0.000	0.857	58.88	8.608	1.6535	1.6478	1.6116
0.000	0.757	58.13	8.709	1.6728	1.6676	1.6314
0.000	0.757	42.72	8.483	1.6294	1.6338	1.5976
0.000	0.757	23.39	8.426	1.6185	1.6349	1.5987
0.000	0.757	6.95	8.494	1.6315	1.6586	1.6224
0.000	0.657	7.00	8.440	1.6211	1.6479	1.6117
0.000	0.657	23.81	8.286	1.5916	1.6075	1.5712
0.000	0.657	42.98	8.437	1.6205	1.6247	1.5885
0.000	0.657	59.81	8.487	1.6303	1.6241	1.5879
		Test 359		Traverse 4		
0.000	0.557	61.14	8.322	1.5984	1.5916	1.5553
0.000	0.557	43.91	8.269	1.5884	1.5920	1.5557
0.000	0.557	23.80	8.289	1.5921	1.6080	1.5718
0.000	0.557	6.91	8.549	1.6421	1.6694	1.6332
0.000	0.507	17.57	3.427	0.6583	0.6665	0.6371
0.000	0.507	62.31	3.381	0.6494	0.6463	0.6173
0.000	0.507	118.07	3.462	0.6649	0.6481	0.6190
0.000	0.507	88.98	3.428	0.6584	0.6488	0.6197

TABLE VI. (Continued)
B) $Re_\infty = 3526$

-x in.	y in.	Δt ^oF	$h \times 10^2$ Btu/sec. ft^2 ^oF	Nu_e	Nu^*	Nu_∞
		Test 363		Traverse 1		
0.906	0.016	51.53	5.806	1.1153	1.1145	1.0798
0.806	0.016	51.58	5.559	1.0678	1.0670	1.0327
0.706	0.016	51.51	5.182	0.9953	0.9946	0.9610
0.606	0.016	51.62	4.497	0.8637	0.8631	0.8309
0.556	0.016	51.83	3.931	0.7550	0.7544	0.7236
0.531	0.016	51.48	3.567	0.6851	0.6846	0.6550
0.506	0.016	51.44	3.445	0.6618	0.6613	0.6321
0.516	0.016	51.58	3.378	0.6488	0.6484	0.6193
0.531	0.016	51.52	3.584	0.6885	0.6880	0.6583
0.516	0.016	51.87	3.360	0.6455	0.6449	0.6160
0.506	0.016	51.67	3.443	0.6613	0.6609	0.6316
		Test 363		Traverse 2		
0.906	0.100	51.67	5.845	1.1228	1.1220	1.0872
0.806	0.100	51.88	5.605	1.0767	1.0758	1.0414
0.706	0.100	51.91	5.322	1.0222	1.0214	0.9875
0.606	0.100	51.68	4.960	0.9527	0.9520	0.9187
0.556	0.100	51.73	4.794	0.9209	0.9202	0.8873
0.531	0.100	51.57	4.789	0.9199	0.9193	0.8864
0.516	0.100	51.66	4.789	0.9199	0.9193	0.8864
0.506	0.100	51.83	4.771	0.9164	0.9157	0.8828
0.496	0.100	51.80	4.567	0.8773	0.8767	0.8443
0.491	0.100	52.02	4.893	0.9399	0.9391	0.9060
0.556	0.100	51.87	4.792	0.9205	0.9198	0.8869
0.706	0.100	51.84	5.332	1.0242	1.0234	0.9895

TABLE VI. (Continued)
B) $Re_\infty = 3526$

-x in.	y in.	Δt °F	$h \times 10^2$ Btu/sec.ft^2 °F	Nu_e	Nu^*	Nu_∞
		Test 363		Traverse 3		
0.906	0.200	51.73	5.941	1.1411	1.1403	1.1054
0.806	0.200	51.77	5.813	1.1167	1.1158	1.0811
0.706	0.200	51.88	5.645	1.0842	1.0834	1.0489
0.606	0.200	51.87	5.551	1.0663	1.0654	1.0311
0.556	0.200	51.94	5.585	1.0727	1.0718	1.0375
0.506	0.200	51.70	5.731	1.1009	1.1001	1.0655
0.486	0.200	51.80	5.798	1.1137	1.1128	1.0781
0.466	0.200	51.76	5.487	1.0540	1.0532	1.0190
0.556	0.200	51.89	5.583	1.0725	1.0716	1.0372
0.486	0.200	51.77	5.800	1.1141	1.1132	1.0785
0.481	0.200	51.74	5.797	1.1135	1.1127	1.0780
0.476	0.200	51.80	5.787	1.1116	1.1107	1.0761
0.471	0.200	51.77	5.698	1.0945	1.0937	1.0591
0.468	0.200	51.58	5.603	1.0763	1.0755	1.0411
0.466	0.200	51.78	5.472	1.0511	1.0503	1.0161
		Test 363		Traverse 4		
0.906	0.300	47.81	6.056	1.1632	1.1641	1.1291
0.806	0.300	47.65	6.005	1.1534	1.1543	1.1193
0.706	0.300	47.96	5.938	1.1406	1.1414	1.1065
0.606	0.300	47.76	5.978	1.1484	1.1493	1.1143
0.506	0.300	47.77	6.184	1.1878	1.1887	1.1535
0.456	0.300	47.77	6.383	1.2260	1.2270	1.1916
0.431	0.300	47.75	6.492	1.2471	1.2481	1.2125
0.416	0.300	47.87	6.380	1.2256	1.2265	1.1911
0.406	0.300	47.77	5.785	1.1112	1.1121	1.0774
0.408	0.300	47.77	5.932	1.1395	1.1404	1.1055
0.411	0.300	47.66	6.170	1.1852	1.1862	1.1510
0.416	0.300	47.62	6.415	1.2322	1.2332	1.1978
0.406	0.300	47.63	5.802	1.1145	1.1154	1.0807

TABLE VI. (Continued)
B) $Re_\infty = 3526$

-x in.	y in.	Δt $^\circ F$	$h \times 10^2$ Btu/sec. ft^2 $^\circ F$	Nu_e	Nu^*	Nu_∞
		Test 363		Traverse 5		
0.906	0.400	47.61	6.198	1.1906	1.1916	1.1564
0.806	0.400	47.60	6.170	1.1851	1.1861	1.1509
0.606	0.400	47.70	6.253	1.2010	1.2020	1.1667
0.506	0.400	47.87	6.425	1.2341	1.2350	1.1995
0.406	0.400	47.64	6.785	1.3033	1.3044	1.2686
0.356	0.400	47.54	6.958	1.3365	1.3376	1.3017
0.331	0.400	47.54	6.958	1.3365	1.3376	1.3017
0.321	0.400	47.77	6.742	1.2950	1.2960	1.2603
0.316	0.400	47.53	6.568	1.2616	1.2627	1.2271
0.311	0.400	47.89	6.234	1.1974	1.1982	1.1630
0.306	0.400	47.70	5.884	1.1303	1.1312	1.0963
		Test 363		Traverse 6		
0.906	0.500	47.88	6.282	1.2066	1.2075	1.1722
0.706	0.500	46.07	6.578	1.2635	1.2653	1.2297
0.506	0.500	47.50	6.607	1.2690	1.2702	1.2345
0.306	0.500	47.63	7.030	1.3503	1.3514	1.3155
0.206	0.500	47.79	7.167	1.3767	1.3778	1.3417
0.156	0.500	47.38	6.931	1.3314	1.3326	1.2967
0.131	0.500	47.65	6.105	1.1726	1.1736	1.1384
0.116	0.500	47.44	5.464	1.0495	1.0505	1.0163
0.081	0.500	47.54	4.145	0.7961	0.7968	0.7654
0.091	0.500	47.67	4.422	0.8494	0.8501	0.8180

TABLE VI. (Continued)
B) $Re_\infty = 3526$

-x in.	y in.	Δt $^\circ F$	$h \times 10^2$ Btu/sec.ft^2 $^\circ F$	Nu_e	Nu^*	Nu_∞
		Test 369		Traverse 1		
0.386	0.819	70.82	6.978	1.3362	1.3257	1.2876
0.386	0.819	61.37	6.982	1.3369	1.3311	1.2930
0.386	0.719	61.61	6.956	1.3319	1.3261	1.2880
0.386	0.619	61.50	6.978	1.3361	1.3303	1.2922
0.386	0.519	61.60	7.009	1.3420	1.3361	1.2980
0.386	0.419	61.34	7.056	1.3510	1.3452	1.3071
0.386	0.369	61.47	7.042	1.3484	1.3425	1.3044
0.386	0.344	61.36	6.929	1.3268	1.3211	1.2830
0.386	0.334	61.46	6.642	1.2718	1.2662	1.2285
0.386	0.329	61.48	6.337	1.2135	1.2082	1.1708
0.386	0.324	61.64	5.870	1.1240	1.1191	1.0823
0.386	0.321	61.49	5.546	1.0619	1.0573	1.0211
0.386	0.339	61.42	6.819	1.3056	1.3000	1.2621
0.386	0.519	61.60	7.022	1.3446	1.3387	1.3006
		Test 369		Traverse 2		
0.486	0.819	61.42	6.916	1.3242	1.3185	1.2805
0.486	0.719	61.31	6.903	1.3218	1.3161	1.2781
0.486	0.619	61.48	6.856	1.3127	1.3070	1.2691
0.486	0.519	61.64	6.793	1.3007	1.2949	1.2570
0.486	0.419	61.56	6.694	1.2817	1.2761	1.2383
0.486	0.319	61.57	6.467	1.2384	1.2329	1.1954
0.486	0.219	61.74	5.990	1.1468	1.1417	1.1048
0.486	0.169	61.45	5.573	1.0670	1.0624	1.0261
0.486	0.144	61.29	5.083	0.9732	0.9690	0.9337
0.486	0.134	61.65	4.782	0.9157	0.9117	0.8771
0.486	0.151	61.41	5.250	1.0052	1.0009	1.9652
0.486	0.194	61.49	5.825	1.1154	1.1105	1.0738
0.486	0.269	61.48	6.276	1.2016	1.1964	1.1591

TABLE VI. (Continued)
B) $Re_\infty = 3526$

-x in.	y in.	Δt ^oF	$h \times 10^2$ Btu/sec. ft^2 ^oF	Nu_e	Nu^*	Nu_∞
		Test 369		Traverse 3		
0.286	0.819	61.53	7.041	1.3481	1.3422	1.3041
0.286	0.719	61.44	7.080	1.3555	1.3497	1.3115
0.286	0.619	61.49	7.139	1.3669	1.3610	1.3228
0.286	0.519	61.55	7.249	1.3880	1.3819	1.3436
0.286	0.469	61.64	7.315	1.4006	1.3945	1.3561
0.286	0.444	61.55	7.340	1.4054	1.3993	1.3610
0.286	0.434	61.39	7.250	1.3883	1.3823	1.3440
0.286	0.429	61.18	7.065	1.3527	1.3470	1.3089
0.286	0.424	61.52	6.751	1.2926	1.2870	1.2491
0.286	0.419	61.46	6.334	1.2128	1.2075	1.1701
0.286	0.569	61.37	7.185	1.3757	1.3697	1.3315
		Test 372		Traverse 1		
0.886	0.000	51.23	5.745	1.1000	1.0994	1.0629
0.786	0.000	51.00	5.467	1.0467	1.0463	1.0102
0.686	0.000	51.05	5.005	0.9582	0.9578	0.9227
0.586	0.000	51.01	4.201	0.8043	0.8040	0.7708
0.536	0.000	51.07	3.484	0.6671	0.6668	0.6359
0.511	0.000	50.84	3.178	0.6085	0.6083	0.5785
		Test 372		Traverse 2		
0.886	0.200	51.04	5.913	1.1322	1.1317	1.0949
0.786	0.200	51.00	5.773	1.1052	1.1048	1.0681
0.686	0.200	50.93	5.630	1.0779	1.0775	1.0412
0.586	0.200	51.03	5.556	1.0637	1.0633	1.0271
0.536	0.200	51.00	5.640	1.0798	1.0794	1.0430
0.511	0.200	51.02	5.717	1.0946	1.0942	1.0576
0.486	0.200	50.79	5.851	1.1203	1.1199	1.0832
0.466	0.200	50.86	5.571	1.0667	1.0663	1.0300

TABLE VI. (Continued)
B) $Re_\infty = 3526$

-x in.	y in.	Δt $^\circ F$	$h \times 10^2$ Btu/sec. ft^2 $^\circ F$	Nu_e	Nu^*	Nu_∞
		Test 372		Traverse 3		
0.186	0.819	51.11	7.076	1.3548	1.3542	1.3161
0.186	0.719	50.99	7.135	1.3660	1.3655	1.3273
0.186	0.569	50.95	7.275	1.3928	1.3923	1.3540
0.186	0.519	50.97	7.340	1.4053	1.4047	1.3664
0.186	0.489	50.96	7.134	1.3658	1.3653	1.3271
0.186	0.474	50.38	5.762	1.1032	1.1030	1.0664
0.186	0.469	50.78	5.184	0.9924	0.9921	0.9566
0.186	0.482	50.95	6.611	1.2657	1.2653	1.2275
0.186	0.479	50.80	6.284	1.2030	1.2026	1.1653
		Test 372		Traverse 4		
0.086	0.819	50.81	7.127	1.3644	1.3640	1.3258
0.086	0.669	50.87	7.203	1.3791	1.3787	1.3404
0.086	0.519	50.69	6.489	1.2424	1.2420	1.2044
0.086	0.499	50.63	3.976	0.7612	0.7610	0.7285
0.086	0.509	50.80	5.112	0.9787	0.9783	0.9429
0.086	0.539	50.98	7.223	1.3828	1.3823	1.3441
0.086	0.559	50.78	7.314	1.4003	1.3999	1.3616
0.086	0.579	50.86	7.291	1.3959	1.3954	1.3571
		Test 373		Traverse 1		
0.886	0.019	49.37	5.778	1.1061	1.1063	1.0697
0.786	0.019	48.98	5.505	1.0538	1.0542	1.0181
0.686	0.019	49.05	5.080	0.9725	0.9728	0.9375
0.586	0.019	49.03	4.277	0.8187	0.8190	0.7856
0.686	0.019	49.39	5.016	0.9601	0.9604	0.9252
0.536	0.019	49.18	3.612	0.6915	0.6917	0.6603
0.511	0.019	49.13	3.310	0.6336	0.6338	0.6036
0.501	0.019	49.35	3.623	0.6936	0.6937	0.6623
0.506	0.019	49.32	3.368	0.6447	0.6449	0.6144

TABLE VI. (Continued)
B) $Re_\infty = 3526$

-x	y	Δt	$h \times 10^2$	Nu_e	Nu^*	Nu_∞
in.	in.	^oF	Btu/sec. ft^2 ^oF			
		Test 373		Traverse 2		
0.086	0.719	49.15	7.146	1.3680	1.3684	1.3302
0.086	0.619	49.11	7.208	1.3798	1.3802	1.3420
0.086	0.519	49.01	6.460	1.2366	1.2370	1.1995
0.086	0.509	48.88	5.068	0.9701	0.9705	0.9352
0.086	0.499	49.36	3.970	0.7599	0.7601	0.7276
0.086	0.494	49.16	4.118	0.7884	0.7887	0.7557
0.086	0.539	49.31	7.208	1.3799	1.3802	1.3420
0.086	0.559	49.12	7.263	1.3904	1.3909	1.3526
0.086	0.579	49.13	7.284	1.3943	1.3948	1.3565
0.086	0.599	49.10	7.283	1.3941	1.3946	1.3563
0.086	0.619	49.06	7.252	1.3882	1.3887	1.3504
0.086	0.819	49.29	7.117	1.3625	1.3629	1.3247
		Test 373		Traverse 3		
-0.014	0.819	59.20	7.129	1.3647	1.3646	1.3264
-0.014	0.719	49.93	7.211	1.3805	1.3805	1.3422
-0.014	0.619	49.98	7.263	1.3904	1.3904	1.3521
-0.014	0.569	50.21	7.028	1.3453	1.3452	1.3071
-0.014	0.544	50.49	5.486	1.0502	1.0500	1.0139
-0.014	0.519	49.83	3.081	0.5899	0.5899	0.5605
-0.014	0.509	49.87	3.091	0.5916	0.5917	0.5622
-0.014	0.499	49.89	4.401	0.8425	0.8425	0.8088
-0.014	0.534	49.86	4.329	0.8288	0.8288	0.7953
-0.014	0.526	49.75	3.431	0.6568	0.6569	0.6262

TABLE VI. (Continued)
B) $Re_\infty = 3526$

-x in.	y in.	Δt ^oF	$h \times 10^2$ Btu/sec.ft^2 ^oF	Nu_e	Nu^*	Nu_∞
		Test 373		Traverse 4		
0.286	0.819	50.02	7.040	1.3476	1.3476	1.3094
0.286	0.719	50.11	7.067	1.3528	1.3527	1.3146
0.286	0.619	50.05	7.127	1.3644	1.3643	1.3261
0.286	0.519	50.03	7.227	1.3835	1.3835	1.3452
0.286	0.469	50.10	7.315	1.4003	1.4002	1.3619
0.286	0.444	50.10	7.339	1.4050	1.4049	1.3666
0.286	0.419	50.24	6.337	1.2131	1.2130	1.1756
0.286	0.416	52.44	5.743	1.0993	1.0983	1.0617
0.286	0.434	52.62	6.880	1.3170	1.3157	1.2777
0.286	0.426	52.73	6.553	1.2545	1.2531	1.2155
		Test 373		Traverse 5		
0.686	0.819	50.10	6.744	1.2911	1.2910	1.2532
0.686	0.719	50.12	6.677	1.2782	1.2781	1.2403
0.686	0.619	50.14	6.601	1.2637	1.2636	1.2259
0.686	0.519	50.04	6.486	1.2416	1.2416	1.2040
0.686	0.419	50.41	6.279	1.2021	1.2019	1.1646
0.686	0.319	50.08	6.060	1.1601	1.1600	1.1230
0.686	0.219	49.92	5.739	1.0986	1.0987	1.0621
0.686	0.119	50.06	5.348	1.0238	1.0237	0.9879
0.686	0.019	50.13	5.075	0.9715	0.9714	0.9361

TABLE VI. (Continued)
B) $Re_\infty = 3526$

-x in.	y in.	Δt ^oF	$h \times 10^2$ Btu/sec.ft^2 ^oF	Nu_e	Nu^*	Nu_∞
		Test 376		Traverse 1		
0.886	0.000	11.98	5.850	1.1202	1.1366	1.0997
0.886	0.000	25.11	5.724	1.0960	1.1064	1.0698
0.886	0.000	70.77	5.802	1.1110	1.1023	1.0657
0.886	0.000	146.86	5.943	1.1379	1.0976	1.0610
0.686	0.000	170.79	5.219	0.9992	0.9554	0.9202
0.686	0.000	82.01	5.073	0.9714	0.9598	0.9246
0.686	0.000	28.68	4.970	0.9516	0.9594	0.9242
0.686	0.000	11.17	4.936	0.9451	0.9592	0.9240
0.536	0.000	17.63	3.431	0.6570	0.6652	0.6343
0.536	0.000	46.71	3.487	0.6677	0.6685	0.6376
0.536	0.000	113.63	3.588	0.6869	0.6707	0.6397
0.536	0.000	225.15	3.752	0.7184	0.6736	0.6425
		Test 376		Traverse 2		
0.886	0.200	120.29	6.085	1.1651	1.1348	1.0979
0.886	0.200	62.90	5.986	1.1462	1.1406	1.1037
0.886	0.200	26.47	5.943	1.1379	1.1481	1.1112
0.886	0.200	6.09	6.223	1.1916	1.2118	1.1744
0.686	0.200	6.59	5.761	1.1030	1.1215	1.0847
0.686	0.200	27.98	5.637	1.0793	1.0883	1.0519
0.686	0.200	66.56	5.691	1.0896	1.0828	1.0464
0.686	0.200	127.63	5.797	1.1101	1.0783	1.0419
0.486	0.200	123.46	5.956	1.1405	1.1096	1.0729
0.486	0.200	64.46	5.856	1.1212	1.1150	1.0783
0.486	0.200	26.90	5.853	1.1206	1.1305	1.0937
0.486	0.200	6.05	6.264	1.1993	1.2197	1.1822
0.461	0.200	6.41	5.919	1.1333	1.1524	1.1154
0.461	0.200	46.36	5.487	1.0506	1.0520	1.0159
0.461	0.200	132.49	5.624	1.0769	1.0442	1.0081

TABLE VI. (Continued)
B) $Re_\infty = 3526$

-x in.	y in.	Δt ^oF	$h \times 10^2$ Btu/sec.ft^2 ^oF	Nu_e	Nu^*	Nu_∞
		Test 376		Traverse 3		
0.286	0.919	99.87	7.107	1.3607	1.3354	1.2974
0.286	0.919	35.78	6.983	1.3370	1.3442	1.3061
0.286	0.919	5.04	7.505	1.4370	1.4619	1.4235
0.286	0.719	5.44	6.963	1.3333	1.3562	1.3181
0.286	0.719	35.71	6.994	1.3392	1.3465	1.3084
0.286	0.719	99.47	7.131	1.3653	1.3402	1.3021
0.286	0.519	96.96	7.287	1.3953	1.3709	1.3326
0.286	0.519	34.92	7.143	1.3676	1.3755	1.3372
0.286	0.449	34.09	7.307	1.3992	1.4076	1.3693
0.286	0.449	95.19	7.402	1.4174	1.3935	1.3551
0.286	0.429	98.25	7.206	1.3797	1.3549	1.3167
0.286	0.429	35.15	7.100	1.3595	1.3671	1.3289
0.286	0.429	5.00	7.564	1.4483	1.4734	1.4349
		Test 376		Traverse 4		
0.506	0.000	5.46	0.905	0.1732	0.1762	0.1594
0.506	0.000	16.09	2.400	0.4595	0.4655	0.4389
0.506	0.000	88.32	3.083	0.5904	0.5819	0.5527
0.506	0.000	252.59	3.460	0.6625	0.6152	0.5852
0.536	0.000	216.43	3.860	0.7391	0.6952	0.6637
0.536	0.000	72.80	3.650	0.6988	0.6928	0.6614
0.536	0.000	10.18	3.754	0.7188	0.7298	0.6978

TABLE VI. (Continued)
C) $Re_\infty = 1757$

-x in.	y in.	Δt $^\circ F$	$h \times 10^2$ Btu/sec. ft^2 $^\circ F$	Nu_e	Nu^*	Nu_∞
		Test 377		Traverse 1		
0.886	0.000	50.40	4.641	0.8892	0.8891	0.8547
0.786	0.000	49.97	4.460	0.8546	0.8546	0.8207
0.686	0.000	50.36	4.096	0.7848	0.7847	0.7518
0.586	0.000	50.75	3.537	0.6776	0.6774	0.6463
0.536	0.000	50.69	3.056	0.5855	0.5854	0.5561
0.511	0.000	50.72	2.919	0.5592	0.5591	0.5303
0.501	0.000	50.73	3.163	0.6060	0.6059	0.5761
0.501	0.000	113.03	3.273	0.6271	0.6124	0.5825
0.511	0.000	112.99	3.016	0.5778	0.5643	0.5354
0.536	0.000	112.92	3.143	0.6021	0.5881	0.5587
0.586	0.000	112.88	3.623	0.6942	0.6780	0.6469
0.686	0.000	113.62	4.200	0.8048	0.7858	0.7529
0.786	0.000	113.40	4.534	0.8688	0.8483	0.8145
0.886	0.000	112.17	4.793	0.9183	0.8971	0.8626
		Test 377		Traverse 2		
0.886	0.000	151.51	4.762	0.9119	0.8781	0.8439
0.786	0.000	151.53	4.549	0.8713	0.8389	0.8052
0.686	0.000	151.26	4.228	0.8097	0.7798	0.7469
0.586	0.000	151.49	3.658	0.7006	0.6746	0.6435
0.536	0.000	151.35	3.203	0.6134	0.5907	0.5613
0.511	0.000	151.55	3.064	0.5868	0.5650	0.5361
0.501	0.000	151.63	3.320	0.6358	0.6122	0.5823
0.501	0.000	17.03	3.080	0.5899	0.5974	0.5678
0.511	0.000	17.14	2.815	0.5391	0.5459	0.5174
0.536	0.000	16.87	2.973	0.5695	0.5767	0.5476
0.586	0.000	17.04	3.474	0.6654	0.6738	0.6428
0.686	0.000	16.82	4.045	0.7747	0.7846	0.7517
0.786	0.000	16.91	4.357	0.8345	0.8451	0.8114
0.886	0.000	16.65	4.666	0.8936	0.9050	0.8705

TABLE VI. (Continued)
C) $Re_\infty = 1757$

-x in.	y in.	Δt °F	$h \times 10^2$ Btu/sec. ft^2 °F	Nu_e	Nu^*	Nu_∞
		Test 379		Traverse 1		
0.886	0.000	53.75	4.600	0.8808	0.8795	0.8453
0.686	0.000	53.73	4.066	0.7784	0.7773	0.7446
0.536	0.000	53.70	3.015	0.5773	0.5765	0.5473
		Test 379		Traverse 2		
0.886	0.100	53.69	4.638	0.8881	0.8869	0.8525
0.786	0.100	53.84	4.455	0.8531	0.8518	0.8179
0.686	0.100	53.66	4.229	0.8096	0.8085	0.7753
0.586	0.100	53.42	3.962	0.7587	0.7577	0.7252
0.536	0.100	53.78	3.859	0.7388	0.7377	0.7056
0.511	0.100	53.66	3.854	0.7380	0.7370	0.7048
0.496	0.100	51.88	3.819	0.7312	0.7307	0.6987
0.491	0.100	53.83	3.757	0.7194	0.7183	0.6865
0.686	0.100	53.73	4.222	0.8084	0.8072	0.7740
		Test 379		Traverse 3		
0.886	0.200	53.85	4.716	0.9030	0.9017	0.8672
0.786	0.200	53.87	4.617	0.8840	0.8827	0.8484
0.686	0.200	53.74	4.517	0.8648	0.8636	0.8296
0.586	0.200	53.85	4.465	0.8550	0.8537	0.8199
0.536	0.200	53.82	4.516	0.8648	0.8635	0.8295
0.486	0.200	53.83	4.633	0.8871	0.8858	0.8515
0.476	0.200	53.79	4.615	0.8837	0.8824	0.8482
0.466	0.200	54.10	4.365	0.8357	0.8344	0.8008
0.461	0.200	54.52	4.138	0.7923	0.7909	0.7580
0.511	0.200	53.92	4.559	0.8729	0.8715	0.8374
0.561	0.200	53.85	4.477	0.8572	0.8559	0.8220

TABLE VI. (Continued)
C) $Re_\infty = 1757$

-x	y	Δt	$h \times 10^2$	Nu_e	Nu^*	Nu_∞
in.	in.	$^\circ F$	Btu/sec. ft^2 $^\circ F$			
		Test 379		Traverse 4		
0.886	0.400	53.31	4.982	0.9540	0.9528	0.9176
0.786	0.400	53.81	4.930	0.9440	0.9426	0.9076
0.686	0.400	53.54	4.974	0.9524	0.9512	0.9161
0.586	0.400	53.55	5.064	0.9696	0.9683	0.9330
0.536	0.400	53.60	5.089	0.9743	0.9730	0.9377
0.486	0.400	53.56	5.241	1.0036	1.0022	0.9666
0.436	0.400	53.38	5.383	1.0307	1.0294	0.9934
0.386	0.400	53.69	5.511	1.0552	1.0537	1.0175
0.336	0.400	53.77	5.506	1.0542	1.0527	1.0166
0.326	0.400	53.42	5.381	1.0303	1.0289	0.9930
0.316	0.400	53.52	5.067	0.9701	0.9688	0.9335
0.311	0.400	53.57	4.823	0.9234	0.9221	0.8874
		Test 379		Traverse 5		
0.400	0.900	53.84	5.460	1.0455	1.0439	1.0079
0.400	0.800	53.69	5.472	1.0478	1.0463	1.0102
0.400	0.700	53.78	5.464	1.0462	1.0447	1.0086
0.400	0.600	53.71	5.471	1.0475	1.0460	1.0099
0.400	0.500	53.56	5.487	1.0506	1.0491	1.0130
0.400	0.400	53.68	5.476	1.0484	1.0469	1.0108
0.400	0.350	53.64	5.422	1.0381	1.0367	1.0007
0.400	0.300	53.99	4.451	0.8523	0.8510	0.8171
0.400	0.310	53.76	4.733	1.9063	1.9050	1.8704
0.400	0.330	53.48	5.309	1.0164	1.0151	0.9793
0.400	0.320	53.49	5.116	0.9796	0.9783	0.9429

TABLE VI. (Continued)
C) $Re_\infty = 1757$

-x in.	y in.	Δt °F	$h \times 10^2$ Btu/sec. ft^2 °F	Nu_e	Nu^*	Nu_∞
		Test 379		Traverse 6		
0.300	0.900	53.70	5.494	1.0520	1.0505	1.0144
0.300	0.800	53.93	5.499	1.0530	1.0514	1.0153
0.300	0.700	53.73	5.542	1.0612	1.0597	1.0235
0.300	0.600	53.98	5.562	1.0649	1.0633	1.0270
0.300	0.500	53.81	5.658	1.0834	1.0818	1.0454
0.300	0.400	53.72	4.526	0.8666	0.8653	0.8313
0.300	0.410	54.11	4.923	0.9426	0.9411	0.9062
0.300	0.405	53.73	4.605	0.8817	0.8805	0.8462
0.300	0.450	53.86	5.694	1.0901	1.0885	1.0521
0.300	0.425	53.79	5.471	1.0476	1.0460	1.0100
0.300	0.420	53.63	5.370	1.0282	1.0268	0.9909
		Test 380		Traverse 1		
0.000	0.900	54.60	5.567	1.0660	1.0641	1.0279
0.000	0.800	54.45	5.616	1.0754	1.0735	1.0372
0.000	0.700	54.56	5.649	1.0817	1.0798	1.0434
0.000	0.600	54.55	5.671	1.0859	1.0840	1.0475
0.000	0.580	54.55	5.594	1.0712	1.0693	1.0330
0.000	0.560	54.38	5.282	1.0114	1.0097	0.9739
0.000	0.540	53.76	4.417	0.8458	0.8445	0.8108
0.000	0.530	54.81	3.720	0.7124	0.7111	0.6794
0.000	0.520	54.25	3.215	0.6157	0.6147	0.5848
0.000	0.505	54.30	3.402	0.6514	0.6504	0.6198
0.000	0.502	54.31	3.678	0.7042	0.7030	0.6715
0.000	0.525	53.85	3.475	0.6654	0.6644	0.6335
0.000	0.550	54.75	4.879	0.9343	0.9326	0.8977

TABLE VI. (Continued)
C) $Re_\infty = 1757$

-x in.	y in.	Δt ^oF	$h \times 10^2$ Btu/sec. ft^2 ^oF	Nu_e	Nu^*	Nu_∞
		Test 380		Traverse 2		
0.100	0.900	54.45	5.567	1.0659	1.0641	1.0279
0.100	0.800	54.47	5.602	1.0726	1.0708	1.0345
0.100	0.700	54.53	5.654	1.0826	1.0807	1.0443
0.100	0.600	54.52	5.699	1.0912	1.0893	1.0528
0.100	0.550	54.44	5.714	1.0941	1.0922	1.0557
0.100	0.535	54.55	5.574	1.0673	1.0655	1.0292
0.100	0.520	55.80	4.946	0.9471	0.9450	0.9099
0.100	0.510	54.04	4.475	0.8569	0.8556	0.8217
0.100	0.500	55.24	3.742	0.7166	0.7151	0.6834
0.100	0.495	54.59	3.732	0.7146	0.7134	0.6816
0.100	0.490	56.78	4.132	0.7912	0.7891	0.7562
0.100	0.492	54.26	3.994	0.7648	0.7635	0.7310
0.100	0.497	54.56	3.714	0.7112	0.7099	0.6782
0.100	0.505	54.21	4.047	0.7749	0.7736	0.7409
		Test 380		Traverse 3		
0.200	0.900	54.46	5.534	1.0596	1.0578	1.0216
0.200	0.800	54.62	5.535	1.0598	1.0580	1.0218
0.200	0.700	54.35	5.593	1.0709	1.0691	1.0328
0.200	0.600	54.34	5.681	1.0878	1.0860	1.0495
0.200	0.550	54.48	5.736	1.0983	1.0964	1.0598
0.200	0.530	54.48	5.754	1.1018	1.0999	1.0633
0.200	0.500	54.47	5.712	1.0937	1.0918	1.0553
0.200	0.480	54.71	5.131	0.9825	0.9807	0.7453
0.200	0.470	54.32	4.635	0.8876	0.8861	0.8518
0.200	0.465	54.42	4.335	0.8302	0.8287	0.7952
0.200	0.462	53.77	4.265	0.8167	0.8155	0.7822
0.200	0.459	55.06	4.274	0.8184	0.8168	0.7834

TABLE VI. (Concluded)
C) $Re_\infty = 1757$

-x in.	y in.	Δt ^oF	$h \times 10^2$ Btu/sec. ft^2 ^oF	Nu_e	Nu^*	Nu_∞
		Test 380		Traverse 4		
0.886	0.300	54.49	4.859	0.9304	0.9288	0.8940
0.786	0.300	54.61	4.786	0.9164	0.9148	0.8802
0.686	0.300	54.46	4.768	0.9130	0.9115	0.8768
0.586	0.300	54.44	4.834	0.9256	0.9240	0.8892
0.536	0.300	54.51	4.913	0.9406	0.9390	0.9041
0.486	0.300	54.59	5.029	0.9630	0.9614	0.9261
0.466	0.300	54.19	5.105	0.9775	0.9759	0.9405
0.461	0.300	54.43	5.127	0.9818	0.9801	0.9447
0.446	0.300	54.49	5.166	0.9891	0.9874	0.9519
0.426	0.300	54.35	5.186	0.9930	0.9914	0.9558
0.406	0.300	54.58	4.606	0.8820	0.8804	0.8462
0.396	0.300	54.57	4.631	0.8868	0.8853	0.8510
0.416	0.300	54.59	5.022	0.9616	0.9599	0.9247
		Test 380		Traverse 5		
0.300	0.900	54.66	5.477	1.0487	1.0468	1.0107
0.300	0.800	54.71	5.486	1.0504	1.0486	1.0124
0.300	0.700	54.74	5.518	1.0566	1.0547	1.0185
0.300	0.600	54.56	5.575	1.0676	1.0657	1.0294
0.300	0.500	54.69	5.637	1.0793	1.0774	1.0410
0.300	0.450	54.57	5.689	1.0894	1.0875	1.0510
0.300	0.425	54.75	5.459	1.0452	1.0433	1.0072
0.300	0.415	54.34	5.163	0.9885	0.9869	0.9514
0.300	0.405	54.76	4.563	0.8736	0.8720	0.8379
0.300	0.402	54.54	4.471	0.8560	0.8545	0.8207
0.300	0.410	54.65	4.901	0.9384	0.9368	0.9018
		Test 380		Traverse 6		
0.686	-0.081	55.08	4.198	0.8037	0.8022	0.7690
0.686	0.000	54.76	4.088	0.7828	0.7813	0.7485
0.686	0.100	54.81	4.249	0.8135	0.8120	0.7788
0.686	0.200	54.82	4.535	0.8683	0.8667	0.8326

TABLE VII

SMOOTH VALUES OF THE NUSSELT NUMBER

A) $Re_{\infty} = 7098$

Polar Angle	Nusselt Number			
Distance from Cylinder Surface in.	0^{o}	30^{o}	60^{o}	90^{o}
0.002	-	-	1.160	0.693
0.004	(0.682)[a]	1.062	1.228	0.661
0.006	(0.676)	1.198	1.299	0.641
0.008	(0.669)	1.280	1.354	0.624
0.010	(0.664)	1.363	1.410	0.614
0.012	(0.658)	1.403	1.450	0.607
0.014	(0.656)	1.409	1.485	0.609
0.016	(0.658)	1.410	1.516	0.615
0.018	(0.661)	1.410	1.543	0.628
0.020	0.667	1.410	1.564	0.647
0.025	0.684	1.410	1.601	0.750
0.030	0.708	1.409	1.621	0.901
0.035	0.730	1.406	1.625	1.043
0.040	0.752	1.402	1.624	1.169
0.045	0.774	1.396	1.622	1.279
0.050	0.796	1.391	1.619	1.371
0.055	0.815	1.387	1.616	1.440
0.060	0.833	1.382	1.614	1.491
0.065	0.850	1.377	1.611	1.532
0.070	0.864	1.372	1.607	1.566
0.075	0.880	1.367	1.602	1.594
0.080	0.894	1.361	1.599	1.611
0.085	0.909	1.357	1.594	1.618
0.090	0.923	1.353	1.589	1.621
0.095	0.938	1.349	1.584	1.614
0.100	0.952	1.346	1.579	1.625
0.200	1.123	1.352	1.492	1.611
0.300	1.204	1.366	1.453	1.590
0.400	1.237	1.381	1.426	1.582
0.500	1.256	1.397	1.404	1.558

a) Values in parenthesis are extrapolated.

TABLE VII (Continued)

B) $Re_{\infty} = 3526$

Polar Angle	Nusselt Number			
Distance from Cylinder Surface in.	0^{o}	30^{o}	60^{o}	90^{o}
0.002	0.609	0.963	0.994	0.753
0.004	0.593	0.999	1.048	0.662
0.006	0.588	1.033	1.099	0.603
0.008	0.584	1.069	1.140	0.578
0.010	0.580	1.102	1.188	0.563
0.012	0.577	1.138	1.227	0.557
0.014	0.576	1.167	1.259	0.557
0.016	0.576	1.175	1.286	0.560
0.018	0.578	1.176	1.307	0.571
0.020	0.581	1.175	1.322	0.587
0.025	0.598	1.173	1.340	0.672
0.030	0.612	1.171	1.350	0.799
0.035	0.628	1.169	1.355	0.915
0.040	0.643	1.167	1.359	1.016
0.045	0.658	1.165	1.361	1.103
0.050	0.670	1.163	1.362	1.175
0.055	0.685	1.161	1.363	1.234
0.060	0.697	1.159	1.362	1.278
0.065	0.711	1.157	1.361	1.312
0.070	0.723	1.155	1.357	1.334
0.075	0.736	1.153	1.353	1.347
0.080	0.748	1.151	1.350	1.351
0.085	0.759	1.149	1.347	1.354
0.090	0.770	1.147	1.344	1.354
0.095	0.781	1.146	1.342	1.354
0.100	0.792	1.144	1.340	1.354
0.200	0.943	1.141	1.311	1.342
0.300	1.016	1.156	1.293	1.332
0.400	1.044	1.171	1.277	1.324
0.500	1.060	1.179	1.264	1.316

TABLE VII (Concluded)

C) $Re_{\infty} = 1757$

Polar Angle	Nusselt Number			
Distance from Cylinder Surface in.	0°	30°	60°	90°
0.002	0.560	0.801	0.786	0.683
0.004	0.550	0.816	0.813	0.638
0.006	0.542	0.823	0.840	0.603
0.008	0.536	0.848	0.862	0.578
0.010	0.532	0.862	0.887	0.563
0.012	0.528	0.878	0.909	0.557
0.014	0.526	0.896	0.932	0.554
0.016	0.524	0.910	0.953	0.558
0.018	0.524	0.916	0.972	0.565
0.020	0.526	0.920	0.990	0.578
0.025	0.534	0.921	1.024	0.582
0.030	0.544	0.922	1.041	0.696
0.035	0.554	0.922	1.049	0.753
0.040	0.564	0.921	1.050	0.807
0.045	0.574	0.920	1.052	0.858
0.050	0.583	0.919	1.054	0.904
0.055	0.593	0.919	1.054	0.945
0.060	0.602	0.918	1.054	0.979
0.065	0.610	0.918	1.052	1.005
0.070	0.618	0.917	1.052	1.021
0.075	0.626	0.916	1.052	1.034
0.080	0.634	0.915	1.051	1.045
0.085	0.641	0.915	1.050	1.050
0.090	0.648	0.914	1.049	1.052
0.095	0.654	0.913	1.047	1.052
0.100	0.661	0.913	1.046	1.052
0.200	0.760	0.909	1.026	1.046
0.300	0.820	0.914	1.011	1.040
0.400	0.853	0.924	1.002	1.033
0.500	0.871	0.938	0.995	1.027

TABLE VIII

STANDARD ERROR OF ESTIMATE OF THE RESULTS

A) $Re_\infty = 7098$

Test	Traverse	N	σ_e
348	1	28	0.0624
	2	13	0.0350
	3	12	0.0184
	4	12	0.0161
	5	9	0.0568
350a	1	27	0.0124
350b	1	12	0.0048
	2	20	0.0060
	3	13	0.0045
	4	16	0.0034
	5	13	0.0186
352	1	13	0.0166
	2	10	0.0899
	3	13	0.0587
	4	9	0.0111
	5	12	0.0109
	6	8	0.0050
359	1	10	0.0349
	2	13	0.0097
	3	11	0.0205
	4	8	0.0897
All tests at $Re_\infty = 7098$		282	0.0353

TABLE VIII (Continued)

B) $Re_\infty = 3526$

Test	Traverse	N	σ_e
363	1	11	0.0122
	2	11	0.0024
	3	15	0.0096
	4	13	0.0038
	5	11	0.0087
	6	11	0.0163
369	1	14	0.0020
	2	13	0.0071
	3	11	0.0042
372	1	6	0.0047
	2	8	0.0054
	3	9	0.0043
	4	8	0.0037
373	1	9	0.0032
	2	12	0.0031
	3	10	0.0011
	4	7	0.0018
	5	9	0.0048
376	1	12	0.0047
	2	15	0.0491
	3	13	0.0372
	4	7	0.0312
All tests at $Re_\infty = 3526$		235	0.0197

TABLE VIII (Concluded)

C) $Re_\infty = 1757$

Test	Traverse	N	σ_e
377	1	14	0.0056
	2	14	0.0086
379	1	3	0.0083
	2	9	0.0016
	3	11	0.0016
	4	12	0.0026
	5	11	0.0013
	6	11	0.0026
380	1	13	0.0018
	2	14	0.0062
	3	12	0.0007
	4	13	0.0007
	5	11	0.0024
	6	4	0.0010
All tests at $Re_\infty = 1757$		148	0.0039

PART III

PROPOSITIONS

PROPOSITION 1

Conventional models for stationary stochastic queues assume that the mean rate of arrival of customers to a service facility is independent of queue length. It is proposed that models which take into account the fact that mean rate of arrival is dependent on queue length are of more general applicability and of greater usefulness.

Conventional models (1, 2) for stationary stochastic queues attempt to describe the waiting-line characteristics of a service facility by assuming that customers arrive at a mean rate, λ, which is independent of queue length. If the mean service rate, μ, is greater than the mean rate of arrival, the probability, P_n, of a queue of length n is given by

$$P_n = \left(\frac{\lambda}{\mu}\right)^n \left(1 - \frac{\lambda}{\mu}\right) \tag{1}$$

and the gross income per unit time is

$$I = C\lambda \tag{2}$$

Thus, by assuming that the mean rate of arrival is independent of queue length, a solution is obtained which predicts that gross income is independent of service rate; and therefore, that the optimum service rate is the one that costs least. In order to obtain a more realistic evaluation of servicing policy, it is customary to assign a cost to customer waiting time (1), and to obtain in this manner a profit function dependent on the servicing rate.

In constructing a model for the description of queue characteristics it should be recognized that, for a competitive enterprise, prospective customers are likely to seek service elsewhere if the queue at the facility is long. Therefore the mean rate of arrival of customers should be considered a function of queue length in order to obtain a model of more general applicability.

If a simple description of this dependence, such as

$$\begin{aligned} \text{mean rate of arrival} &= \lambda', \quad 0 \leqslant n < N \\ &= 0, \quad n \geqslant N \end{aligned} \tag{3}$$

is used, the probability of a queue of length n is found to be

$$\begin{aligned} P'_n &= \frac{\left(\frac{\lambda'}{\mu'}\right)^n \left(1 - \frac{\lambda'}{\mu'}\right)}{1 - \left(\frac{\lambda'}{\mu'}\right)^{N+1}} \qquad 0 \leqslant n \leqslant N \\ &= 0 \qquad\qquad\qquad\qquad n > N \end{aligned} \tag{4}$$

and the gross income per unit time is given by

$$I' = C\lambda' \left[1 - \frac{\left(\frac{\lambda'}{\mu'}\right)^N \left(1 - \frac{\lambda'}{\mu'}\right)}{1 - \left(\frac{\lambda'}{\mu'}\right)^{N+1}} \right] \tag{5}$$

Thus the gross income predicted by this model increases as the rate of servicing increases, and it is not necessary to introduce costs extraneous to the model in order to make the servicing policy amenable to analysis.

Finally, the parameters introduced in the description of mean rate of arrival as a function of queue length, such as the value of N

in the model described, may be established by observation of the queue, by sampling opinion of customers, and from estimates of management. Hence, by reconciling these independent estimates, these values can be assigned with considerable certainty.

PROPOSITION 2

It is proposed that an effort be made to determine the electronic energy levels of a metal in the solid state near the melting point and in the liquid state near the freezing point in order to elucidate some aspects of the solid-liquid phase transition.

Phase transition from solid to liquid is traditionally regarded as a change in the "order" of the crystal lattice at the intermolecular level (3). However, it may be inferred from information available in the literature (4, 5, 6) that intramolecular changes may occur in the vicinity of phase transition or in the process of change of phase.

Such changes are probably caused by the "order-disorder" characteristics of the material (5) near the transition point, but it is possible that the point of transition is determined by intramolecular changes. A detailed knowledge of the distribution of energy among the electrons in the solid and liquid states in the vicinity of phase transition would probably lead to more definite conclusions as to whether transition is determined by intramolecular changes.

PROPOSITION 3

It is proposed that in general-purpose digital computers a command to halt operation is not necessary and that small general-purpose computers could be made more effective by replacing the "halt" command by one more useful in programming.

The logic of general-purpose computers usually includes an explicit command which halts arithmetic and logical action by setting the computer in a closed cycle during which all registers and memory locations remain unchanged (7). Apart from the explicit command structure, however, every computer has non-addressable logic which inhibits the performance of "forbidden" operations by setting the computer in a similar cycle. Thus a programmed halt could be obtained, in the absence of an explicit command, by use of a "forbidden" operation such as division by zero.

In order to use this method of halting the action, a few memory locations may be required. In small general-purpose computers, which usually have 16 to 32 commands, the availability of an additional command for arithmetic or logic would more than compensate this loss of a few memory locations out of the usual 4000 to 5000 available.

PROPOSITION 4

It is proposed that the rate of condensation of a one-component vapour may reach a maximum as the temperature of the condenser surface is decreased while maintaining constant vapour temperature.

Nusselt (8) derived an expression for the heat transfer coefficient from an inclined plate to a condensing vapour. The solution, which is valid for laminar flow of the condensate film, may be expressed in terms of a mean value of the heat transfer coefficient:

$$h_m = \frac{4}{3}\left[\frac{\sigma_f^2 \Lambda k_f^3 \sin\phi}{4\eta_f \ell (t_v - t_s)}\right]^{1/4} \qquad (1)$$

From this expression, which has been verified experimentally (9, 10), the mean rate of condensation may be expressed as

$$\dot{m} = \frac{4}{3}\left[\frac{\sigma_f^2 k_f^3 \sin\phi (t_v - t_s)^3}{4\eta_f \ell \Lambda^3}\right]^{1/4} \qquad (2)$$

In equations 1 and 2 the latent heat of the substance, Λ, is a function of the vapour temperature, t_v, whereas the specific weight, σ_f, thermal conductivity, k_f, and viscosity, η_f, of the condensate film are functions of an "average" film temperature. The average film temperature, t_f, may be taken as (9)

$$t_f = \frac{3}{4} t_s + \frac{1}{4} t_v \qquad (3)$$

By differentiating equation 2 at constant vapour temperature there results

$$\left(\frac{\partial \dot{m}}{\partial t_f}\right)_{t_v} = \dot{m}\left[\frac{3}{4}\frac{1}{k_f}\left(\frac{\partial k_f}{\partial t_f}\right) + \frac{1}{2}\frac{1}{\sigma_f}\left(\frac{\partial \sigma_f}{\partial t_f}\right) - \frac{1}{4}\frac{1}{\eta_f}\left(\frac{\partial \eta_f}{\partial t_f}\right) - \frac{1}{t_v - t_s}\right] \quad (4)$$

From equation 4 it follows that a local maximum at constant vapour temperature will exist provided

$$\frac{3}{k_f}\left(\frac{\partial k_f}{\partial t_f}\right) + \frac{2}{\sigma_f}\left(\frac{\partial \sigma_f}{\partial t_f}\right) - \frac{1}{\eta_f}\left(\frac{\partial \eta_f}{\partial t_f}\right) - \frac{4}{t_v - t_s} = 0 \quad (5)$$

Figure P1 shows the locus of equation 5 for water. The calculated results indicate that the rate of condensation will go through a maximum only when the vapour temperature is above 300 ^{o}F. Below this temperature the predicted surface temperature is below the freezing point, so the analysis of Nusselt is not applicable. Experimental results to confirm the existence of a local maximum are not available.

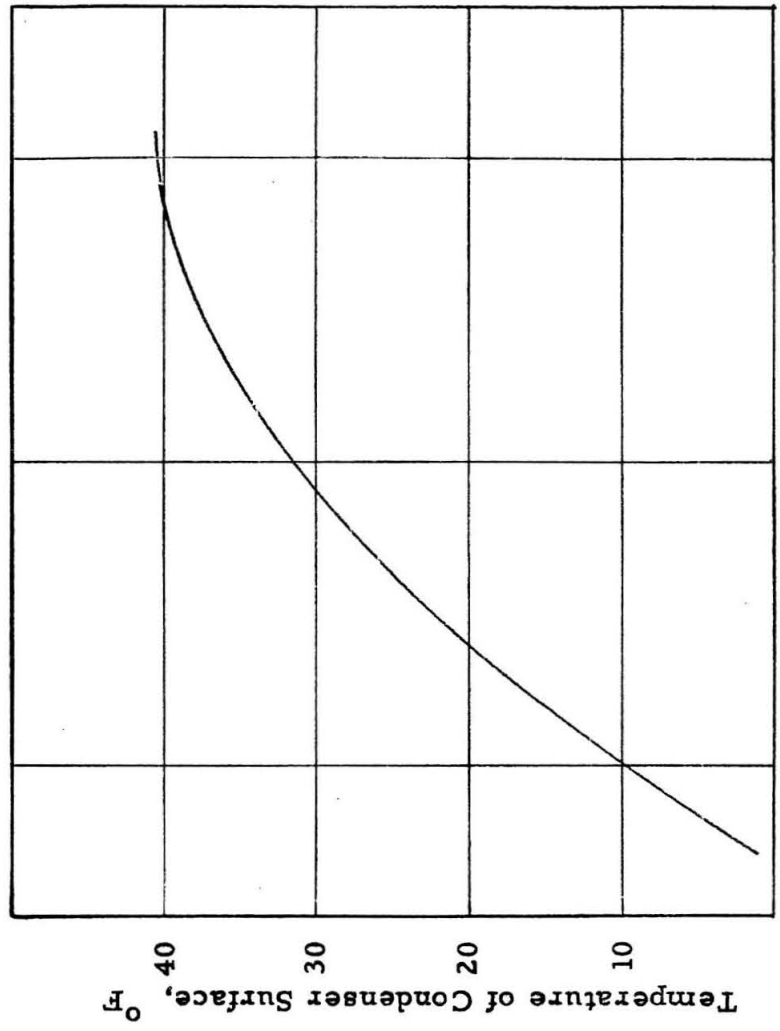

Figure P1: Relation Between Temperature of Condenser Surface and Vapour Temperature for Maximum Rate of Condensation of Water

PROPOSITION 5

It is proposed that experiments in two-dimensional, non-isothermal, laminar flow be conducted in order to establish whether the relation between shear stress and velocity derivatives obtained under such conditions is the same as that for isothermal flow.

The momentum equations for a fluid may be written in terms of stresses (11, 12, 13) in the form

$$\rho \frac{Du_i}{D\theta} = F_i + \sum_{j=1}^{3} \frac{\partial \tau_{ji}}{\partial x_j} \quad , \qquad i = 1, 2, 3 \tag{1}$$

In order to solve these equations it is often assumed that the stresses are given by (12, 13):

$$\tau_{ji} = \eta \left(\frac{\partial u_i}{\partial x_j} + \frac{\partial u_j}{\partial x_i} \right), \quad i \neq j \tag{2}$$

and

$$\tau_{ii} = -P + \eta \left[2 \frac{\partial u_i}{\partial x_i} - \frac{2}{3} \nabla \cdot \vec{u} \right] + \eta^* \nabla \cdot \vec{u} \tag{3}$$

It has been verified experimentally (14) that many fluids satisfy equations 2 and 3 under isothermal conditions. Under such conditions, the phenomenological coefficient η, known as the viscosity of the fluid, is a function of temperature and pressure.

Combining equations 1, 2, and 3, there results

$$\rho \frac{Du_i}{D\theta} = F_i - \frac{\partial P}{\partial x_i} + \sum_{j=1}^{3} \frac{\partial}{\partial x_j} \left[\eta \left(2 \frac{\partial u_i}{\partial x_i} - \frac{2}{3} \delta_{ij} \nabla \cdot \vec{u} \right) \right] + \frac{\partial}{\partial x_i} \eta^* \nabla \cdot \vec{u}$$

$$i = 1, 2, 3 \qquad (4)$$

Equation 4 is often applied to problems of non-isothermal flow (11, 13, 15), even though experimental verification of the validity of equations 2 and 3 for this case is not available.

If equation 4 is restricted to the case of steady, uniform, laminar, two-dimensional flow between parallel plates, it can be simplified to

$$F_1 - \frac{\partial P}{\partial x_1} + \frac{\partial}{\partial x_2} \left(\eta \frac{\partial u_1}{\partial x_2} \right) = 0 \qquad (5)$$

$$F_2 - \frac{\partial P}{\partial x_2} = 0 \qquad (6)$$

From equations 5 and 6 the validity of the representation of the shear stresses may be verified if the pressure gradient, temperature, and velocity fields are measured in experiments which satisfy the restrictions mentioned above, provided the dependence of viscosity on temperature is known for isothermal conditions and the components of the body forces are known.

REFERENCES

1. Churchman, C. W., Ackoff, R. L., and Arnoff, E. L., Introduction to Operation Research, John Wiley and Sons, Inc., New York (1957).

2. Feller, W., "Chance Processes and Fluctuations" in Modern Mathematics for the Engineer - Second Series, edited by E. F. Beckenbach, McGraw-Hill Book Co., Inc., New York (1961).

3. Frenkel, J., Kinetic Theory of Liquids, Oxford University Press, Oxford (1946).

4. Goetz, A., Phys. Rev. 33, 373 (1929).

5. Makinson, R. E. B., and Roberts, A. P., Aust. J. Phys. 13, 437 (1960).

6. Powles, J. G., Arch. des Sciences (Geneve) 13, 467 (1961).

7. Phister, M., Jr., Logical Design of Digital Computers, John Wiley and Sons, Inc., New York (1958).

8. Nusselt, W., Z. Ver. deut. Ing. 60, 541 (1916).

9. McAdams, W. H., Heat Transmission, McGraw-Hill Book Co., Inc., New York (1954).

10. Coulson, J. M., and Richardson, J. F., Chemical Engineering, McGraw-Hill Book Co., Inc., New York (1956).

11. Schlichting, H., Boundary Layer Theory, McGraw-Hill Book Co., Inc., New York (1955).

12. Longwell, P. A., Mechanics of Fluid Flow, Department of Chemical Engineering, California Institute of Technology, Pasadena, California (1958).

13. Bird, R. B., Stewart, W. E., and Lightfoot, E. N., Transport Phenomena, John Wiley and Sons, New York (1960).

14. Hatschek, E., The Viscosity of Liquids, D. Van Nostrand Co., New York (1929).

15. Yamagata, K., Mem. Fac. Eng. Kyushu University (Japan) 8, 366 (1940).

NOMENCLATURE

Roman

C	gross income per customer serviced
D	substantial derivative operator, $\frac{\partial}{\partial \theta} + \vec{u} \cdot \nabla$, sec.$^{-1}$
F	component of body force in x_i direction, lb./cu. ft.
h_m	mean heat transfer coefficient, Btu/sq. ft. sec. ^{o}F
I	total gross income
k	thermal conductivity, Btu/sq. ft. sec. (^{o}F/ft.)
ℓ	length of condenser surface, ft.
$\dot{m}$	rate of condensation, lb./sq. ft. sec.
n	number of customers in a queue
N	maximum number of customers in a queue
P	pressure, lb./sq. ft.
P_n	probability of a queue of length n
t	temperature, ^{o}F
$\vec{u}$	local velocity vector, ft./sec.
u_i	component of local velocity in x_i direction, ft./sec.
x_1, x_2, x_3	Cartesian coordinates, ft.

Greek

δ_{ij}	Kronecker delta
η	viscosity, lb. sec./sq. ft.
η^*	bulk viscosity, lb. sec./sq. ft.
θ	time, sec.
λ	mean rate of arrival of customers
Λ	latent heat of vapourization, Btu/lb.

μ	mean rate of service
ρ	density, lb. sec.^{2}/ft.^{4}
σ	specific weight, lb./cu. ft.
σ_{ji}	components of stress acting in x_i direction on a plane perpendicular to x_j direction, lb./sq. ft.
ϕ	angle between plate and horizontal

Subscripts

i, j	dummy variables
f	condensate
s	condensate surface
v	vapour

Superscript

'	proposed model
$\rightarrow$	vector